

5-1-2012

## Investigating the Use of Pozzolans in Portland Cement Concrete and Inorganic Polymer Mortar

Omar Abdelmalek Saleh  
University of Nevada, Las Vegas, omar\_a\_saleh@hotmail.com

Follow this and additional works at: <https://digitalscholarship.unlv.edu/thesesdissertations>



Part of the [Civil Engineering Commons](#), and the [Materials Science and Engineering Commons](#)

---

### Repository Citation

Saleh, Omar Abdelmalek, "Investigating the Use of Pozzolans in Portland Cement Concrete and Inorganic Polymer Mortar" (2012). *UNLV Theses, Dissertations, Professional Papers, and Capstones*. 1620.  
<https://digitalscholarship.unlv.edu/thesesdissertations/1620>

This Thesis is protected by copyright and/or related rights. It has been brought to you by Digital Scholarship@UNLV with permission from the rights-holder(s). You are free to use this Thesis in any way that is permitted by the copyright and related rights legislation that applies to your use. For other uses you need to obtain permission from the rights-holder(s) directly, unless additional rights are indicated by a Creative Commons license in the record and/or on the work itself.

This Thesis has been accepted for inclusion in UNLV Theses, Dissertations, Professional Papers, and Capstones by an authorized administrator of Digital Scholarship@UNLV. For more information, please contact [digitalscholarship@unlv.edu](mailto:digitalscholarship@unlv.edu).

INVESTIGATING THE USE OF POZZOLANS IN PORTLAND CEMENT  
CONCRETE AND INORGANIC POLYMER MORTAR

By

Omar Abdelmalek Saleh

Bachelor of Science in Civil Engineering  
University of Mosul, Ninawa, Iraq  
1995

A thesis submitted in partial fulfillment  
of the requirements for the

Master of Science in Engineering

Department of Civil and Environmental Engineering  
Howard R. Hughes College of Engineering  
The Graduate College

University of Nevada, Las Vegas  
May 2012

Copyright by Omar Abdelmalek Saleh 2012

All Rights Reserved



## THE GRADUATE COLLEGE

We recommend the thesis prepared under our supervision by

**Omar Abdelmalek Saleh**

entitled

### **Investigating the Use of Pozzolans in Portland Cement Concrete and Inorganic Polymer Mortar**

be accepted in partial fulfillment of the requirements for the degree of

#### **Master of Science in Engineering**

Department of Civil and Environmental Engineering

Aly Said, Committee Chair

Moses Karakouzian, Committee Member

Samaan Ladkany, Committee Member

Jan Pedersen, Graduate College Representative

Ronald Smith, Ph. D., Vice President for Research and Graduate Studies  
and Dean of the Graduate College

**May 2012**

## Abstract

The use of pozzolans offers promising signs for a change in the cement industry. Pozzolan in its natural and artificial forms can be used to improve cement properties or to synthesize new cement. This study investigates the use of pozzolans in portland cement concrete and inorganic polymer mortar (geopolymer mortar).

This thesis is divided into two phases. Phase 1 investigates the use of natural pozzolan as a partial replacement of portland cement in concrete. In this phase two types of class N pozzolan are used separately to develop concrete mixtures contain different percentages of class N pozzolan. Fresh concrete properties are evaluated along with hardened concretes properties. The properties of the new concretes are compared to those of a control concrete mixture made without the use of pozzolan.

Phase 2 focuses on synthesizing geopolymer mortars using artificial pozzolan as well as natural pozzolan in two separate applications. The pozzolan was used as a base material to synthesize the geopolymer binder. An alkaline solution and heat curing were deployed to enhance the polymerization process. Geopolymer mortars were synthesized using different alkaline solutions and curing temperatures. Some of the geopolymer mortar specimens then were exposed to 800°C to study the geopolymer mortars resistance to heat. Factors that affect the geopolymer mortars properties were investigated. Geopolymer mortars properties were evaluated before and after they were exposed to 800°C.

## Acknowledgements

I would like to express my sincere thanks to my advisor and committee chair, Dr. Aly M. Said, for his encouragement, advice and suggestions. His demand for excellence allowed me to complete this thesis.

I also would like to take this opportunity to thank my committee members Dr. Moses Karakouzian, Dr. Samaan Ladkany, and Dr. Jan Pedersen for their comments and encouragement.

I am grateful for all the help I received from Dr. Jacimaria Batista. I am appreciative to Mohamed Zeidan for his assistance and daily support. I am also thankful for the help I received from Mark Elkouz and Oscar Quiroz.

I am grateful to Dr. Anmar Al\_Talib for his help and support. My appreciation to Dr. Khalid Saleh for the help I received from him throughout my study.

My thanks and love is due to my wife for her support, encouragement and patience throughout this journey and to my kids for their love and spirit brought to me. My love and thanks to my parents and siblings for their encouragements and support.

## Table of Contents

Abstract.....	iii
Acknowledgments.....	iv
Table of Contents.....	v
List of Tables.....	x
List of Figures.....	xi
Chapter 1 - Introduction.....	1
1.1.Pozzolans Types and Definitions.....	2
1.2.Research Significance.....	3
1.3.Aim of this Thesis.....	4
1.4.Scope of Work.....	4
1.4.1. Phase 1: Investigating the use of class N pozzolans as a partial replacement of OPC in concrete.....	4
1.4.1.1. Properties of the raw materials.....	5
1.4.1.2. Fresh concrete properties.....	5
1.4.1.3. Hardened concrete properties.....	5
1.4.2. Phase 2: Synthesizing geopolymer mortars.....	5
1.4.2.1. Factors that affect the properties of the hardened geopolymer mortars.....	6
1.4.2.2. Properties of the raw materials.....	6
1.4.2.3. Changes in hardened geopolymer properties that were monitored.....	6
1.5.Organization of the Thesis.....	6
Chapter 2 – Phase 1: The Use of Class N Pozzolan as a Partial Replacement of Ordinary Portland Cement in Concrete.....	8
2.1 Overview.....	8
2.2 Literature Review.....	9
2.2.1 Pozzolan Effect on Fresh Concrete Properties.....	9
2.2.2 Pozzolan Effect on Concrete Strength and Modulus of Elasticity.....	10
2.2.3 Pozzolan Effect on Concrete Rapid Chloride Ion Permeability.....	11

2.3 Materials Used in Phase 1 .....	12
2.3.1 Aggregate .....	12
2.3.2 Class N Pozzolan .....	13
2.3.3 Portland Cement.....	17
2.3.4 Water.....	17
2.3.5 Super-Plasticizer/High Range water Reducer.....	17
2.4 Phase 1 Standard Tests.....	18
2.4.1 X-ray Fluorescence Spectroscopy (XRF) .....	18
2.4.2 X-Ray Diffraction Analysis (XRD) .....	19
2.4.3 Compressive Strength Test of Mortar Cubes.....	20
2.4.4 Strength Activity Index with Portland Cement.....	21
2.4.5 Slump Test .....	21
2.4.6 Air Content Test.....	22
2.4.7 Concrete Unit Weight Test .....	23
2.4.8 Temperature of Freshly Mixed Concrete (Adiabatic Temperature) .....	24
2.4.9 Compressive Strength Test of Cylindrical Concrete Specimens .....	25
2.4.10 Splitting Tensile Strength Test.....	26
2.4.11 Static Modulus of Elasticity Test.....	27
2.4.12 Dynamic Young's Modulus of Elasticity Test.....	28
2.4.13 Rapid Chloride Ion Penetration Test (RCPT).....	29
2.4.14 Rapid Chloride Ion Migration Test (RMT) .....	29
2.5 Investigating the use of Pozzolete in Concrete .....	30
2.5.1 Methodology .....	30
2.5.1.1 Concrete Proportion .....	30
2.5.1.2 Mixing Procedure.....	31
2.5.1.3 Testing.....	33
2.5.2 Test Results and Discussions .....	33
2.5.2.1 Fresh Concrete Properties .....	34
2.5.2.2 Temperature of the Freshly Mixed Concrete .....	34
2.5.2.3 Compressive Strength .....	35
2.5.2.4 Splitting Tensile Strength and Modulus of Elasticity .....	37



2.5.2.5 Rapid Chloride Ion Permeability Test and Rapid Chloride Ion Migration Test.....	39
2.6 Investigating the use of Lassenite SR in Concrete.....	41
2.6.1 Methodology.....	41
2.6.1.1 Concrete Proportion.....	41
2.6.1.2 Mixing Procedure.....	42
2.6.1.3 Testing.....	43
2.6.2 Test Results and Discussions.....	44
2.6.2.1 Tests for the Fresh Concrete Properties.....	44
2.6.2.2 Temperature of the Freshly Mixed Concrete.....	44
2.6.2.3 Concrete Strength and Modulus of Elasticity.....	45
2.6.2.4 Rapid Chloride Ion Permeability Test and Rapid Chloride Ion Migration Test.....	47
Chapter 3 – Phase 2: Synthesizing Geopolymer Mortars.....	50
3.1 Overview.....	50
3.2 Literature Review.....	54
3.3 Materials used in Phase 2.....	54
3.3.1 Fly Ash.....	54
3.3.2 Class N Pozzolan.....	56
3.3.3 Fine Aggregate.....	59
3.3.4 Sodium Silicate Solution ( $\text{Na}_2\text{Si}_3\text{O}_7$ ).....	59
3.3.5 Potassium Hydroxide (KOH).....	59
3.3.6 Water.....	59
3.4 Phase 2 Standard Tests.....	59
3.4.1 Mortar Flow Test.....	59
3.4.2 Compressive Strength Test of Geopolymer Mortar Cubes.....	60
3.4.3 X-ray Fluorescence Spectroscopy (XRF).....	60
3.4.4 X-Ray Diffraction Analysis (XRD).....	60
3.4.5 Mercury Intrusion Porosimetry (MIP).....	61
3.5 Fine Aggregate Saturated Surface-Dry Condition (SSD) Preparation.....	62
3.6 Potassium Hydroxide Solution (KOH) Preparation.....	63

3.7 Geopolymer Mortars Specimen Preparation.....	63
3.8 Geopolymer Mortars Exposure to 800°C .....	64
3.9 Fly Ash Based Geopolymer Mortars .....	65
3.9.1 Methodology .....	65
3.9.1.1 Fly Ash based Geopolymer Mortars Mix Proportion .....	65
3.9.1.2 Fly Ash based Geopolymer Mortars Mixing Procedure.....	66
3.9.1.3 Fly Ash based Geopolymer Mortars Testing.....	67
3.9.2 Fly Ash based Geopolymer Tests Results and Discussions.....	68
3.9.2.1 Fly Ash based Geopolymer Mortars Compressive Strength .....	68
3.9.2.1.1 Effect of the Curing Regime and Age of Testing .....	68
3.9.2.1.2 Effect of the Sodium Silicate to Potassium Hydroxide Ratio..	73
3.9.2.1.3 Effect of the Exposure to 800°C .....	75
3.9.2.2 Changes in Volume and Mass after the Exposure to 800°C.....	76
3.9.2.3 X-Ray Diffraction Analysis (XRD).....	77
3.9.2.4 Mercury Intrusion Porosimetry (MIP).....	80
3.10 Metakaolin Based Geopolymer .....	82
3.10.1 Methodology .....	82
3.10.1.1 Metakaolin based Geopolymer Mortars Mix Proportion.....	82
3.10.1.2 Metakaolin based Geopolymer Mortars Mixing Procedure .....	82
3.10.1.3 Metakaolin based Geopolymer Mortars Testing .....	84
3.10.2 Metakaolin based Geopolymer Tests Results and Discussions .....	84
3.10.2.1 Metakaolin based Geopolymer Mortars Compressive Strength.....	84
3.10.2.1.1 Effect of the Curing Regime and Age of Testing .....	84
3.10.2.1.2 Effect of the Sodium Silicate to Potassium Hydroxide Ratio..	89
3.10.2.1.3 Effect of the Exposure to 800°C .....	91
3.10.2.2 Changes in Volume and Mass after the Exposure to 800°C.....	92
3.10.2.3 X-Ray Diffraction Analysis (XRD).....	93
3.10.2.4 Mercury Intrusion Porosimetry (MIP).....	96
Chapter 4 – Conclusion and Recommendations .....	98
4.1 Developing Concrete Mixture Proportions Incorporating Class N Pozzolans .....	98
4.2 Performance of the New Concretes .....	98

4.3 Pozzolan based Geopolymer Mortars .....	100
4.4 Performance and Heat Resistant of the Geopolymer Mortars .....	100
4.5 Future Recommendation.....	102
References.....	103
VITA.....	118

## List of Tables

Table 1	ASTM C 618 (2003) requirements for class N pozzolan.....	15
Table 2	Pozzolete and Lassenite SR X-ray fluorescence spectroscopy .....	16
Table 3	Portland cement properties.....	17
Table 4	Super-Plasticizers properties .....	18
Table 5	Details of concrete mixtures and their proportions by mass per cubic yard of concrete .....	31
Table 6	Fresh concrete properties.....	34
Table 7	The average compressive strength and splitting tensile strength .....	36
Table 8	Concrete modulus of elasticity.....	38
Table 9	RCPT and RMT results .....	40
Table 10	Details of concrete mixtures and their proportions by mass per cubic yard of concrete .....	42
Table 11	Fresh concrete properties.....	44
Table 12	The average compressive strength and splitting tensile strengths for concrete mixtures incorporating Lassenite SR.....	46
Table 13	RCPT and RMT results .....	48
Table 14	Fly ash ASTM C 618 (2003) requirements.....	55
Table 15	Metakaolin ASTM C 618 (2003) requirements .....	56
Table 16	Fly ash and Metakaolin X-ray fluorescence spectroscopy.....	58
Table 17	Fly ash based geopolymer mortars compressive strength.....	70
Table 18	Fly ash based geopolymer mortars changes in mass and volume .....	77
Table 19	Fly ash based geopolymer mortars XRD results .....	78
Table 20	Flay ash based geopolymer mortars MIP results.....	81
Table 21	Metakaolin based geopolymer mortars compressive strength .....	86
Table 22	Metakaolin based geopolymer mortars changes in mass and volume.....	93
Table 23	Metakaolin based geopolymer mortars XRD results .....	94
Table 24	Metakaolin based geopolymer mortars MIP results.....	97

## List of Figures

Figure 1	Class N pozzolan sources .....	9
Figure 2	Particle distribution curve for coarse aggregate .....	12
Figure 3	Particle distribution curve for fine aggregate .....	13
Figure 4	Pozzolete .....	13
Figure 5	Pozzolete X-ray diffraction analyses.....	14
Figure 6	Lassenite SR .....	14
Figure 7	Lassenite SR X-ray diffraction analysis .....	15
Figure 8	X-ray fluorescence spectrometer .....	19
Figure 9	X-Ray diffraction spectrometer .....	20
Figure 10	Mortar cube compressive strength test .....	21
Figure 11	Concrete slump test .....	22
Figure 12	Air meter type B .....	23
Figure 13	Concrete unit weight test preparation.....	24
Figure 14	Temperature of freshly mixed concrete test setting .....	24
Figure 15	Sulfur capping preparation .....	26
Figure 16	Cylindrical concrete specimens' compressive strength test setting .....	26
Figure 17	Concrete splitting tensile strength test setting .....	27
Figure 18	Concrete static modulus of elasticity test setting .....	28
Figure 19	Concrete dynamic Young's modulus of elasticity using E-meter MK II.....	28
Figure 20	Concrete rapid chloride ion penetration test setting .....	29
Figure 21	Specimen after rapid chloride ion migration test .....	30
Figure 22	Steel drum mixer .....	31
Figure 23	Concrete mixing procedure .....	32
Figure 24	Change in adiabatic temperature for different mixtures.....	35
Figure 25	Relationship between concrete compressive strength and the curing age.....	37
Figure 26	Relationship between the percentages of Pozzolete and concrete compressive strength .....	37
Figure 27	Relationship between the percentages Pozzolete and concrete splitting tensile strength at 28 days .....	38
Figure 28	RMT for N1P10 specimens at 28, 56, and 90 days.....	41

Figure 29	Concrete mixing procedure .....	43
Figure 30	Change in adiabatic temperature for different mixtures.....	45
Figure 31	Relationship between concrete compressive strength and the curing age.....	47
Figure 32	Concrete splitting tensile strength .....	47
Figure 33	NP0 & NP5 Chloride ion penetration depths at 28 days.....	49
Figure 34	Fly ash .....	54
Figure 35	Fly ash X-ray diffraction analysis .....	55
Figure 36	Metakaolin.....	57
Figure 37	Metakaolin X-ray diffraction analysis.....	57
Figure 38	Geopolymer mortar flow test .....	59
Figure 39	X-Ray diffraction single crystal structure .....	60
Figure 40	Micromeritics AutoPore IV and penetrometer filled with mercury .....	62
Figure 41	Cone test for surface moisture.....	63
Figure 42	Geopolymer mortars specimens inside an oven .....	64
Figure 43	Geopolymer mortar specimens inside the furnace .....	65
Figure 44	Fly ash based geopolymer mortar mixing .....	66
Figure 45	Fly ash based geopolymer mortars mixing procedure.....	67
Figure 46	Relationship between the curing temperature and the compressive strength for fly ash geopolymer mortars made with Sodium silicate to potassium hydroxide ratios of 0.5, 0.75, and 1.00. ....	71
Figure 47	Relationship between the curing temperature and the compressive strength for fly ash geopolymer mortars made with Sodium silicate to potassium hydroxide ratios of 1.25 and 1.50. ....	72
Figure 48	Effect of increasing the curing temperature from 45°C to 75°C on the compressive strength of different geopolymer mortars .....	73
Figure 49	Effect of the sodium silicate to potassium hydroxide ratio by mass on the compressive strength of the fly ash based geopolymer mortars cured at different temperatures .....	74
Figure 50	Fly ash based geopolymer before and after the exposure to 800°C .....	76
Figure 51	Quantitative Rietveld X-ray fine structure analysis for fly ash based geopolymer mortar FA-1.25-45 .....	79

Figure 52	Quantitative Rietveld X-ray fine structure analysis for fly ash based geopolymer mortar FA-1.25-75 .....	79
Figure 53	Quantitative Rietveld X-ray fine structure analysis for fly ash based geopolymer mortar FA-1.25-75-800 .....	80
Figure 54	Relationship between the threshold diameter and the cumulative intrusion for fly ash based geopolymer mortars .....	81
Figure 55	Metakaolin based geopolymer mortars preparation .....	83
Figure 56	Metakaolin based geopolymer mortars mixing procedure .....	83
Figure 57	Relationship between the curing temperature and the compressive strength for metakaolin geopolymer mortars made with Sodium silicate to potassium hydroxide ratios of 0.75, 1.00, and 1.25. ....	87
Figure 58	Relationship between the curing temperature and the compressive strength for metakaolin geopolymer mortars made with Sodium silicate to potassium hydroxide ratio of 1.50. ....	88
Figure 59	Effect of increasing the curing temperature from 45°C to 75°C on the compressive strength of different geopolymer mortars.....	88
Figure 60	Effect of the sodium silicate to potassium hydroxide ratio by mass on the compressive strength of the metakaolin based geopolymer mortars cured at different temperatures .....	90
Figure 61	Metakaolin based geopolymer mortar before and after exposure to 800°C ...	92
Figure 62	Quantitative Rietveld X-ray fine structure analysis for the metakaolin based geopolymer mortar Meta-1.25-45 .....	95
Figure 63	Quantitative Rietveld X-ray fine structure analysis for the metakaolin based geopolymer mortar Meta-1.25-75 .....	95
Figure 64	Quantitative Rietveld X-ray fine structure analysis for the metakaolin based geopolymer mortar Meta-1.25-75-800 .....	96
Figure 65	Relationship between the threshold diameter and the cumulative intrusion for metakaolin based geopolymer mortar.....	97

## Chapter 1

### Introduction

Durability of concrete structures exposed to harsh environments such as highway bridges, airports runways, concrete dams etc. is a challenge that cannot be easily met using ordinary portland cement. The deterioration of concrete structures in the past few decades has become a matter of great concern to the concrete industry. In addition to the durability concern, concretes made with ordinary portland cement possess low early strength, low fire resistance and low resistance to chemical attack (Gourley & Johnson, 2005). Hence, concretes made with ordinary portland cement have several weaknesses, which are difficult and expensive to overcome.

As a result, new materials are being investigated to improve cement properties or to synthesize new cement. This study has investigated the use of pozzolan as a partial replacement of cement as well as a base material to manufacture new cements. Pozzolans can be used as partial replacement of ordinary portland cement (OPC) in concrete to reduce concrete heat of hydration, improve concrete durability, and reduce the cost of concrete (ACI 211.1, 1991). Pozzolans also have environmental benefits by reducing the use of portland cement. Portland cement manufacturing is associated with high CO<sub>2</sub> emission (Meyer, 2009). Pozzolans can be used as mineral admixtures in concrete (ASTM C 618, 2003) or as components of blended cement when manufacturing portland-pozzolan cement (ASTM C 595, 2003). Most of the mass concrete dams built around the world contain pozzolans (ACI 232.2 R, 2003). Portland-pozzolan cement was used in the United States by the California Division of Highways in the 1930s to build the Golden Gate Bridge, the San Francisco-Oakland Bay Bridge (Meissner, 1949) and the California



State Water Project (Tuthill & Adams 1972). Similar cement was used by the US Army Corps of Engineers to build the Bonneville Dam on the Columbia River in 1943 (Waugh, 1963). A pozzolan added at mixer was used in building the Friant Dam in 1942 (Davis, 1950). The use of pozzolan in concrete applications required a complete evaluation for its effect on concrete properties.

Pozzolans with high percentages of silicon and aluminum can be used as base materials to synthesize inorganic polymer binder called geopolymer. Geopolymer was introduced to the world by Professor Joseph Davidovits as a non-flammable and non-combustible material (Davidovits, 1989). Geopolymer is inorganic aluminosilicate polymer that can be synthesized from materials of geological origins or byproducts that contain high percentages of silicon and aluminum (Hardjito, Wallah, Sumajouw, & Rangan, 2004a). Geopolymer can be used as cement for concrete and mortar, material for coating and adhesives, binder for fiber composites and waste encapsulation (Davidovits, 2008).

In this thesis, pozzolans of both natural and artificial origins were used in the development of high performance cement binders. First, natural pozzolans were used as a partial replacement of portland cement in concrete mixtures, then both natural and artificial pozzolans were used to synthesize geopolymer mortars in two separate applications.

## **1.1 Pozzolans Types and Definitions**

The American Concrete Institute (ACI) defines pozzolan as:

a siliceous or siliceous and aluminous material, which in itself possesses little or no cementitious value but will, in finely divided form and in the presence of

moisture, chemically react with calcium hydroxide at ordinary temperatures to form compounds possessing cementitious properties; there are both natural and artificial pozzolans. (ACI 232.2 R, 2003).

Class N pozzolan is a designation of the natural pozzolan in the raw or calcined State (ACI 232.1 R, 2000). The American Society of Testing and Materials (ASTM) covers the specifications of class N pozzolan for the use as a mineral admixture in concrete in its ASTM C 618 specification (ASTM C 618, 2003). The American Concrete Institute defines natural pozzolan as “either a raw or calcined natural material that has pozzolanic properties (for example, volcanic ash or pumicite, opaline chert and shales, tuffs, and some diatomaceous earths)” (ACI 232.1 R, 2000).

Fly ash is an artificial pozzolan generated as a byproduct of coal burning, especially at power plants. In 2010, the United States generated 68 million tons of fly ash (American Coal Ash Association). Although fly ash can be used in concrete, blended cement and several other applications, a huge amount of the generated fly ash in 2010, more than 62%, was a waste product. Class F fly ash is produced from burning anthracite or bituminous coal (ASTM C 618, 2003). The ACI defines fly ash as “the finely divided residue that results from the combustion of ground or powdered coal and that is transported by flue gases from the combustion zone to the particle removal system” (ACI 232.2 R, 2003).

## **1.2 Research Significance**

This research is significant for the development of pozzolan based high performance cement binders for use in concrete and mortar. The new binders would reduce the use of OPC in concrete and eliminate its use in mortar. This research is also

significant for the development of high early strength concrete as well as high early strength and heat resistant inorganic polymer mortars.

### **1.3 Aim of this Thesis**

The aims of this thesis are:

1. To develop mixtures proportions for the use of class N pozzolans as a partial replacement of OPC in concrete;
2. To study and evaluate the performance of the new concretes;
3. To synthesize pozzolan based geopolymer mortars;
4. To study and evaluate the performance and heat resistant of the geopolymer mortars;

### **1.4 Scope of Work**

This thesis is divided into two phases. Phase 1 covers the use of natural pozzolans as a partial replacement of OPC in concrete. Phase 2 covers the use of both natural and artificial pozzolans to synthesize geopolymer mortars.

**1.4.1 Phase 1: Investigating the use of class N pozzolan as a partial replacement of OPC in concrete.** In this phase of the thesis, the use of class N pozzolan as a partial replacement of OPC in concrete mixtures was studied. Class N pozzolans from two different sources were used in this phase. Several percentages of pozzolans were used to prepare several concrete mixtures. The properties of the new concretes were investigated using several standardized tests. The test results were evaluated and compared to the tests results of a control concrete mixture made without pozzolan. The properties that were evaluated included:

**1.4.1.1 Properties of the raw materials.** The properties of the raw materials were studied by conducting the following investigations:

- Elemental analysis-Using X-ray fluorescence spectroscopy analysis
- Crystal structure-Using X-Ray diffraction analysis
- Strength activity index-Following ASTM C 311 (2000)
- Particles distribution-Following ASTM C 136 (2001)

**1.4.1.2 Fresh concrete properties.** The effect of class N pozzolan on fresh concrete properties was investigated following several standardized tests as follows:

- Slump-Following ASTM C 143 (2003)
- Unit weight-Following ASTM C 138 (2001)
- Air content-Following ASTM C 231 (2003)
- Temperature of freshly mixed concrete-Following ASTM C 1064 (2003)

**1.4.1.3 Hardened concrete properties.** The effect of class N pozzolan on hardened concrete properties was studied following several standardized tests as follows:

- Compressive strength-Following ASTM C 39 (2003)
- Splitting tensile strength-Following ASTM C 496 (2004)
- Static modulus of elasticity-Following ASTM C 469 (2002)
- Dynamic Young's modulus of elasticity-Following ASTM C215 (2002)
- Rapid chloride ion penetration-Following ASTM C 1202 (1997)
- Rapid chloride ion migration-Following the procedure proposed by Luping and Nilsson (1993)

**1.4.2 Phase 2: Synthesizing geopolymer mortars.** In this phase, class N pozzolan and class F fly ash were used separately to synthesize geopolymer mortars. The

geopolymer mortars were evaluated for their strength and heat resistant. Properties of the raw materials were analyzed and the factors that affect hardened geopolymer properties were studied. The changes in the hardened geopolymer properties associated with these factors are evaluated. The scope of work was carried as follows:

#### ***1.4.2.1 Factors that affect the properties of the hardened geopolymer mortars.***

The effect of each of the following factors on the geopolymer properties was studied:

- Initial curing temperatures
- Sodium silicate to potassium hydroxide ratio by mass
- Exposure to 800°C

***1.4.2.2 Properties of the raw materials.*** The following analyses were used to evaluate the properties of the raw materials:

- Elemental analysis-Using X-ray fluorescence spectroscopy analysis
- Crystal structure-Using X-Ray diffraction analysis

#### ***1.4.2.3 Changes in hardened geopolymer properties that were monitored.***

Changes in the following hardened properties were monitored:

- Change in mass and volume
- Change in compressive strength-Following ASTM C 109
- Change in the crystal structure-Using X-Ray diffraction analysis
- Change in Pores Structure-Using Mercury Intrusion Porosimetry

### **1.5 Organization of the Thesis**

This thesis consists of four chapters. The first chapter is an introduction to the use of pozzolans in concrete and geopolymer. The second chapter covers Phase 1 of the thesis, which investigates the use of class N pozzolan as a partial replacement of OPC in

concrete. Chapter three covers Phase 2 of the thesis, which focuses on synthesizing geopolymer mortars. Finally, chapter four presents the conclusion and recommendations.

**PHASE 1: The Use of Class N Pozzolan as a Partial Replacement  
of Ordinary Portland Cement in Concrete**

**2.1 Overview**

In this phase of the thesis, two class N pozzolans of volcanic origins are used independently as a partial replacement of OPC in concrete mixtures. The properties of the new concretes are evaluated using several standardized tests. The tests results are compared to the tests results of a control concrete mixture made without pozzolan to evaluate the performances of the pozzolans.

Class N pozzolan is used in this study because class N pozzolan is available and accessible in open fields mining. Unlike the production of OPC, the production of class N pozzolan required a very simple process that does not consume a lot of energy. Hence, the use of class N pozzolan as a partial replacement of OPC in concrete will reduce the cost and carbon footprint of concrete.

The U.S. Green Building Council (U.S.G.B.C.) encourages the use of regionally available building materials and credits projects that use regional materials. LEED 2009 new construction defined regional materials as “building materials or products that have been extracted, harvested or recovered, as well as manufactured within 500 miles of the project site” (USGBC, 2009). Thus, the two class N pozzolan used in this study, which was performed in Las Vegas, Nevada, were of origins that are located within the 500 miles limits. The first pozzolan was Pozzolete which is volcanic pozzolan from Panaca, Nevada. The second pozzolan was Lassenite SR which is volcanic ash contains diatoms

remains from ancient seabed in Long Valley, Nevada. Bothe locations are illustrated in Figure 1.



1) Panaca, Nevada. 2) Long Valley, Nevada

Figure 1. Class N pozzolan sources, Retrieved from (<http://www.mapquest.com>).

## 2.2 Literature Review

Several studies evaluated the performance of class N pozzolan from different sources as a partial replacement of OPC and yielded diverse results. In general introducing class N pozzolan into the concrete mixture would change fresh concrete and hardened concrete properties and affect concrete durability. The following sections provide literature review for the effect of class N pozzolan when used in concrete on different concrete properties.

**2.2.1 Pozzolan Effect on fresh concrete properties.** Previous studies concluded that mineral admixtures including class N pozzolan could have a big impact on the water requirement of concrete (Mather, 1956). Hence, selecting a desired slump is the first step in the recommended class N pozzolan proportioning method suggested by Lovewell and Hyland (1974). Super-plasticizer can be used to maintain a workable concrete mixture when class N pozzolan is used (Chen, Soles & Malhorta, 1993; Ghrici, Kenia & Said-



Mansour, 2007; Güneysi, Ozturan & Gesoglu, 2011; Papadakis & Tsimas, 2005; Shannag, 2000; Tagnit-Hamou, Petrov & Luke, 2003; López & Castro, 2010; Nili & Salehi, 2010; Nili & Zaheri, 2011; Ramezani pour, Pilvar, Mahdikhani & Moodi, 2011; Uzal, Turanli & Mehta, 2007). Increasing the water/cement ratio (w/c) is another option to overcome the reduction in concrete workability associated with using class N pozzolan (Davraz & Gunduz, 2005; Kouloumbi, Batis & Malami 1994; Temiz, Kose & Koksak 2007). Mehta (1999) reported that the extra water needed by the pozzolan during mixing will be consumed in the pozzolanic reaction at a later stage.

Class N pozzolan is used in mass concrete to lower the heat of hydration (ACI 207.1R, 1996). Townsend (1966) reported that pozzolan provide approximately 50% less heat of hydration than an equal amount of portland cement. A reduction in the heat of hydration of concrete containing class N pozzolan was also reported by ACI 232.1R (2000); Shannag and Yeginobali (1995). The use of class N pozzolan in concrete not only reduces concrete hydration peak temperature but it also reduces the slope of the cooling zone ( Nili & Salehi, 2010). Unlike its effect on concrete workability and heat of hydration, class N pozzolan does not have a major effect on concrete unit weight and air content (Ballard et al. 2008; Irassar, Maio & Batic, 1996; Kaid, Cyr, Julien & Khelafi, 2009; Khan & Alhozaimy, 2005, 2011).

**2.2.2 Pozzolan Effect on concrete strength and modulus of elasticity.** The use of class N pozzolan as a partial replacement of OPC in concrete effects the hardened concrete properties like compressive strength, tensile strength and modulus of elasticity. Class N pozzolan's effect on hardened concrete properties is highly related to the age of testing, pozzolan percentage of replacement and the source of pozzolan. A reduction in

concrete early compressive strength or concrete compressive strength in general could be associated with the use of class N pozzolan in concrete (Irassar et al., 1996; Khan & Alhozaimy, 2005, 2011; López & Castro, 2010; Mehta, 1981; Nili & Zaheri, 2011; Shannag & Yeginobali, 1995; Sideris & Savva, 2001; Uzal et al., 2007). However, class N pozzolan might increase concrete strength (Chen et al., 1993; Davraz & Gunduz, 2005; Targan, Olgun, Erdogan & Sevinc 2003). Splitting tensile strength of concrete incorporating class N pozzolan follows the same trend as its compressive strength (Uzal et al., 2007; Yeginobali, 1995). On the other hand, no significant effect on concrete modulus of elasticity was reported.

**2.2.3 Pozzolan Effect on concrete rapid chloride ion permeability.** The resistance to rapid chloride ion permeability is an important concrete property that affects its durability. Pozzolan's ability to reduce concrete permeability is the most important property that encourages its use a partial replacement of concrete (Davis, 1950). A study conducted by Papadakis and Tsimas (2005) yielded a higher efficiency factor against chlorides ( $k=1$ ) in concrete when class N pozzolan was used. In general the literature shows that class N pozzolan would improve concrete resistance to chloride ion permeability in most cases (Ballard et al. 2008; Kouloumbi et al., 1994; Tagnit-Hamou et al., 2003; Uzal et al., 2007). However, class N pozzolan could cause an increase in concrete chloride ion permeability (Khan & Alhozaimy, 2005, 2011). Shi (2003) analyzes the RCPT published results of hundred concrete mixtures made with different supplementary cementitious materials (SCM's) including class N pozzolan and concluded that the RCPT is not a valid test to evaluate the permeability of concrete made with different proportions or containing different materials. Furthermore, Shi reported

that the chloride migration test (RMT) should be used instead of RCPT to compare concrete permeability.

### 2.3 Materials Used in Phase 1

All materials were stored at room temperature  $73\pm 3^{\circ}\text{F}$  to maintain a constant mixing temperature. When a material was used in different mixtures it was taken from the same batch to reduce differences that could accompany using different batches.

**2.3.1 Aggregate.** Both coarse and fine aggregates were obtained from a concrete ready-mix plant and they can be described as follows:

- **Coarse aggregate.** Well graded crushed natural gravel with bulk specific gravity of 2.86, absorption ratio of 0.91%, dry rodded unit weight of  $97.8 \text{ lb/ft}^3$ , water content of about 0.1% and nominal size of  $\frac{3}{4}$  inch. The sieve analysis of the coarse aggregate is shown in Figure 2.

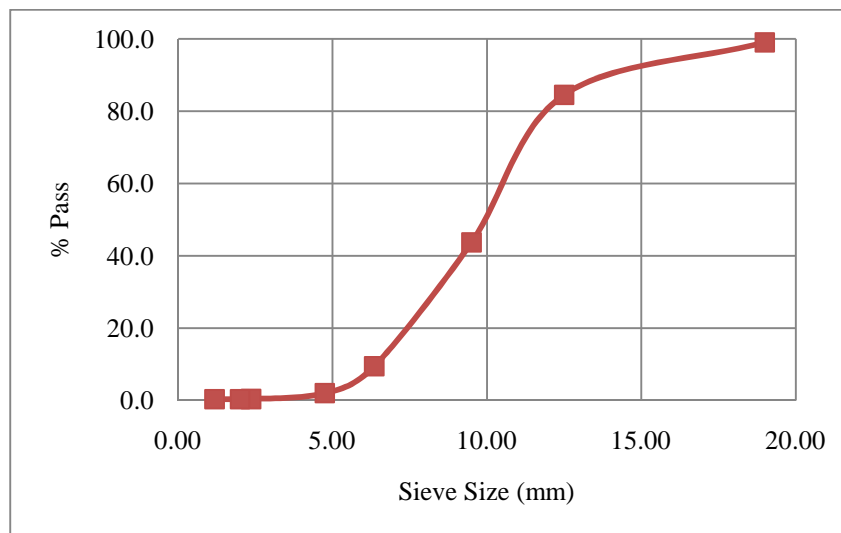


Figure 2. Particle distribution curve for coarse aggregate.

- **Fine aggregate.** Well graded natural sand with bulk specific gravity of 2.72, absorption of 0.65%, water content of 0.18%, and fineness modulus of 2.67. The sieve analysis of the fine aggregate is demonstrated in Figure 3.

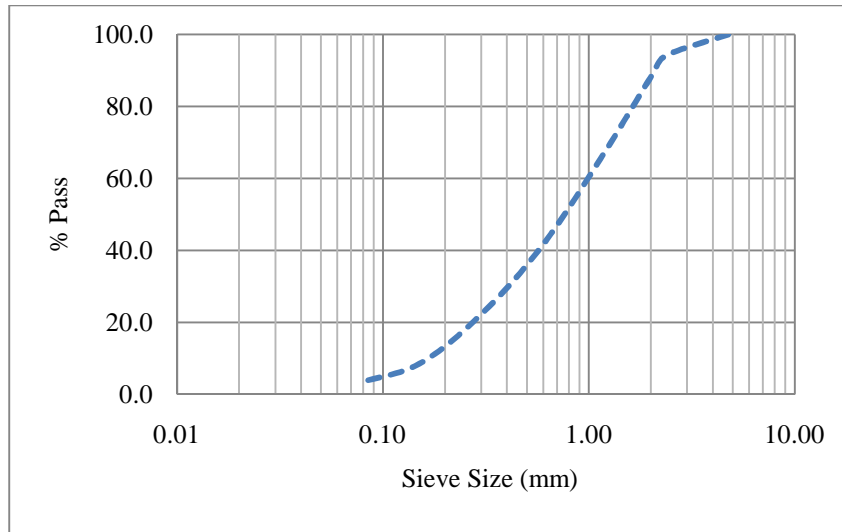


Figure 3. Particle distribution curve for fine aggregate.

**2.3.2 Class N pozzolan.** Two types of ASTM C 618 (2003) class N pozzolan were used in Phase 1. Both pozzolans were of volcanic origin. Important properties of the two pozzolan were compared to ASTM C 618 (2003) requirements as presented in Table 1. The X-ray fluorescence spectroscopy (XRF) analyses of the two pozzolans is presented in Table 2. The two pozzolan can be described as follows:

- **Pozzolete.** Class N Pozzolete is shown in Figure 4. Pozzolete is volcanic pozzolan from Panaca, Nevada. The X-ray diffraction analysis (XRD) of Pozzolete is illustrated in Figure 5.



Figure 4. Pozzolete.

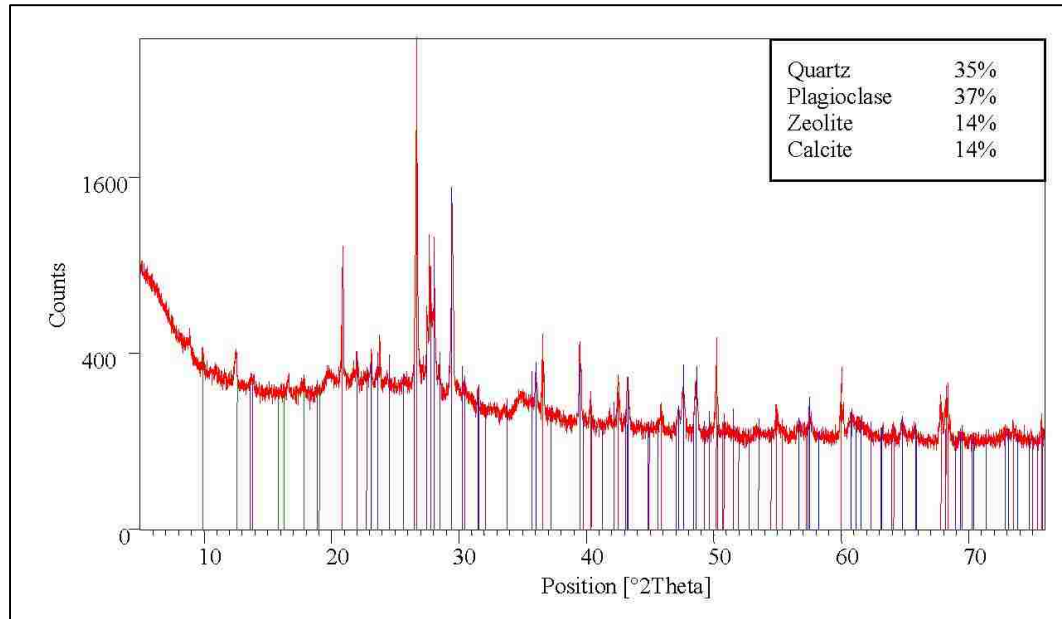


Figure 5. Pozzolete X-ray diffraction analysis.

- **Lassenite SR.** Class N Lassenite SR is shown in Figure 6. Lassenite SR is volcanic ash available 30 miles north of Reno, Nevada. Figure 7 shows the X-ray diffraction analysis (XRD) of Lassenite SR.



Figure 6. Lassenite SR.

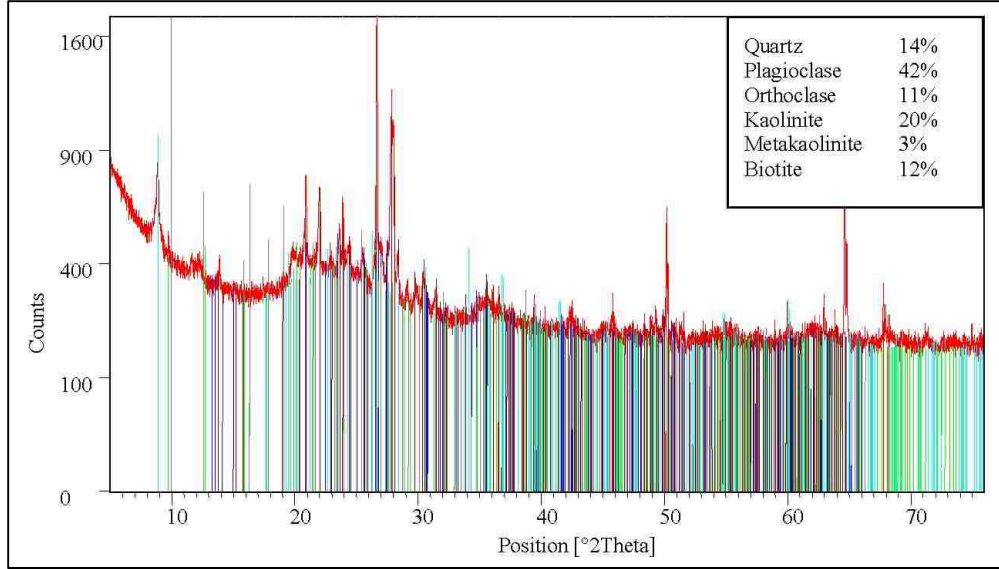


Figure 7. Lassenite SR X-ray diffraction analysis.

Table 1. ASTM C 618 (2003) requirements for class N pozzolan.

	ASTM C 618	Pozzolete	Lassenite SR
SiO <sub>2</sub> , %	-	67.83	72.22
Al <sub>2</sub> O <sub>3</sub> , %	-	11.01	16.09
Fe <sub>2</sub> O <sub>3</sub> , %	-	1.86	4.84
Oxide Sum,%	Min. 70	80.70	93.15
So <sub>3</sub> , %	Max. 04	-	0.34
H <sub>2</sub> O, %	Max. 03	2.81	2.19
LOI, %	Max. 10	9.73	5.89
Amount retained on No 325, %	Max. 34	-	32.90
28 days activity index, % of control	Min. 75	80	82
Specific gravity	-	2.29	2.50

Table 2. Pozzolete and Lassenite SR X-ray fluorescence spectroscopy.

Oxide	Pozzolete	Lassenite SR	Element	Detection limit	Pozzolete	Lassenite SR
	wt%				(ppm)	
SiO <sub>2</sub>	67.83	72.22	Sc	5	13	12
Al <sub>2</sub> O <sub>3</sub>	11.01	16.09	V	5	27	134
TiO <sub>2</sub>	0.241	0.596	Ni	-	9	11
Fe <sub>2</sub> O <sub>3</sub>	1.86	4.84	Cu	-	13	48
MgO	4.24	1.13	Ga	5	15	21
Na <sub>2</sub> O	2.75	4.21	Rb	5	148	75
K <sub>2</sub> O	4.16	1.76	Sr	5	603	283
MnO	0.078	0.066	Y	5	38	14
CaO	8.16	2.08	Zr	5	173	159
P <sub>2</sub> O <sub>5</sub>	0.073	0.172	Nb	5	23	7
Total	100.40	103.16	Ba	20	316	627
			La	20	7	29
			Hf	5	7	6
			Pb	10	49	15
H <sub>2</sub> O-	2.81	2.19	Th	10	19	14
H <sub>2</sub> O+	8.21	3.70	U	5	1	6

**2.3.3 Portland cement.** Commercial type II/V portland cement meets the ASTM C 150 (2004) specifications was used. The cement was supplied by a local concrete ready-mix plant. Important properties of the cement are given in Table 3.

Table 3. Portland cement properties.

Oxide (%)	Portland Cement
Specific gravity	3.15
SiO <sub>2</sub>	20.64
Al <sub>2</sub> O <sub>3</sub>	3.40
Fe <sub>2</sub> O <sub>3</sub>	3.40
CaO	63.50
MgO	4.70
SO <sub>3</sub>	2.40
Na <sub>2</sub> O	0.46
LOI %	1.20

**2.3.4 Water.** Tap-water with temperature 70±3°F was used.

**2.3.5 Super-plasticizer or high range water-reducer.** Two types of super-plasticizer were used separately, ADVA 380 and EUCON 37. Both super-plasticizers comply with ASTM C 494 (2004) requirements. Properties of the super-plasticizers are shown in Table 4.



Table 4. Super-Plasticizers properties.

Property	ADVA 380	Eucon 37
State of Matter	Liquid	Liquid
Added Chloride	No	No
Color	Brown	Brown
Weight per Gallon	8.9 lb/gal	10.03 lb/gal
Base	Polycarboxylate Polymer	Naphthalene Sulfonate
PH	5-7	8-10
Recommended Dosage	4-16 fl oz/100 lbs of cement	6-18 fl oz/100 lbs of cement

## 2.4 Phase 1 Standard Tests

Several standardized tests were followed to evaluate the properties of the raw materials as well as fresh concretes properties and hardened concretes properties. These tests included:

**2.4.1 X-ray fluorescence spectroscopy (XRF).** Samples of class N pozzolan and class F fly ash were sent to the Geoscience Department at the University of Nevada, Las Vegas to perform the XRF analyses. The XRF analyses were performed using a PANalytical Axios advanced sequential X-ray fluorescence spectrometer shown in Figure 8. The major and trace elements in the pozzolans were identified using this test.



Figure 8. X-ray fluorescence spectrometer, (Retrieved from unlv.edu).

**2.4.2 X-ray diffraction analysis (XRD).** Samples of class N pozzolans and fly ash were sent to the Geoscience Department at the University of Nevada, Las Vegas to perform the XRD analyses. Quantitative analyses at position  $2^\circ$  Theta for class N pozzolan and class F fly ash were performed using a PANalytical X'PERT Pro X-ray diffraction spectrometer shown in Figure 9. The atomic structure of the minerals was analyze to find information about the crystal structure of class N pozzolan and class F fly ash used in this thesis.



Figure 9. X-Ray diffraction spectrometer, (Retrieved from unlv.edu).

**2.4.3 Compressive strength test of mortar cubes.** Mortar cubes compressive strength was tested for all mortar mixtures at previously specified ages. All specimens used in the test were 2x2x2 inch. The ultimate resisted load was determined following ASTM C 109/C 109M (2002) and using a hydraulic operated machine. See Figure 10. The loading rate ranged between 200 and 400 lb/sec. The compressive strength computed using the following equation:

$$\text{Compressive Strength (psi)} = P/A$$

Where: P: Maximum applied load (lb)

A: Specimen cross-sectional area (in<sup>2</sup>)

The average of three tests on specimens from the same batch was reported.



Figure 10. Mortar cube compressive strength test.

**2.4.4 Strength activity index with portland cement.** Standard portland cement mortars and mortars with 20% of their portland cement replaced with class N pozzolan were prepared following ASTM C 311 (2002). After 28 days of curing the compressive strength of the mortar cubes was computed following section (2.4.3). Using the compressive strength test results the pozzolan strength activity index was calculated as follows:

$$\text{Strength Activity Index} = (A/B) \times 100$$

Where: A: Average compressive strength of the standard mortar cubes

B: Average compressive strength of mortar cubes with pozzolan

**2.4.5 Slump test.** The slump test was performed on the fresh concrete to measure the concrete workability. ASTM C 143 (2003) standard was followed to perform the slump test. The American Concrete Institute (ACI) recommends concrete slump for various type of construction to be between 2-4 inches which can be increased when chemical admixtures are used (ACI 211.1, 1991). Hence, the concrete slump for all

mixtures was maintained to be between 3-5 inches. The slump test is illustrated in Figure 11.



Figure 11. Concrete slump test.

**2.4.6 Air content test.** The air content test was performed on the fresh concrete following the pressure method presented in ASTM C 231 (2003) standard using air meter type B. The ACI recommends approximate air content for concrete depending on concrete slump and the nominal aggregate size used in concrete (ACI 211.1, 1991). The nominal aggregate size of the present study is  $\frac{3}{4}$  inch. Hence, an air content of less than 2.0% was observed for all concrete mixtures. Air content test setting is shown in Figure 12.



Figure 12. Air meter type B.

**2.4.7 Concrete unit weight Test.** The fresh concrete unit weight was computed following ASTM C 138 (2001) standard. A steel container of a known volume and weight was filled with concrete. The concrete was placed in three layers of approximately equal volume. Each layer was tamped 25 times with the tamping rode. The test setting is demonstrated in Figure 13. The unit weight was computed as follows:

$$\gamma_c = (M_c - M_m) / V_m$$

Where:  $\gamma_c$ : Concrete Unit Weight lb/ft<sup>3</sup>

$M_c$ : Mass of the Container filled with concrete (lb)

$M_m$ : Mass of the Container (lb)

$V_m$ : Volume of the Container (ft<sup>3</sup>)



Figure 13. Concrete unit weight test preparation.

**2.4.8 Temperature of freshly mixed concrete (Adiabatic temperature).** The temperature of the fresh concrete was monitored according to ASTM C 1064 (2003) standard. A data logger and thermocouples were used and the temperature was recorded in 3 minutes intervals for at least 44 hours. The thermocouples were inserted in the middle of 6x12 inches cylindrical specimen to insure a 3” concrete cover around the thermocouples end. The specimens were sealed and stored at room temperature  $73\pm 3^{\circ}\text{F}$ . The collected data then was evaluated using computer software. The average of two tests on specimens from the same batch was reported for each mixture. Figure 14 shows the adiabatic temperature test setting.



Figure 14. Temperature of freshly mixed concrete test setting.

**2.4.9 Compressive strength test of cylindrical concrete specimens.** All the concrete specimens used in the compressive strength tests were 4x8 inch cylindrical specimens. Before performing the compressive strength test the specimens were capped using either unbounded caps in according to ASTM C 1231 (2000), or using sulfur mortar following ASTM C 617 (1998). See Figure 15. Specimen capping method was chosen according to the age of concrete and the expected strength. When sulfur capping was used, the specimens were left to harden for at least 16 hours before testing. The ultimate resisted load was determined according to ASTM C 39 (2003) using a hydraulic operated machine, shown in Figure 16. The loading rate ranged between 20 and 50 psi/sec. The compressive strength was computed using the following equation:

$$\text{Compressive Strength (psi)} = P/A$$

Where: P: Maximum applied load (lb)

A: Specimen cross-sectional area (in<sup>2</sup>)

The average of three tests on specimens from the same batch was reported.





Figure 15. Sulfur capping preparation.



A- Test with unbounded capping

B- Test with sulfur capping

Figure 16. Cylindrical concrete specimens' compressive strength test setting.

**2.4.10 Splitting tensile strength test.** The concrete splitting tensile strength test was performed using 4x8 inch cylindrical specimens. The specimens were cured for 28 days before testing. The test was performed following ASTM C 496 (2004). A hydraulic operated machine was used to measure the maximum load that can be applied on the specimen. See Figure 17. The loading rate was 100 to 200 psi/min. The splitting tensile strength was computed using the following equation:

$$T=2P/(\pi ld)$$

Where: T= Tensile strength (psi)

P= Maximum applied load (lb)

l= Specimen length in inch

d= Specimen diameter in inch

The average of three tests performed on specimens from the same batch was reported.



Figure 17. Concrete splitting tensile strength test setting.

**2.4.11 Static modulus of elasticity Test.** The static modulus of elasticity test for concrete in compression was performed on 4x8 cylindrical concrete specimens. The test was performed on the concrete after 28 days of curing. The test was performed according to ASTM C 469 (2002). A compressometer with a digital gage was used to measure the deformation and a hydraulic operated machine was used to apply the compression load. See Figure 18. The loading rate was  $35 \pm 5$  psi/s. The strain was recorded at each 2000 lb increase in loading. The test was stopped when the load reached 40% of that recorded as the ultimate load during the 28 days compressive strength test. The static modulus of elasticity was computed using the following equation:

$$E = S/\epsilon$$

Where: E= Static modulus of elasticity (psi)

S= Stress corresponding to 40% of ultimate load (psi)

$\epsilon$  = longitudinal strain produced by S stress

The average of three tests performed on specimens from the same batch was reported.



Figure 18. Concrete static modulus of elasticity test setting.

**2.4.12 Dynamic Young's modulus of elasticity Test.** The concrete dynamic Young's modulus of elasticity was tested using E-meter MK II and following ASTM C 215 (2002). After 28 days of curing, the test specimens' dimensions were measured and their masses were computed. The information was entered in the E-meter. During the test the specimen was supported so that it can freely vibrate in the longitudinal direction. To test the specimen the specimen was impacted from one end and the signal was picked up from the other end. The test was repeated three times on each specimen. The average of the three readings was reported for each specimen. The average of three tests performed on specimens from the same batch was considered. The test setting is shown in Figure 19.



Figure 19. Concrete dynamic Young's modulus of elasticity using E-meter MK II.

**2.4.13 Rapid chloride ion penetration test (RCPT).** The rapid chloride penetration was performed to evaluate concrete resistance against chloride ion penetration at different ages. The RCPT was conducted following ASTM C 1202 (1997) standard. The test was performed on the concrete specimens at ages 28, 56 and 90 days. The six hours adjusted passed charged was considered because specimen were bigger than 3.75 inch in diameter. Each test was performed on two specimens from the same batch and the average of the two tests was reported. Figure 20 illustrates the test setting.



Figure 20. Concrete rapid chloride ion penetration test setting.

**2.4.14 Rapid chloride ion migration test (RMT).** The concrete rapid migration test was performed according to the procedure proposed by Luping and Nilsson (1993). The test was performed to physically evaluate the ion migration through the concrete specimen. After the RCPT specimens were removed from testing cells, they rinsed with tap-water and split in half using a diamond saw. Each half then was sprayed with silver nitrate ( $\text{AgNO}_3$ ) which forms a white precipitate of silver chloride after 5 minutes. This white mark represents the chloride ion penetration depth. Ten reading of the penetration depth were taken. The average and maximum penetration depth were reported. Figure 21 shows specimen after the RMT.



Figure 21. Specimen after rapid chloride ion migration test.

## 2.5 Investigating the use of Pozzolete in Concrete

The following two sections will present the methodology and testing results for concrete incorporating volcanic pozzolan. Test results for all mixtures will be compared and pozzolan performance will be discussed.

### 2.5.1 Methodology.

**2.5.1.1 Concrete proportion.** Pozzolete was used as a partial replacement of OPC in four different percentages (0%, 10%, 20% and 30%) by mass. The mixture proportion was designed following ACI proportioning method presented in ACI 211.1 (1991). To maintain workable mixture, ADVA 380 super-plasticizer was used. Suitable amount of the super-plasticizer (SP) was used for each mixture in order to maintain a similar workability. Because Pozzolete had a great impact on concrete workability, several trial mixtures were mixed to adjust the amount of SP for each mixture. Table 5 presents all four mixtures and their proportion by mass per cubic yard of concrete.

Table 5. Details of concrete mixtures and their proportions by mass per cubic yard of concrete.

Mixture	Cement (lb)	Pozzolete (lb)	Water (lb)	Coarse aggregate dry (lb)	Fine aggregate dry lb	Super- plasticizer (fl oz/100 lbs cement)
N1P0	858.0	00.0	342.2	1,663.6	1,242.8	3.0
N1P10	772.2	85.8	341.0	1,663.6	1,213.8	7.0
N1P20	686.4	171.6	339.7	1,663.6	1,171.0	11.0
N1P30	600.6	257.4	339.0	1,663.6	1,142.6	13.0

**2.5.1.2 Mixing procedure.** The same mixing procedures and times were followed in preparing all concrete mixtures. An electrical powered steel drum mixer was used to mix the concrete. The mixer is shown in Figure 22.



Figure 22. Steel drum mixer.

All materials were weighted according to their proportion and placed next to the mixer before the mixing procedure started. The mixing procedure is shown in Figure 23.

In the case of the control mixture (concrete was made without the use of pozzolan) the rest of the water was added with the super-plasticizer and mixed for 4 minutes. The total mixing time was maintained to be 12 minutes. Specimens were prepared following ASTM C 192 (2002).

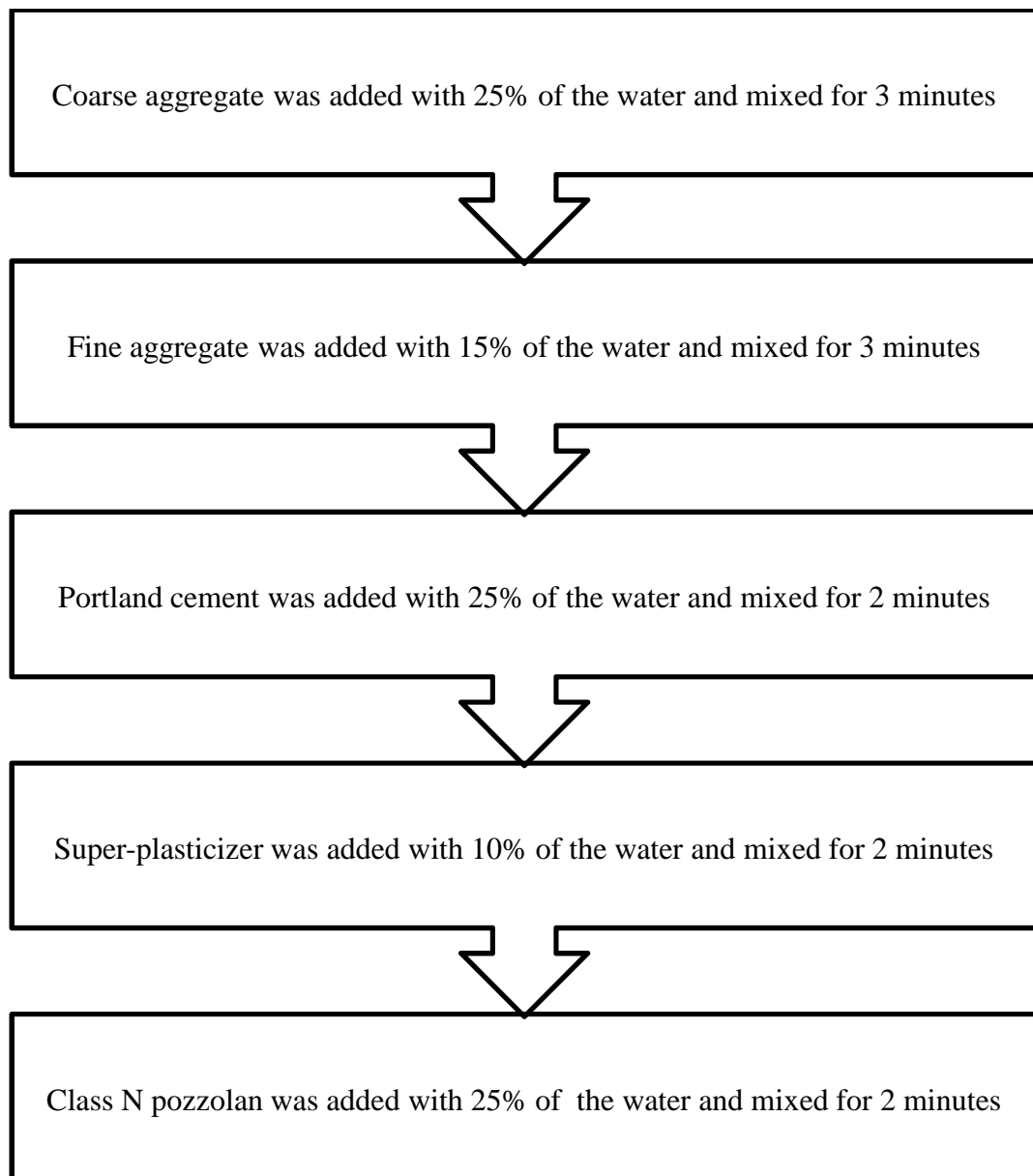


Figure 23. Concrete mixing procedure.

**2.5.1.3 Testing.** A slump test was conducted on each trial and final concrete mixture following section 2.4.5. To insure similar concrete workability almost a constant slump (3 to 3.5 inch) was maintained for all concrete mixtures. The air content test was performed on the fresh concrete following the pressure method presented in section 2.4.6 and the fresh concrete unit weight test was performed according to section 2.4.7. The temperature of freshly mixed concrete was monitored according to the procedure presented in section 2.4.8. Cylindrical concrete specimens of diameter 4 inch and height of 8 inch were prepared according to ASTM C 192 (2002) to be used in other tests. The 4x8 inch cylindrical specimens were covered immediately after molding to prevent water lost and kept for 24 hours at room temperature in a vibration free environment. The next day the specimens were removed from the molds and placed in a curing room with relative humidity of around 98% and temperature of  $73\pm 3^{\circ}\text{F}$  until testing time. Concrete compressive strength was tested for all the mixtures at ages 3,7,28, 90,180 and 360 days following the procedure prescribed in section 2.4.9. The specimens were capped using unbounded caps for compressive strength tests at early ages (3 and 7 days) and sulfur capping at later ages (28 days and older). The splitting tensile strength test and static modulus of elasticity test were performed on all mixtures following sections 2.4.10 and 2.4.11 respectively. The dynamic Young's modulus of elasticity was tested according to section 2.4.12. The rapid chloride penetration test was performed according to section 2.4.13 and the rapid migration test was performed following section 2.4.14.



**2.5.2 Test results and discussions.** The following sections will presents the results of all tests performed on concrete incorporating Pozzolete and their control mixture.

**2.5.2.1 Fresh concrete properties.** Table 6 presents the concrete fresh properties. As shown in Table 6 there was insignificant decrease in concrete unit weight with the increase of Pozzolete. On the other hand, there was insignificant increase in concrete air content with the increase of pozzolan. This comes in agreement with the finding of Irassar et al. (1996). Table 5 shows increase in the amount of super-plasticizer associated with increase of Pozzolete percentage. The use of more super-plasticizer to maintain workable concrete is a result of the negative effect of Pozzolete on concrete workability.

Table 6. Fresh concrete properties.

Mixture	Unit weight lb/ft <sup>3</sup>	Air content %	Slump (in)
N1P0	155.60	1.8	3.5
N1P10	155.20	1.8	3.5
N1P20	154.80	2.1	3.0
N1P30	153.60	2.1	3.0

**2.5.2.2 Temperature of the freshly mixed concrete (Adiabatic temperature).**

Figure 24 presents the changes in the adiabatic temperature with time for the first 44 hours for all four concrete mixtures. As shown in Figure 24, the temperature increased during acceleration and setting period until reached a peak temperature then started to decrease. Figure 24 also shows that all mixtures reached their peak temperature, which can be an indicator of the hydration reaction, in 12-14 hours. Compared to its control mix

(N1P0), the concrete mixture with 10% Pozzolete (N1P10) showed similar peak temperature but at an earlier time. Whereas the mixture with 20% Pozzolete (N1P20) showed a lower peak temperature almost two hours after the N1P0, and the mixture with 30% Pozzolete (N1P30) showed the lowest peak temperature compared to the control mixture. This is an indicator of the lower reactivity of Pozzolete compare to OPC. Hence the peak temperature decreases with the increase of Pozzolete in concrete. Figure 24 shows that the reduction in temperature after reaching the peak temperature for mixtures containing Pozzolete is slower than the control mix which indicates the existence of the hydration reaction for a longer time period for mixtures containing Pozzolete. Hence mixtures containing Pozzolete have a lower cooling slope. This seems to agree with the finding of ACI 232.1R (2000); Nili and Salehi (2010); Shannag and Yeginobali (1995) and Twonsend (1966).

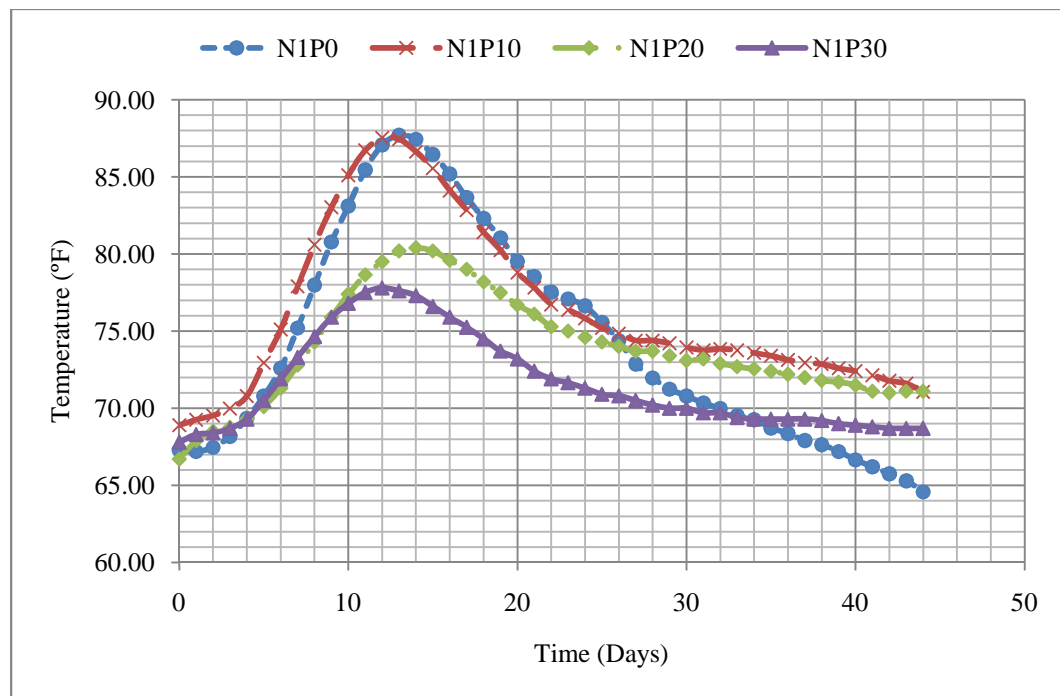


Figure 24. Change in adiabatic temperature for different mixtures.

**2.5.2.3 Compressive strength.** Table 7 presents the average compressive strength reported to the nearest 10 psi of at least 3 specimens from the same batch for all four mixtures at different ages. The standard deviation of the tested specimens at different ages ranged between 9 and 485 psi. As presented in Table 7, the use of Pozzolete in concrete caused a reduction in concrete compressive strength at all ages. This comes in agreement with the reduction in reactivity that follows the increase of Pozzolete in concrete discussed in section 2.5.2.2. However, all concrete mixtures showed compressive strength higher than 7850 psi at the age of 28 days. In general all mixtures continued to gain strength with age. Figure 25 shows the development of the compressive strength with time for all four mixtures and Figure 26 illustrates the relationship between the percentages of Pozzolete and concrete compressive strength at ages 28, 90, 180 and 360 days. The reduction in concrete compressive strength with the use of Pozzolete comes in agreement with the finding of these studies (Khan & Alhozaimy, 2005, 2011; López & Castro, 2010; Naseer et al., 2008; Nili & Zaheri, 2011; Sideris & Savva, 2001).

Table 7. The average compressive strength and 28 days splitting tensile strength.

Pozzolete %	Compressive strength (psi)						Splitting tensile strength at 28 days (psi)
	Time (days)						
	3	7	28	90	180	360	
0	5,500	7,140	9,030	10,330	11,490	12,410	890
10	5,450	6,510	8,180	9,900	10,290	12,150	855
20	5,150	6,360	8,040	9,590	9,820	10,970	835
30	4,460	5,850	7,890	8,920	9,620	10,460	810

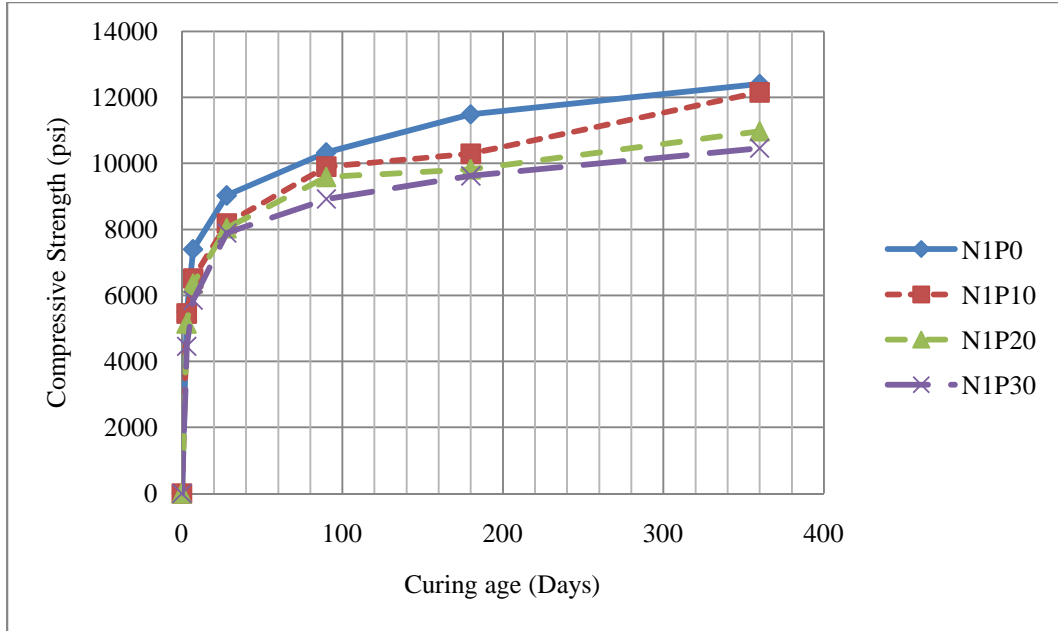


Figure 25. Relationship between concrete compressive strength and the curing age.

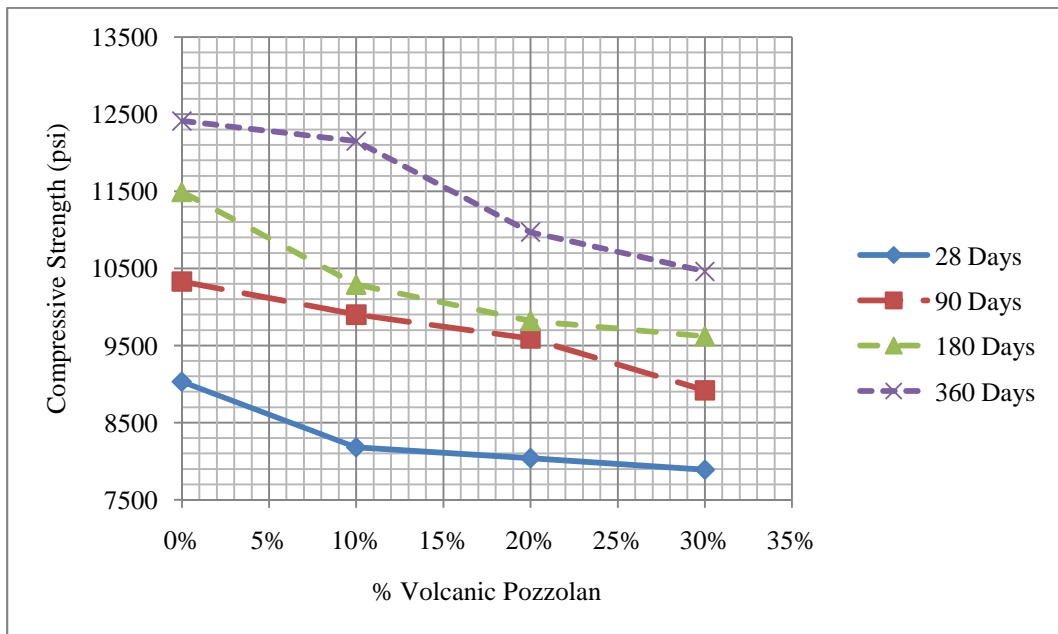


Figure 26. Relationship between the percentages of Pozzolete and concrete compressive strength at different curing age.

**2.5.2.4 Splitting tensile strength and modulus of elasticity.** The 28 days splitting tensile strength results for all mixture is presented in Table 7. The 28 days splitting

tensile strength followed the same trend as the compressive strength and decreased with the increase of Pozzolete as illustrated in Figure 27. This finding is in agreement with the finding of Shannag and Yeginobali (1995). All concretes exhibited a splitting tensile strength close to 10% of their compressive strength. Likewise, the static and young's modulus of elasticity at the age of 28 days decreased with the increase of Pozzolete.

Table 8 presents the results of the Static and young's modulus of elasticity.

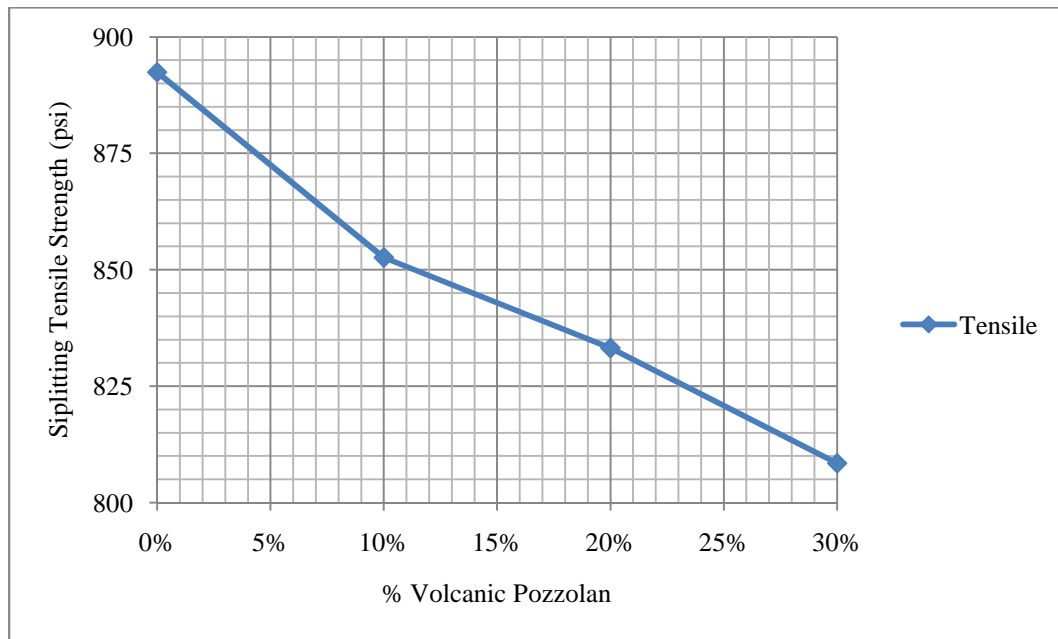


Figure 27. Relationship between the percentages Pozzolete and concrete splitting tensile strength at 28 days.

Table 8. Concrete modulus of elasticity.

Mixture	Static modulus of elasticity (Gpa)	Young's modulus of elasticity (Gpa)
N1P0	27.8	26.1
N1P10	25.4	21.9
N1P20	24.6	21.6
N1P30	23.9	21.5

### ***2.5.2.5 Rapid chloride ion permeability test and rapid chloride ion migration***

*test.* The RCPT and RMT were conducted following section 2.4.13 and 2.4.14 respectively. The test results for ages 28, 56 and 90 days are presented in Table 9. The penetrability was evaluated according to the adjusted charge passed, the average physical penetration and maximum physical penetration. The 28 days RCPT and RMT results show increase in adjusted charge passed, average penetration and maximum penetration with the increase of the Pozzolete. This increase in early age permeability is in agreement with the finding of Khan and Alhozaimy (2005, 2011). At the age of 56 days all concretes showed better chloride ion penetration resistance and the improvement was more noticeable for concretes with higher percentage of Pozzolete. Furthermore, concrete with 10% Pozzolete shows lower chloride ion penetration depth than the control mix. As the curing time increased the resistance to chloride ion penetration continued to improve. Although concretes with higher percentages of Pozzolete showed better penetrability evaluation at the age of 90 days, starting at 56 days for N1P10 and N1P20, their penetration depth is relatively higher than the control mix. In general the chloride ion penetration decreased with the increase of the curing time for all mixtures as shown in Figure 28. The gap in adjusted charge passed, the average physical penetration and maximum physical penetration between mixtures with different percentages of Pozzolete relatively dissipated after 90 days.

Table 9. RCPT and RMT results.

Test age	Mixture	N1P0	N1P10	N1P20	N1P30
28 days	Adjusted charge passed (coulombs)	2,944	4,222	4,282	4,237
	Penetrability evaluation (ASTM C 1202, 1997)	Moderate	High	High	High
	Ave. penetration depth (in)	0.66	0.85	0.99	1.02
	Max. penetration depth (in)	1.10	1.12	1.2	1.50
56 days	Adjusted charge passed (coulombs)	2,334	2,301	2,290	2,673
	Penetrability evaluation (ASTM C 1202, 1997)	Moderate	Moderate	Moderate	Moderate
	Ave. penetration depth (in)	0.52	0.50	0.59	0.77
	Max. penetration depth (in)	0.83	0.9	0.94	0.82
90 days	Adjusted charge passed (coulombs)	2,214	2,094	1,787	1,745
	Penetrability evaluation (ASTM C 1202, 1997)	Moderate	Moderate	Low	Low
	Ave. penetration depth (in)	0.45	0.42	0.59	0.5
	Max. penetration depth (in)	0.73	0.76	0.83	0.7

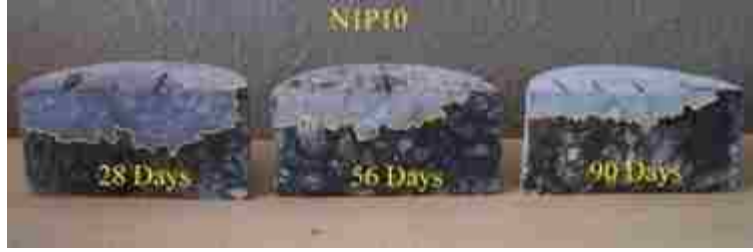


Figure 28. RMT for N1P10 specimens at 28, 56, and 90 days.

## 2.6 Investigating the use of Lassenite SR in Concrete

The methodology and testing results for mixture containing Lassenite SR pozzolan will be presented in the following sections. These results will be compared to test results of a control mixture containing no pozzolan and the performance of concrete containing Lassenite SR pozzolan will be evaluated.

### 2.6.1 Methodology.

**2.6.1.1 Concrete proportion.** Lassenite SR class N pozzolan has a big impact on concrete workability. Hence, low dosage (5%) of Lassenite SR was used in this study as a partial replacement of OPC in concrete. Concrete mixture containing 5% Lassenite SR was prepared (NP5) and its properties was compared to a control mixture that was made without pozzolan (NP0). The mixture proportion was designed following ACI proportioning method presented in ACI 211.1 (1991). EUCON 37 high range water-reducing admixture was use to maintain workable mixture. The proportions of both mixtures by mass per cubic yard of concrete are presented in Table 10.



Table 10. Details of concrete mixtures and their proportions by mass per cubic yard of concrete.

Mixture	Cement (lb)	Lassenite SR (lb)	Water (lb)	Coarse aggregate dry (lb)	Fine aggregate dry (lb)	Super- plasticizer (fl oz/100 lbs Cement)
NP0	858.0	-	342.2	1,663.6	1,243.2	4
NP5	815.1	42.9	337.4	1,663.6	1,231.0	16

**2.6.1.2 Mixing procedure.** The mixer prescribed in section 2.5.1.2 was used to prepare the concrete. The same mixing time was followed to prepare both mixtures. All materials were proportioned according to their mass and placed next to the mixer before the mixing procedure starts. The mixing procedure is illustrated in Figure 29.

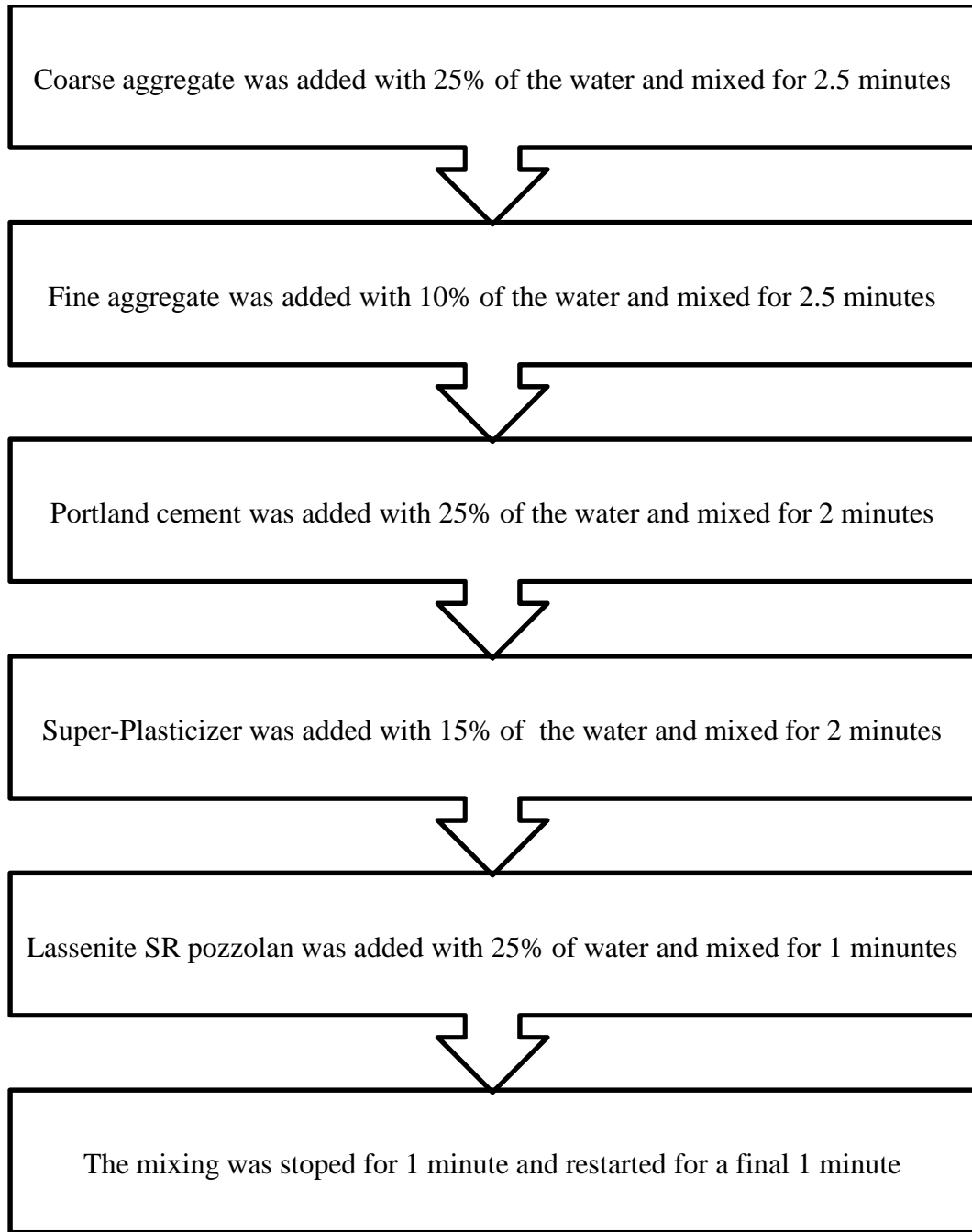


Figure 29. Concrete mixing procedure.

**2.6.1.3 Testing.** Fresh concrete properties and hardened concrete properties were evaluated following the same testing procedure prescribed in section 2.5.1.3. The tests results are presented and discussed in the following sections.

**2.6.2 Test results and discussion.** The tests results of concrete incorporating Lassenite SR class N pozzolan will be presented in the following sections and compared to the tests results of a control mixture containing no pozzolan.

**2.6.2.1 Tests for the fresh concrete properties.** The fresh concrete unit weight, air content, and slump were tested to evaluate the fresh concrete properties. Table 11 presents the fresh concrete properties tests results for NP5 and NP0. As presented in Table 11, Lassenite SR did not affect concrete unit weight and air content. Concrete workability, on the other hand, was significantly reduced when Lassenite SR was used. Hence, a large amount of super-plasticizer was used to produce a workable mixture.

Table 11. Fresh concrete properties.

Mixture	Unit weight lb/ft <sup>3</sup>	Air content %	Slump (in)
NP0	155.60	1.8	3.5
NP5	155.55	1.8	5.0

**2.6.2.2 Temperature of the freshly mixed concrete (Adiabatic temperature).** To study the effect of Lassenite SR on concrete heat of hydration the change in the adiabatic temperatures of two specimens from the same batch was recorded and averaged for each mixture and plotted against time as shown in Figure 30. After the temperature of both mixtures increased during the acceleration and setting period, they reached their peak then the temperature started to decrease gradually until relatively constant temperature was recorded. As shown in Figure 30 NP0 reached its peak temperature two hours before NP5. Moreover, the peak temperature of NP0 was 0.5 degree higher than the peak temperature of the NP5. Hence, Lassenite SR caused a reduction in concrete reactivity,

which reduces concrete heat of hydration. Both concretes had the same cooling slope for the first 10 hours after NP5 peak, followed by a lower temperature for NP5 than NP0 for the rest of the testing period. This lower cooling temperature is evidence of the lower reactivity of the pozzolan. The reduction in the heat of hydration with the use of Lassenite SR comes in agreement with the findings of previous studies by ACI 232.1R, (2000); Nili and Salehi (2010); Shannag and Yeginobali (1995) and Twonsend (1966).

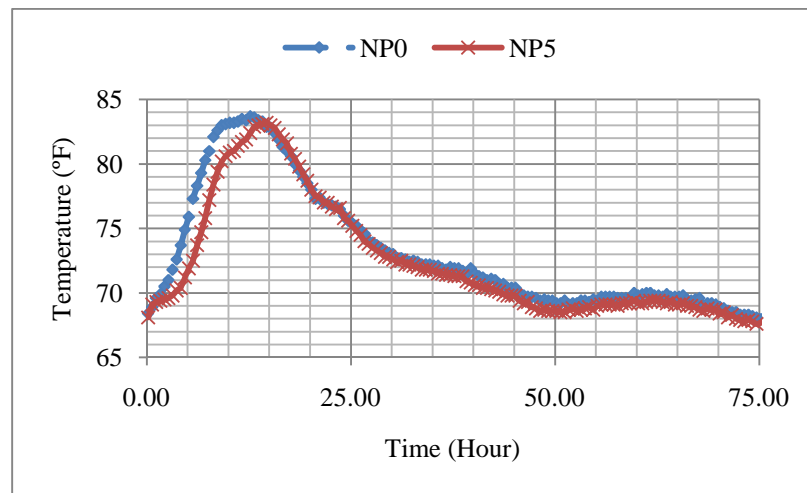


Figure 30. Change in adiabatic temperature for different mixtures.

**2.6.2.3 Concrete strength and modulus of elasticity.** Table 12 presents the average compressive strength, splitting tensile strength and modulus of elasticity for both mixtures. It can be noted that Lassenite SR improved concrete strength at early ages. The increase in compressive strength at 3 days was 36.7%. At 7 days NP5 continue to show higher compressive strength than the control mix by 20.0%. It should be noted that the gap in compressive strength that results between the two mixtures decreases with time. After 28 days of curing NP5 shows only 4.2% higher compressive strength than its conventional mix. At 90 days of curing specimens from both mixtures yielded similar

compressive strength. At the age of 180 days the control mix shows 490 psi increase in compressive strength over NP5. The development of compressive strength is illustrated in Figure 31. Note that both concretes continue to gain strength with time.

The splitting tensile strength of NP5 was 15.7% higher than that of its conventional mix. The splitting tensile strength of both concretes was around 10% of their compressive strengths. Lassenite SR had no major effect on concrete modulus of elasticity. It should be noted that the improvement in concrete early strength is a result of less porous concrete with stronger binding paste produced by using both Lassenite SR and the super-plasticizer. The increase in concrete strength with the use of class N pozzolan supports the finding of Ballard et al. (2008); Chen et al. (1993) and Tagnit-Hamou et al. (2003). Figure 32 illustrates the tensile strength for both mixtures.

Table 12. The average compressive strength and splitting tensile strengths.

Mixture	Compressive strength (psi)					Splitting tensile strength at 28 days (psi)	Static modulus of elasticity (Gpa)
	Time (days)						
	3	7	28	90	180		
NP0	5,500	7,140	9,030	10,330	11,490	890	27.8
NP5	7,520	8,570	9,410	10,340	11,000	1,030	27.2

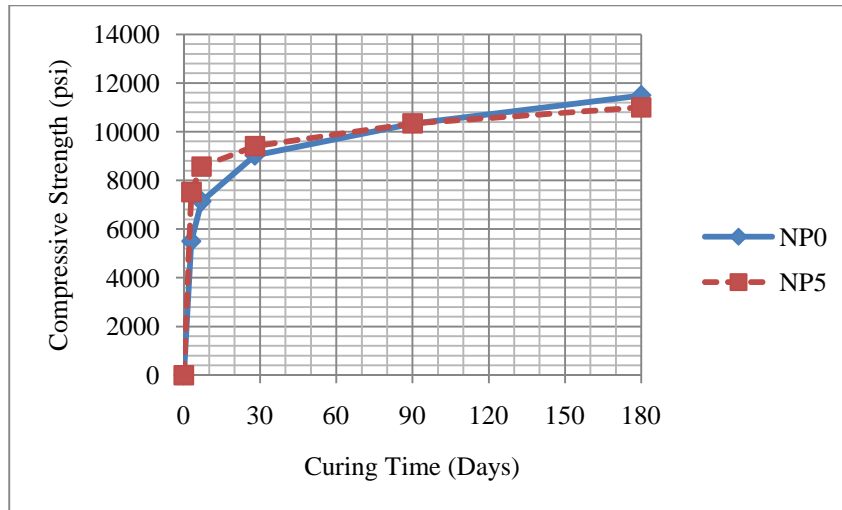


Figure 31. Relationship between concrete compressive strength and the curing age.

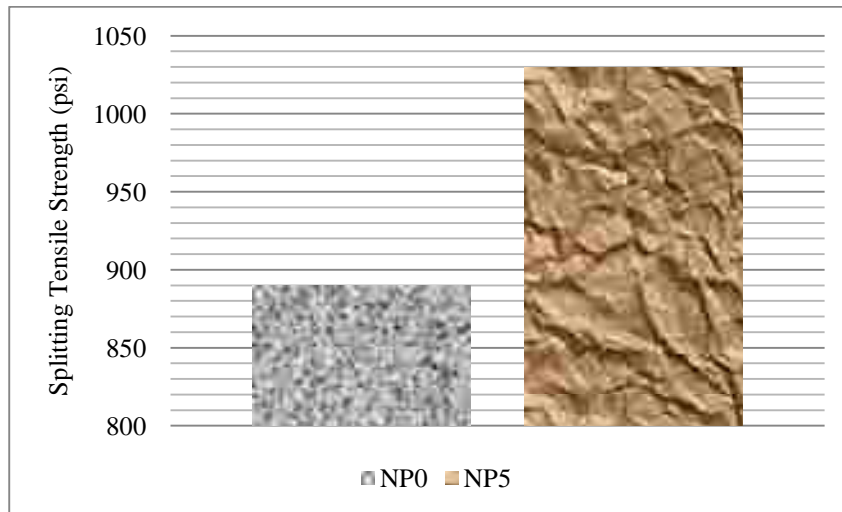


Figure 32. Concrete splitting tensile strength.

#### 2.6.2.4 Rapid chloride ion permeability test and rapid chloride ion migration

*test.* Table 13 presents the RCPT and RMT tests results for both mixtures at ages 28, 56 and 90 days of curing. Specimen penetrability was evaluated according to ASTM C 1202 (1997) adjusted charged passed and RMT average and maximum physical penetration. From Table 13 it can be projected that the use of Lassenite SR caused a major increase in concrete resistance to chloride ion penetration. The control mixture (NP0) reported a

moderate penetration according to ASTM C 1202 (1997) at the age of 28 days while concrete containing NP5 reported a low penetration at the same age. Furthermore, the use of Lassenite SR caused 0.31 inch reduction in the average physical penetration and 0.44 inch reduction in the maximum penetration. Unlike NP0, there were no major changes in the rapid chloride penetration resistance for NP5 even after 90 days of curing. Concrete containing Lassenite SR pozzolan showed better resistance to rapid chloride ion penetration at all ages. See Figure 33.

Table 13. RCPT and RMT results.

Test age	Mixture	NP0	NP5
28 days	Adjusted charge passed (coulombs)	2,944	1,703
	Penetrability evaluation (ASTM C 1202, 1997)	Moderate	Low
	Ave. penetration depth (in)	0.66	0.35
	Max. penetration depth (in)	1.10	0.66
56 days	Adjusted charge passed (coulombs)	2,334	1,736
	Penetrability evaluation (ASTM C 1202, 1997)	Moderate	Low
	Ave. penetration depth (in)	0.52	0.36
	Max. penetration depth (in)	0.83	0.50
90 days	Adjusted charge passed (coulombs)	2,214	1,364
	Penetrability evaluation (ASTM C 1202, 1997)	Moderate	Low
	Ave. penetration depth (in)	0.45	0.36
	Max. penetration depth (in)	0.73	0.50



Figure 33. NP0 and NP5 Chloride ion penetration depths at 28 days.



## **PHASE 2: Synthesizing Geopolymer Mortars**

### **3.1 Overview**

The use of ordinary portland cement (OPC) as the primary binder in concrete is conventional. However, it is associated with several disadvantages as mentioned in chapter 1. In recent years a special attention was directed to reduce or eliminate the use of OPC in construction. The alternative should be a high performance material with low impact on the surrounding environment and can be produced at a reasonable cost. Synthesizing geopolymer, which is the focus of this chapter, could be the path to achieve this objective.

In this phase of the thesis, two types of geopolymer mortars are synthesized in an attempt to create OPC free mortars. The first geopolymer is manufactured using fly ash as the base material. The fly ash is used because it is a byproduct material, which makes the geopolymer a sustainable product. The second geopolymer is created using class N pozzolan as a base material. The class N pozzolan used in this phase is a highly reactive metakaolin commercially known as Optipozz. The metakaolin was used because it is a material of geological origin, which makes the geopolymer an environmentally friendly product. The geopolymer mortars properties are evaluated before and after they were exposed to 800°C following several standardized tests.

### **3.2 Literature Review**

When the portland cement is mixed with water to create portland cement binder, the main product of the reaction are the calcium-silicate-hydrate (C-S-H) gels (Taylor, 1986). The portland cement binder chemical, physical and mechanical properties depend

on the C-S-H gels (Fernández-Jiménez, Pastor, Martín, & Palomo, 2010). Unlike portland cement binder, geopolymer properties depend on the silicon-oxo-aluminate (Si-O-Al) bond, which is known as Sialate. The geopolymer bond or the Sialate can take one of the three basic forms as a repeating unit. (Davidovits, 1999):

- Poly (sialate), [-Si-O-Al-O-].
- Poly (sialate-siloxo), [-Si-O-Al-O-Si-O-].
- Poly (sialate-disiloxo), [-Si-O-Al-O-Si-O-Si-O-].

As mentioned in chapter 1, geopolymer can be synthesized from materials contain high percentages of silicon and aluminum. Several studies used ASTM C 618 (2003) class N pozzolan to synthesize geopolymer (Bondar, Lynsdale, Milestone, Hassani & Ramezani pour, 2010, 2011a, 2011b; Duxson, 2006; Duxson, Lukey & van Deventer, 2006, 2007; Duxson, Mallicoat, Lukey, Kriven & Van Deventer, 2007; Kong, Sanjayan, Sagoe-Crentsil, 2007, 2008; Najafi Kani & Allahverdi, 2009; Najafi Kani, Allahverdi & Provis, 2011; Pacheco-Torgal, Moura, Ding & Jalali, 2011; Yip, Provis, Lukey, van Deventer, 2008; Yunsheng, Wei & Zongjin, 2008). Others recognized ASTM 618 (2003) class F fly ash to be an ideal byproduct candidate to synthesize geopolymer (Bakharev, 2006; Chindaprasirt, Chareerat & Sirivivatnanon, 2007; Doležal et al., 2006; Edouard, 2011; Fernández-Jiménez et al, 2010; Hardjito et al., 2004a, 2004b, 2005a, 2005b; Hardjito & Rangan 2005; Jirasit & Lohaus, 2005; Kong & Sanjayan, 2008, 2010; Kumar S., Kumar R., Alex, Bandopadhyay & Mehrotra, 2005; Lee, 2000; Lloyd & Rangan, 2009; Mandal, Thokchom & Roy, 2011; Palomo, Grutzeck & Blanco, 1999; Pan, Sanjayan & Rangan, 2009; Pan & Sanjayan, 2010; Rangan, Hardjito, Wallah & Sumajouw, 2005; Sumajouw, Hardjito, Wallah & Rangan, 2005; Sun, 2006; Temuujin,

Van Riessen & MacKenzie, 2010; Van Jaarsveld & Van Deventer, 1999a, 1999b; Wallah, Hardjito, Sumajouw & Rangan, 2005a, 2005b; Wallah & Rangan, 2006; Wu & Sun, 2010).

To induce the silicon (Si) and aluminum (Al) atoms in the source materials to dissolve and form the geopolymer paste, high alkaline solutions and heat curing are deployed. The reaction process of creating the geopolymer is called polymerization. The chemical reaction during the polymerization process could take 24 to 48 hours (Hardjito et al., 2004a). The alkaline solution used in the polymerization is usually a combination of sodium/potassium hydroxide (NaOH/KOH) and sodium/potassium silicate (Bakharev, 2006; Chindaprasirt, et al., 2007; Davidovits, 1999; Doležal et al., 2006; Fernández-Jiménez et al, 2010; Hardjito et al., 2004a, 2004b, 2005a, 2005b; Hardjito & Rangan 2005; Kong & Sanjayan, 2008, 2010; Kong et al., 2007, 2008; Lloyd & Rangan, 2009; Mandal et al, 2011; Palomo, Grutzeck & Blanco, 1999; Pan et al., 2009; Pan & Sanjayan, 2010; Temuujin et al., 2010; Wallah et al., 2005a, 2005b; Wallah & Rangan, 2006). Xu and Van Deventer (2000) reported higher strength for geopolymer synthesized using potassium hydroxide (KOH). An alkaline solution of potassium hydroxide and sodium silicate provides the best activator and a concentration of 5 to 7.5 M KOH dissolves the greatest amount of Al ions after breaking the Al-Si bonds in the source material (Bondar et al., 2010). The optimum ratio of the alkaline silicate solution to the alkaline hydroxide solution will depend on the types and concentrations of the alkaline solutions used.

Geopolymer shows better resistance to elevated temperatures than ordinary portland cement. Fernández-Jiménez et al. (2010) reported that portland cement strength declines radically at high temperature (400°-600°C) while alkali activated fly ash

maintains its strength or experience a higher strength when exposed to the same range of temperature for 1 hour. Metakaolin based geopolymer on the other hand retained 66% of its compressive strength after exposure to 800°C for 1 hour (Kong et al, 2007). The heat resistant of fly ash based geopolymer depends on the chemical composition of the geopolymer and the temperature for which the geopolymer will be exposed. Bakharev (2006) reported that fly ash based geopolymer prepared using sodium alkaline activator showed less heat resistant than geopolymer prepared using potassium alkaline activators. Hence, the potassium alkaline activator increases the thermal stability of the geopolymer. Alkali activated fly ash represents a perfect base for various materials to be applied at 800°C (Provis & Van Deventer, 2009). After exposing the geopolymer to 800°C for 1 hour, fly ash based geopolymer paste did not show any surface damage while metakaolin based geopolymer paste showed macro cracks of 0.1-0.2 mm (Kong et al, 2007). However, geopolymer composites (mortars and concretes) could experience thermal damages under elevated temperatures. These damages are caused by the contradicted thermal behavior between the geopolymer matrix and the aggregate (Kong & Sanjayan, 2008). In general, geopolymer composites with higher ductility will retain higher strength after exposure to high temperatures (Pan et al., 2009). Kong and Sanjayan (2010) reported that specimen size and aggregate size have a significant impact on geopolymer composite behavior at 800°C.

Another factor that could affect geopolymer properties is the curing regime. Van Dam (2010) reported that curing regime has a major impact on geopolymer properties and the optimum curing temperature depends on the source material and the alkaline solution. Increasing the curing temperature up to 75°C increased geopolymer

compressive strength; however, no significant increase in compressive strength was reported when the curing temperature increased beyond 75°C (Hardjito et al., 2004a).

Besides the curing temperature, the delay time after molding and the initial curing period are other factors that affect geopolymer strength. Delay time of 1 hour before the heat curing will increase the geopolymer strength; however, increasing the delay time more than 1 hour will have no significant effect on geopolymer strength (Chindaprasirt et al, 2007). Geopolymer subjected to longer initial curing will develop higher compressive strength (Rangan et al., 2005, Hardjito et al., 2004a).

### 3.3 Materials used in Phase 2

Each material used in this phase was taken from the same batch to reduce differences that could accompany using different batches. All materials were stored at room temperature  $73\pm 3^{\circ}\text{F}$  to maintain a constant mixing temperature.

**3.3.1 Fly ash.** The fly ash used in this study was ASTM C 618 (2003) class F fly ash supplied by a local coal plant. See Figure 34. Important properties of the fly ash were compared to ASTM requirements as presented in Table 14. The fly ash XRF is presented in Table 16 while the XRD is illustrated in Figure 35.



Figure 34. Fly ash.

Table 14. Fly ash ASTM C 618 (2003) requirements.

	ASTM C 618	Fly Ash
SiO <sub>2</sub> , %	-	58.03
Al <sub>2</sub> O <sub>3</sub> , %	-	24.85
Fe <sub>2</sub> O <sub>3</sub> , %	-	1.199
Oxide Sum, %	Min. 70	84.08
So <sub>3</sub> , %	Max. 5	0.84
H <sub>2</sub> O, %	Max. 3	0.35
LOI,%	Max. 6	1.02
Specific Gravity	-	2.35

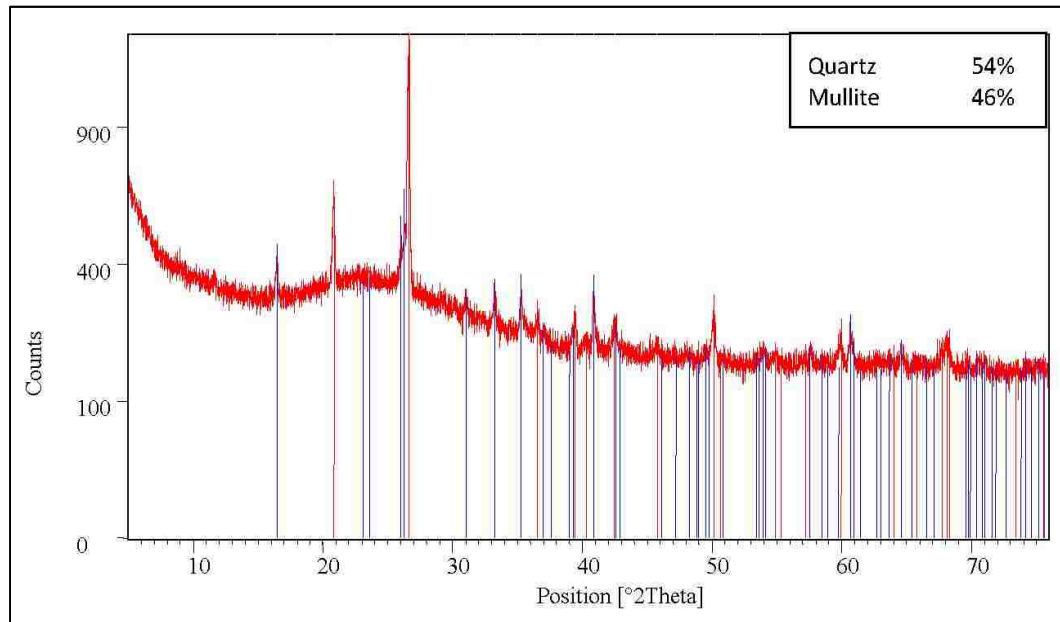


Figure 35. Fly ash X-ray diffraction analysis.

**3.3.2 Class N pozzolan.** The class N pozzolan used in this phase was Burgess Optipozz shown in Figure 36. Optipozz is high reactivity metakaolin classified as class N pozzolan under ASTM C 618 (2003). The pozzolan was supplied by Burgess Pigment. Important properties of the metakaolin were compared to ASTM requirements as presented in Table 15. The metakaolin XRF is presented in Table 16 while the XRD is illustrated in Figure 37.

Table 15. Metakaolin ASTM C 618 (2003) requirements.

Property	ASTM C 618	Metakaolin
SiO <sub>2</sub>	-	52.62
Al <sub>2</sub> O <sub>3</sub>	-	45.00
Fe <sub>2</sub> O <sub>3</sub>	-	1.391
Oxide Sum,%	Min. 70	99.01
SO <sub>3</sub> , %	Max. 4	0.34
H <sub>2</sub> O, %	Max. 3	0.25
LOI, %	Max. 10	1.43
Amount Retained on No 325, %	Max. 34	9.10
Strength Activity Index 28 days, % of control	Min. 75	85
Specific Gravity	-	2.49



Figure 36 Metakaolin.

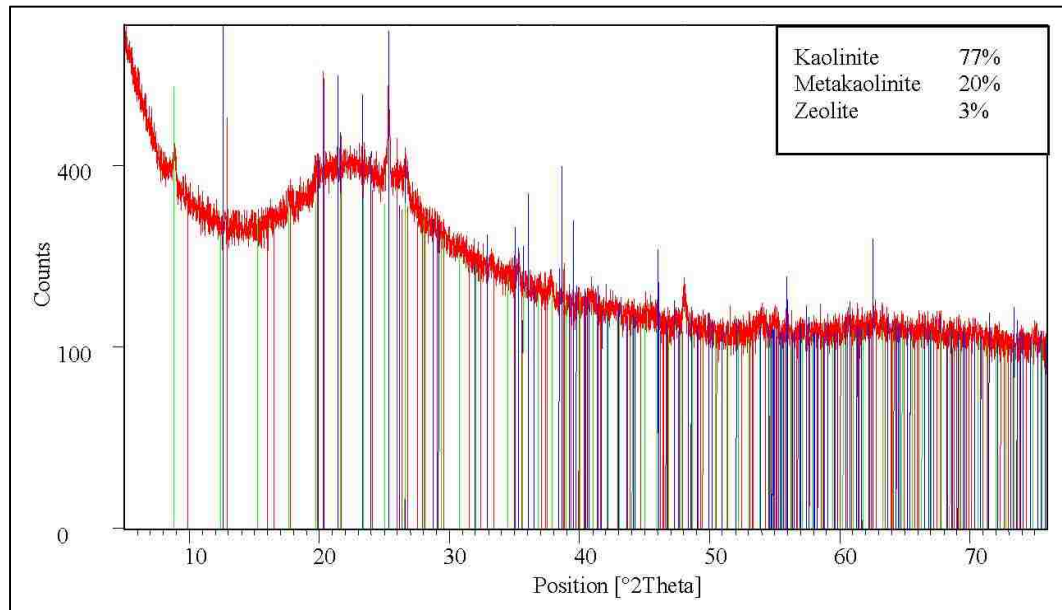


Figure 37. Metakaolin X-ray diffraction analysis.



Table 16. Fly ash and Metakaolin X-ray fluorescence spectroscopy.

Oxide	Fly ash	Metakaolin	Element	Detection limit	Fly ash	Metakaolin
	wt%				(ppm)	
SiO <sub>2</sub>	58.03	52.62	Sc	5	21	26
Al <sub>2</sub> O <sub>3</sub>	24.85	45.00	V	5	184	289
TiO <sub>2</sub>	1.199	1.391	Ni	-	29	43
Fe <sub>2</sub> O <sub>3</sub>	4.43	0.51	Cu	-	63	34
MgO	1.35	0.00	Ga	5	41	70
Na <sub>2</sub> O	2.27	0.49	Rb	5	56	11
K <sub>2</sub> O	1.10	0.25	Sr	5	1947	108
MnO	0.019	0.003	Y	5	45	13
CaO	5.36	0.12	Zr	5	410	89
P <sub>2</sub> O <sub>5</sub>	0.339	0.096	Nb	5	27	32
Total	98.95	100.48	Ba	20	3138	420
			La	20	49	74
			Hf	5	21	0
			Pb	10	46	49
H <sub>2</sub> O-	0.34	0.25	Th	10	46	33
H <sub>2</sub> O+	0.68	1.17	U	5	0	0

**3.3.3 Fine aggregate.** The fine aggregate prescribed in section 2.3.1.2 was used in this phase.

**3.3.4 Sodium silicate solution ( $\text{Na}_2\text{Si}_3\text{O}_7$ ).** A 3.22 weight ratio sodium silicate, 37.5% solution in water with PH of 11.3 and specific gravity of 10.62 lbs/gal supplied by Science Company was used.

**3.3.5 Potassium hydroxide (KOH).** Potassium hydroxide pellets with 85% minimum potassium hydroxide, 2% maximum potassium carbonate and 10-15% water were used. The potassium hydroxide was supplied by VWR International, LLC.

**3.3.6 Water.** Distilled water was used to eliminate performance disparities that accompany using tap water.

### 3.4 Phase 2 Standard Tests

Several standardized tests were followed to evaluate the properties of the raw materials, along with the properties of fresh geopolymer mortars properties and hardened geopolymer mortars properties. These tests included:

**3.4.1 Mortar flow test.** The flow of the geopolymer mortars was determined using a flow table and flow mold conforming to the requirement of specification ASTM C 230 (2003). The flow test was conducted on each geopolymer mixture following ASTM C 109 (2002). Figure 38 illustrates the flow test.



Figure 38. Geopolymer mortar flow test.

**3.4.2 Compressive strength test of geopolymer mortar cubes.** The same test prescribed in section 2.4.3 was used to determine geopolymer mortars compressive strength.

**3.4.3 X-ray fluorescence spectroscopy (XRF).** The XRF analysis was used to identify the major and traced elements in the fly ash and the metakaolin. The same test prescribed in section 2.4.1 was conducted on samples from the two materials.

**3.4.4 X-ray diffraction analysis (XRD).** The XRD analysis was used to find information about the changes in the crystal structure of the geopolymer when cured with different curing temperatures and after exposing the geopolymer mortars to 800°C. Samples of the geopolymer were ground to pass sieve #200. The samples then were sent to the Harry Reid Center for Environmental Studies at the University of Nevada, Las Vegas to perform the XRD. The XRD was conducted via high resolution X-ray diffractometry using Bruker-AXS D8 Advance Vario with primary Johansson-type monochromator, a goniometer radius of 435 mm and an ultra-fast silicon-strip position sensitive detector (LynxEye). See figure 39. The test results then were analyzed by Rietveld analysis using Bruker-AXS TOPAS 4.2.



Figure 39. X-Ray diffraction single crystal structure.

**3.4.5 Mercury intrusion porosimetry (MIP).** The mercury intrusion porosimetry test (MIP) was used to evaluate the porosity and to study the pores structure of the geopolymer mortars. Small samples of the geopolymer mortars ( $2.5 \pm 1$  gram) were dried in a conventional oven at  $60^{\circ}\text{C}$  for three days. The samples then were left to cool to room temperature inside the oven before they were transferred to a dessicator where they put under a low pressure ( $-23$  INHG from the atmosphere) for 24 hours. The MIP test was performed using Micromeritics AutoPore IV Mercury Porosimeter shown in Figure 40. During testing the test sample was located in a glass penetrometer and the test was carried in two steps.

- Low pressure: The sample was placed in a low pressure vacuum and subjected to a low pressure of 30 psia. The Mercury was introduced to the testing sample at the end of this step.
- High Pressure: The sample was placed in a high pressure chamber and subjected to a high pressure up to 30,000 psia using hydraulic oil.

The test results provide the cumulated intrusion associated with applied pressure. Using the Washburn equation (Washburn, 1921) the pore size for the geopolymer mortars was calculated as follows:

$$d = \frac{-4 \gamma \cos\Phi}{P}$$

Where: d: pore diameter

$\gamma$ : surface tension of Mercury (485 dyne/cm)

$\Phi$ : Contact angle of Mercury ( $130^{\circ}$ )

P: Applied pressure

The pores diameters then were plotted against the cumulated intrusions. Pore diameter of  $0.1\mu\text{m}$  is usually used as a boundary to divide the pores into micro pores and macro pores. Pores with diameter  $\geq 0.1\mu\text{m}$  are macro pores and pores with diameter  $<0.1\mu\text{m}$  are micro pores. The threshold pore diameter, which is defined as the diameter corresponding to the maximum rate of intrusion per change in pressure (Cook, Hover, 1999), was computed too.



Figure 40. Micromeritics AutoPore IV and penetrometer filled with mercury.

### 3.5 Fine Aggregate Saturated Surface-Dry Condition (SSD) Preparation

The fine aggregate used in this phase of the research was in saturated surface-dry condition (SSD). The SSD condition was obtained following the procedure prescribed in section 6 of ASTM C 128 (2001). The aggregate was immersed in water for  $24 \pm 4$  hours. Afterward, the excess water was removed and the aggregate was dried using moving currents of warm air. The aggregate was frequently stirred to insure homogenous drying.

The SSD condition was obtained following the cone test for surface moisture prescribed in ASTM C 128 (2001) as illustrated in Figure 41.



Figure 41. Cone test for surface moisture.

### 3.6 Potassium Hydroxide Solution (KOH) Preparation

The 7.5 M KOH solution was prepared 24±3 hour before geopolymer mixing time. The solution was prepared by dissolving 420.8 gram of KOH pellets in distilled water to make 1 liter (1000 ml) of KOH solution. The solution then was stored at room temperature 73 ±3°F until mixing time.

### 3.7 Geopolymer Mortars Specimen Preparation

The specimens were prepared using 2” cube plastic molds. The geopolymer mortar was placed in two layers. Each layer was tamped according to ASTM C 109 (2002) and vibrated for 1 minute. After molding, the specimens were put for 1 hour at room temperature inside heat resistance plastic bags previously tested to retain humidity. After the delay time, the specimens were subjected to initial curing for 3 days inside a forced air drying oven. See Figure 42. To study the effect of the initial curing on the properties of the geopolymer mortars three different curing temperatures (45°, 60°, and

75°) were used. At the end of the curing period the oven was turned off and the specimens were left to cool to room temperature for 6 hours before unmolding to avoid the thermal cracking that accompanies rapid reduction in temperature.



Figure 42. Geopolymer mortars specimens inside an oven.

### 3.8 Geopolymer Mortars Exposure to 800°C

At the age of six days, four specimens from each geopolymer mortar were taken, their dimensions were measured, and their masses were computed before they were put in a furnace and exposed to 800°C. See Figure 43. The temperature was increased in 5°C/min increments until it reached 800°C, then was maintained for 1 hour at 800°C before the furnace was turned off and the specimens left to cool to room temperature for 16-20 hours inside the furnace.



Figure 43. Geopolymer mortar specimens inside the furnace.

### 3.9 Fly Ash Based Geopolymer Mortar

The following sections will cover the preparation and testing of the fly ash based geopolymer mortars. Tests results of different geopolymer mortars will be compared and discussed.

#### 3.9.1 Methodology.

**3.9.1.1 Fly ash based geopolymer mortars mix proportion.** The fly ash and fine aggregate in the fly ash geopolymer mortar mixtures were proportioned following the cement and sand proportions of the standard cement mortar suggested by ASTM C 109 (2002) respectively. A 500 grams of fly ash and 1,375 grams of fine aggregate were used to prepare six 2x2x2 inch cubes of geopolymer mortar. The alkaline solution used to prepare the geopolymer was a combination of potassium hydroxide solution and sodium silicate solution (water glass). To study the effect of the alkaline solution on the



properties of the geopolymer, five different ratios of sodium silicate to potassium hydroxide (0.5, 0.75, 1.00, 1.25, and 1.50) were used. The alkaline solution to fly ash ratio by mass was kept constant at 0.49 to maintain a mortar flow of  $110 \pm 5\%$  following ASTM C 109 (2002).

**3.9.1.2 Fly ash based geopolymer mortars mixing procedure.** This procedure was followed in mixing all fly ash based geopolymer mortars. The mixing was conducted using an electrically driven mechanical mixer of the kind equipped with a paddle and a mixing bowl. See Figure 44. The fly ash geopolymer mortars mixing procedure is illustrated in Figure 45.



Figure 44. Fly ash based geopolymer mortar mixing.

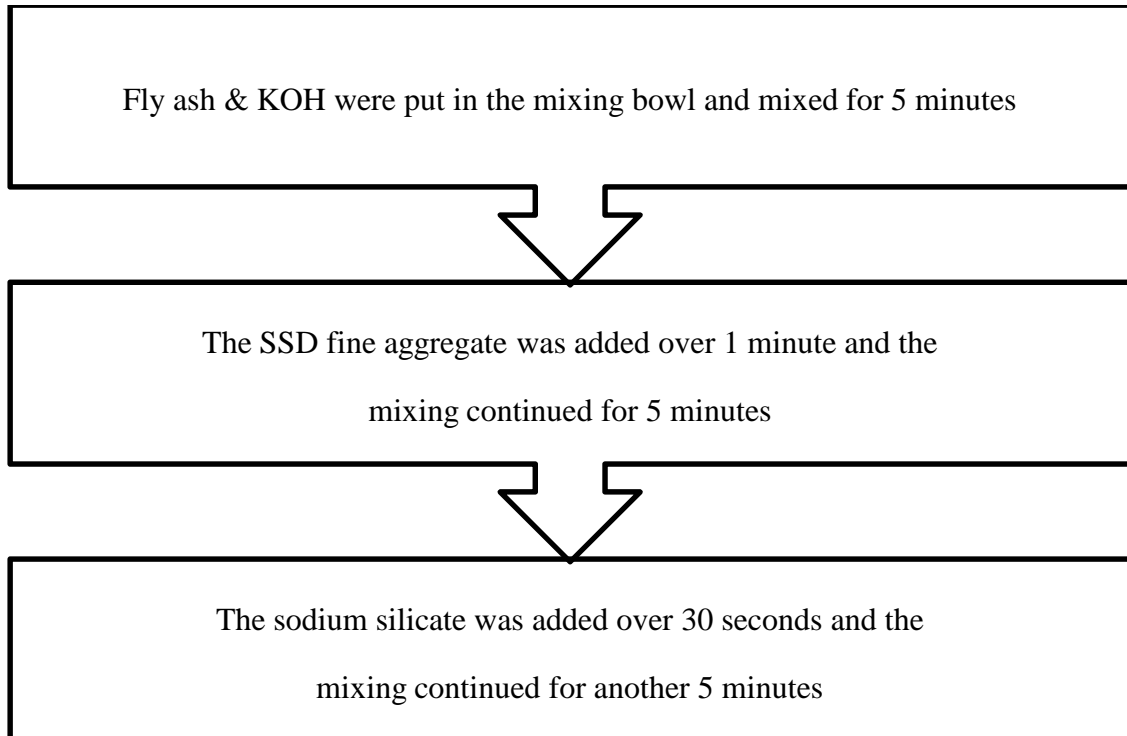


Figure 45. Fly ash based geopolymer mortars mixing procedure

The total mixing time was 16.5 minutes. After mixing, the geopolymer mortar specimens were prepared according to section 3.7. The mixture was named as follows:

FA-X-Y

Where: FA: Is flay ash

X: Is the sodium silicate to potassium hydroxide ratio.

Y: Is the initial curing temperature.

The number 800 was added at the end of the name if the specimen was exposed to 800°C i.e. FA-X-Y-800.

**3.9.1.3 Fly ash based geopolymer mortars testing.** Immediately after mixing, a flow test was conducted on the new geopolymer mortars to insure a flow of  $110 \pm 5\%$ . The test was performed according to section 3.4.1. At the end of the initial heat curing,

three specimens from each geopolymer were used to perform the 3 day compressive strength test which was performed according to section 3.4.2. In the meantime, the rest of the specimens were left in sealed plastic containers at room temperature. The compressive strength at 7 days was tested for each geopolymer using three specimens. Simultaneously, three specimens exposed to 800°C following section 3.8 were tested for compressive strength after their dimensions were measured and masses were computed. Samples were chosen for the X-ray diffraction analysis (XRD), the mercury intrusion porosimetry (MIP), and the scanning electron microscope (SEM).

**3.9.2 Fly ash based geopolymer tests results and discussions.** The following sections will present the results of all tests performed on the fly ash based geopolymer mortars:

**3.9.2.1 Fly ash based geopolymer mortars compressive strength.** This section will discuss the effect of the curing regime, alkaline solution, and the exposure to 800°C on the development of the geopolymer mortars compressive strength. The compressive strength results for all the fly ash geopolymer mortars are shown in Table 17.

**3.9.2.1.1 Effect of the curing regime and the age of testing.** Figure 46 and figure 47 shows the compressive strength of the fly ash geopolymer mortars prepared at different initial curing temperatures. As shown in both Figures (46 and 47), the fly ash geopolymer mortars compressive strength increase with the increase of the initial curing temperature. Table 17 shows that when the initial curing temperature increased from 45°C to 60°C, the geopolymer mortars compressive strength increase ranged between 790 and 3070 psi. The increase depends on sodium silicate to potassium hydroxide ratio by mass. When the curing temperature increased from 60°C to 75°C, the increase in

compressive strength ranged between 350 and 2010 psi. This increase depends on the sodium silicate to potassium hydroxide ratio. It should be noted that this range of temperature (60° to 75°C) had more effect on geopolymer mortars with a sodium silicate to potassium hydroxide ratio ranged between 0.75 and 1.25. Figure 48 illustrates the change in compressive strength for geopolymer mortars made with different sodium silicate to potassium hydroxide ratios that accompany the increase of the initial curing temperature from 45°C to 75°C. From Figure 48, it is clear that fly ash based geopolymer mortars made with a sodium silicate to potassium hydroxide ratio of 1.25 shows more than 5000 psi increase in compressive strength. The increase of the compressive strength with the increase of the initial curing temperature seems to agree with the finding of other studies by Van Jaarsveld, Van Deventer and Lukey (2002); Van Dam (2010). Fly ash based geopolymer mortars showed no major change in compressive strength after the initial curing. The increase in strength at the age of 7 days was less than 17% for all fly ash based geopolymer mortars tested in this study. This agrees with the finding of previous studies by Kong and Sanjayan (2008); Lloyd and Rangan (2009).

Table 17. Fly ash based geopolymer mortars compressive strength.

Geopolymer mortars cured at 75°C				
Mortar Name	Sodium silicate to potassium hydroxide ratio by mass	Compressive Strength (psi)		
		3 Days	7 Days	7 Days Exposed to 800°C
FA-0.50-75	0.50	5160	5630	-
FA-0.75-75	0.75	7630	7750	2580
FA-1.00-75	1.00	7250	7420	2700
FA-1.25-75	1.25	7990	7950	3030
FA-1.50-75	1.50	3310	3540	-
Geopolymer mortars cured at 60°C				
FA-0.50-60	0.50	4890	5220	-
FA-0.75-60	0.75	5900	6530	2770
FA-1.00-60	1.00	5240	6050	2720
FA-1.25-60	1.25	5480	5240	3000
FA-1.50-60	1.50	2960	3330	-
Geopolymer mortars cured at 45°C				
FA-0.50-45	0.50	2300	2510	-
FA-0.75-45	0.75	3600	3860	2885
FA-1.00-45	1.00	3530	3850	2490
FA-1.25-45	1.25	2410	2540	2833
FA-1.50-45	1.50	2170	2600	-

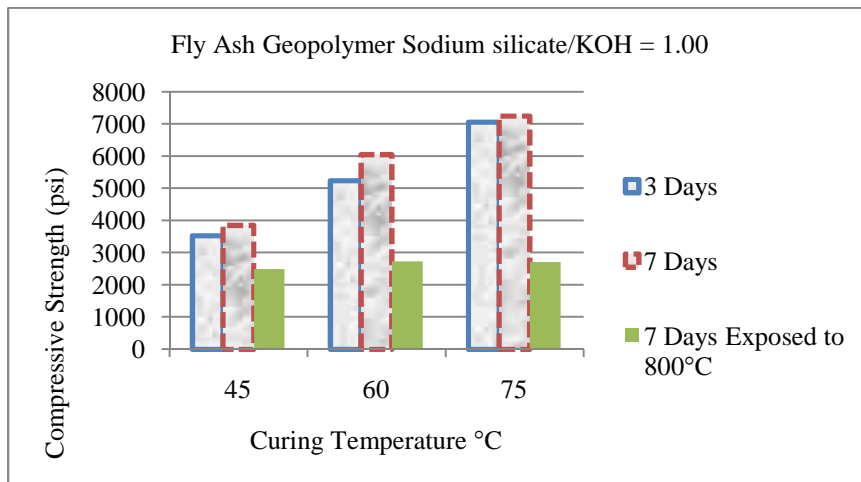
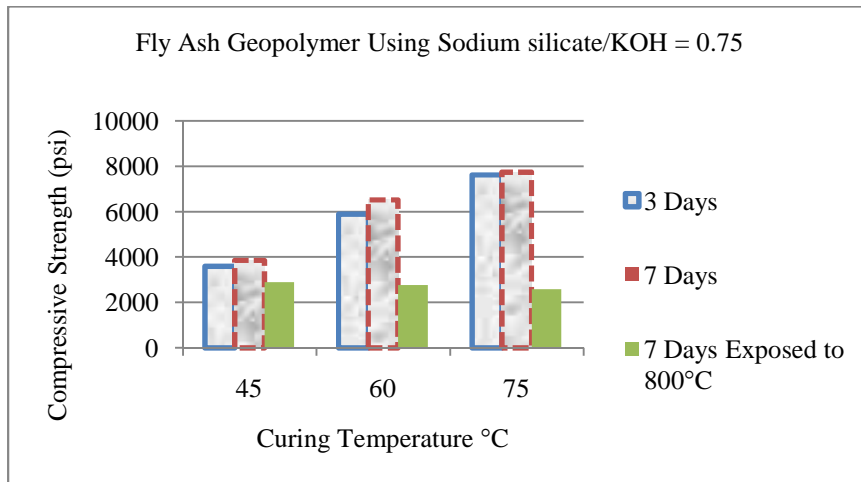
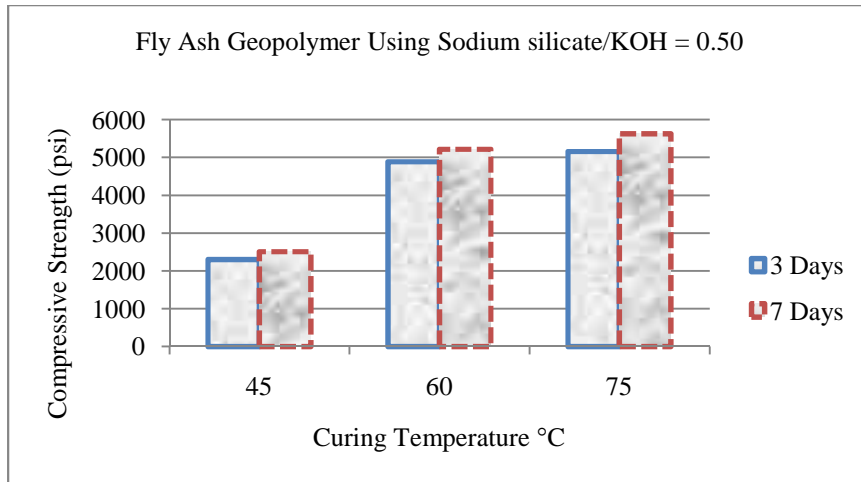


Figure 46. Relationship between the curing temperature and the compressive strength for fly ash geopolymer mortars made with Sodium silicate to potassium hydroxide ratios of 0.5, 0.75, and 1.00.

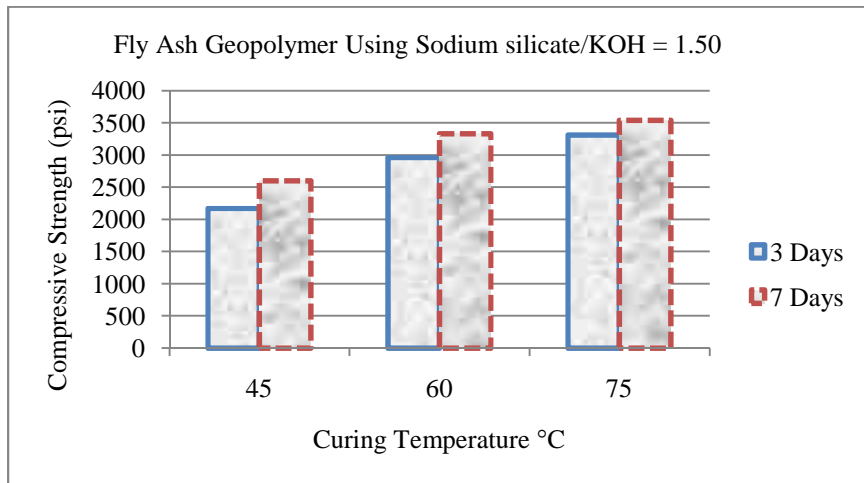
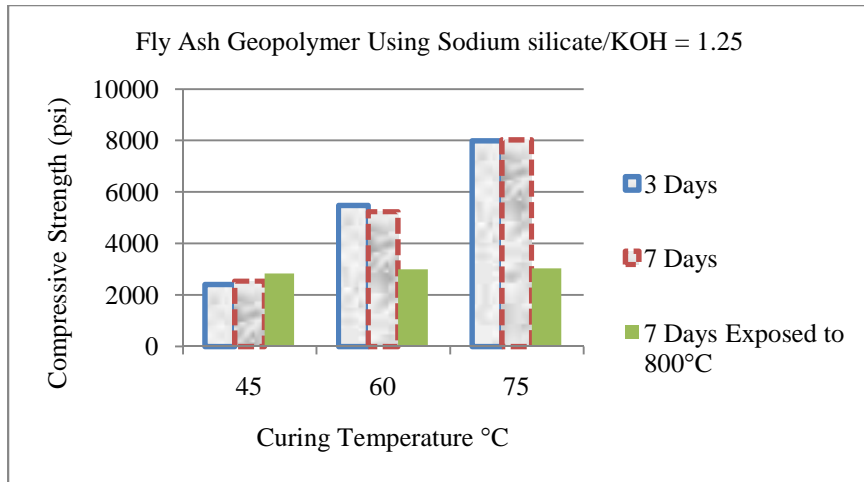


Figure 47. Relationship between the curing temperature and the compressive strength for fly ash geopolymer mortars made with Sodium silicate to potassium hydroxide ratios of 1.25 and 1.5.

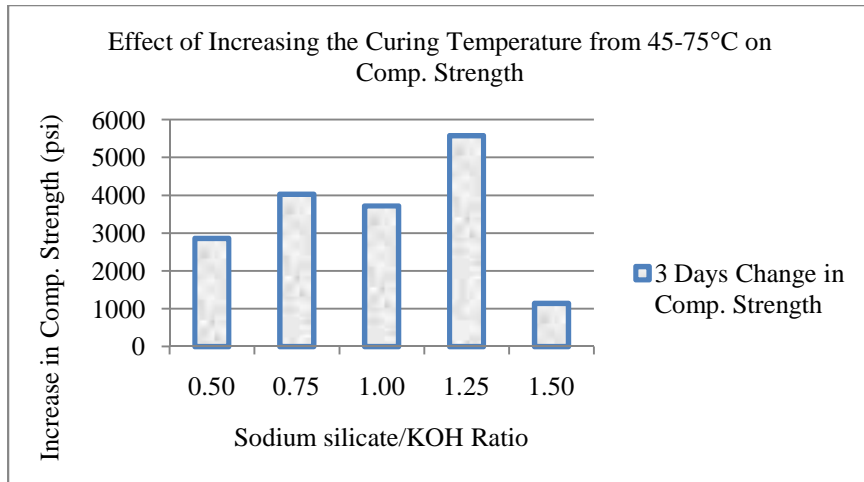


Figure 48. Effect of increasing the curing temperature from 45°C to 75°C on the compressive strength of different geopolymer mortars.

3.9.2.1.2 *Effect of the sodium silicate to potassium hydroxide ratios.* Figure 49 shows the compressive strength results of geopolymer mortars made with different sodium silicate to potassium hydroxide ratios. It can be noted from Figure 49, that the effect of the sodium silicate to potassium hydroxide ratio on the geopolymer compressive strength is highly related to the initial curing temperature. In general, geopolymer mortars containing sodium silicate to potassium hydroxide ratios that range from 0.75 to 1.25 show higher compressive strength. Figure 49 also shows higher compressive strength for specimens made with sodium silicate to potassium hydroxide ratios of 0.75 and 1.00 when the curing temperature was 45°C. However, specimens cured at 60°C show higher compressive strength when the sodium silicate to potassium hydroxide ratio is 0.75. The results presented in Table 17 testify that a combination of a sodium silicate to potassium hydroxide ratio of 1.25 and a curing temperature of 75°C resulted in the highest compressive strength. It should be noted that the alkaline silicate solution to alkaline hydroxide solution optimal ratio depends on the type of the alkaline silicate solution used (Hardjito et al., 2004a).



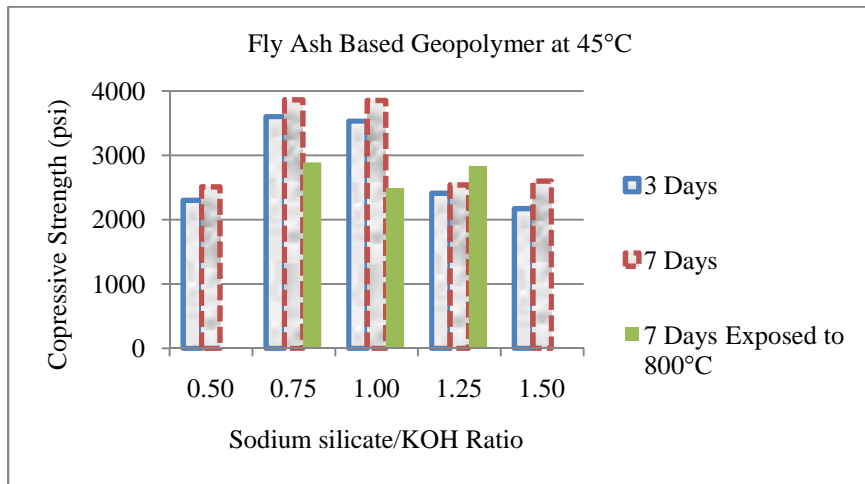
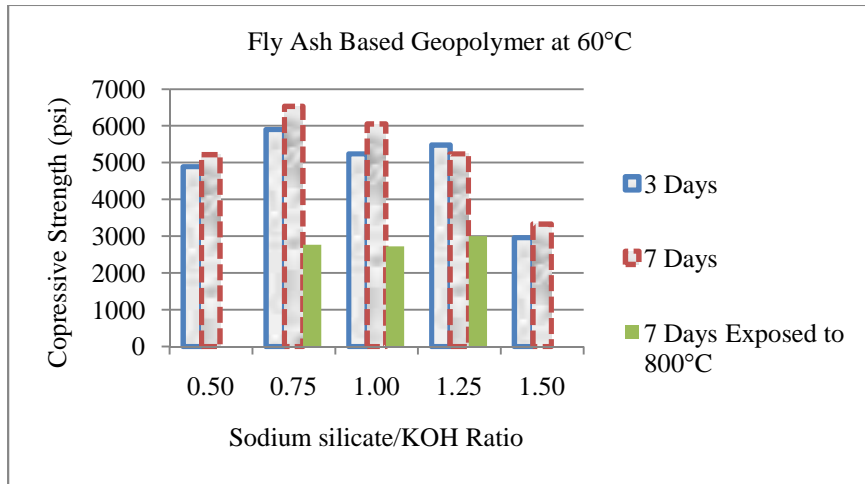
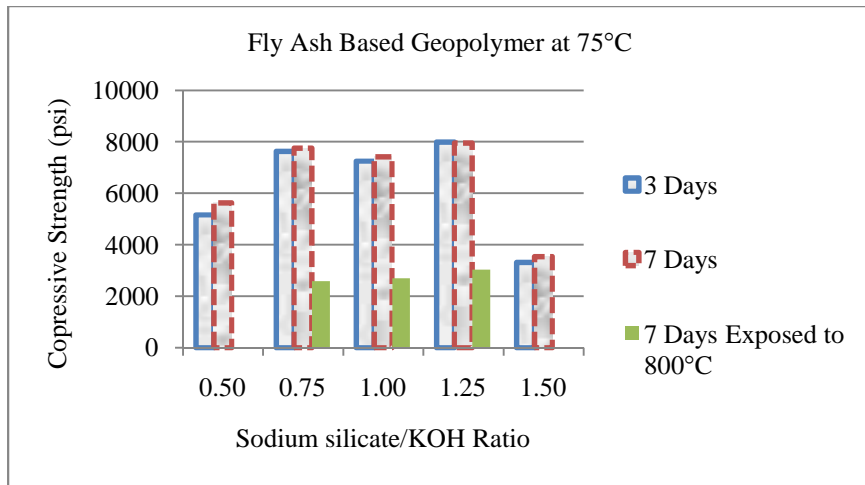


Figure 49. Effect of the sodium silicate to potassium hydroxide ratio by mass on the compressive strength of the fly ash based geopolymer mortars cured at different temperatures.

3.9.2.1.3 *Effect of the exposure to 800°C.* As presented in section 3.8, geopolymer mortars were exposed to 800°C to study their resistance to heat. Figure 50 shows a specimen before and after exposure to 800°C. The compressive strength of different mixtures after the heat exposure is illustrated in Table 17 and Figures 46 and 47. In general, all specimens maintained some of their compressive strength after they were exposed to 800°C. This compressive strength ranged between 2,490 and 3,030 psi, which disagrees with the finding of previous study by Kong and Sanjayan (2010). The loss in strength after the geopolymer mortars were exposed to 800°C was higher for mixtures that recorded higher compressive strength without the exposure to 800°C. It should be noted that specimens made with a sodium silicate to potassium hydroxide ratio of 1.25 and cured at 45°C showed a gain of 293 psi in compressive strength. This strength gain after the exposure to 800°C for specimens with lower initial strength is in agreement with the finding of previous study by Pan et al. (2009). Geopolymer mortars loss in strength due to the exposure to an elevated temperature is a result of the differential thermal expansion between the aggregate and the geopolymer (Kong & Sanjayan, 2008).



Figure 50. Fly ash based geopolymer before and after the exposure to 800°C.

**3.9.2.2 Changes in volume and mass after the exposure to 800°C.** Table 18 illustrates the changes in mass and volume of the geopolymer mortars after their exposure to 800°C. In general, all geopolymer mortars experienced loss in mass. This loss in mass ranged between 19% and 24%. The loss in mass of the geopolymer mortars after the exposure to 800°C increased with the decrease of the initial curing temperature. The geopolymer mortars loss in mass after the exposure to an elevated temperature is caused by the loss of water from the geopolymer mortars (Kong & Sanjayan, 2008). Unlike the change in mass, the change in the geopolymer mortars' volume after they exposed to 800°C was from an increase of 0.3% to a decrease of 1.8 %. However, most mortars showed an increase in volume after they were exposed to 800°C. This increase is a result

of the aggregate expansion which predominates over the contraction in the geopolymer binder (Kong & Sanjayan, 2008).

Table 18. Fly ash geopolymer mortars changes in mass and volume.

Mixture name	Reduction in mass (%)	Increase in volume (%)
Geopolymer mortars cured at 75°C		
FA-0.75-75	19.6	0.2
FA-1.00-75	20.0	0.1
FA-1.25-75	19.2	0.0
Geopolymer mortars cured at 60°C		
FA-0.75-60	23.3	0.2
FA-1.00-60	23.4	0.2
FA-1.25-60	23.6	0.2
Geopolymer mortars cured at 45°C		
FA-0.75-45	24.3	0.0
FA-1.00-45	23.1	0.3
FA-1.25-45	24.4	1.8

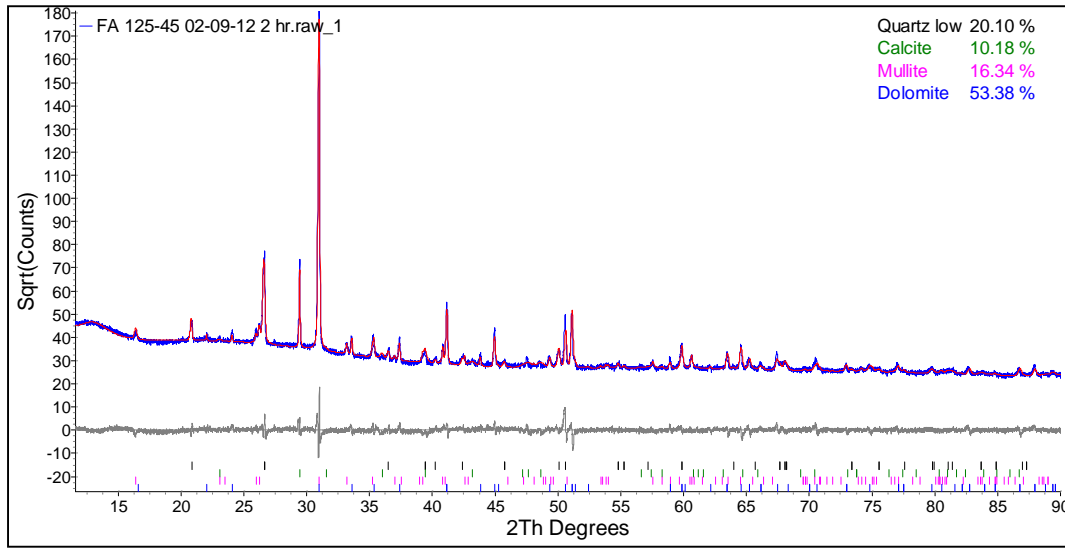
**3.9.2.3 X-ray diffraction analysis (XRD).** Quantitative Rietveld X-ray fine structure analysis was performed on the geopolymer mortars with a sodium silicate to potassium hydroxide ratio of 1.25. This sodium silicate to potassium hydroxide ratio was chosen because it was associated with the highest geopolymer mortars compressive strength as mentioned in section 3.9.2.1.2. The XRD was performed to study the effect of different initial curing temperatures as well as the exposure to 800°C on the crystal

structure of the geopolymer mortars. Hence, three specimens were used for this test. Two specimens were initially cured at 75°C one of which was exposed to 800°C (FA-1.25-75 and FA-1.25-75-800). The third specimen was initially cured at 45°C (FA-1.25-45). The analysis results are shown in Table 19 and Figures 51, 52, and 53. As presented in Table 19, the crystal structure is highly affected by the initial curing temperature. The XRD results show an increase in Dolomite when the initial curing temperature increased from 45°C to 75°C. On the other hand, there was a decrease in the percentages of Calcite, Mullite and Quartz low. Moreover, a trace of Microdine (intermediate) was found in samples initially cured at 75°C. Exposing the geopolymer mortars to 800°C for one hour caused a significant increase in the percentage of Calcite. Moreover, CaO and Periclase were found in the mortars after the exposure to 800°C. In general, the initial curing and the exposure to 800°C changed the crystal structure of the geopolymer mortars.

Table 19. Fly ash based geopolymer mortars XRD results.

	Fly Ash	Geopolymer mortar name		
		FA-1.25-45	FA-1.25-75	FA-1.25-75-800
CaO %	-	-	-	3.91
Calcite %	-	10.18	5.95	48.42
Dolomite %	-	53.38	67.94	-
Microdine Intermediate %	-	-	2.8	-
Mullite %	46	16.34	9.17	9.97
Periclase %	-	-	-	21.81
Quartz Low %	54	20.1	14.14	15.89

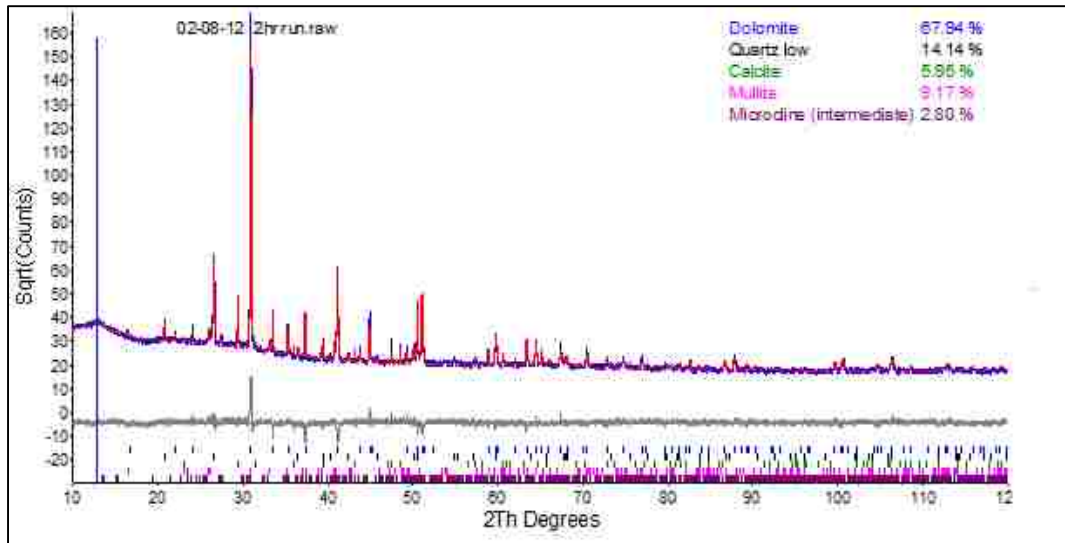
### FA-1.25-45



Refinement residual ( $R_{WP}$ ) 6.7 %

Figure 51. Quantitative Rietveld X-ray fine structure analysis for fly ash based geopolymer mortar FA-1.25-45.

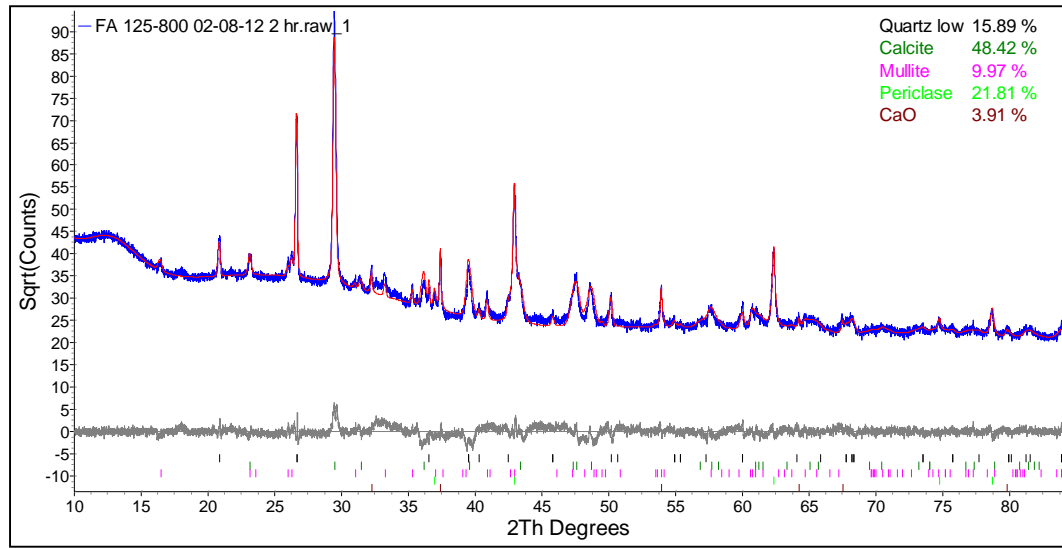
### FA-1.25-75



Refinement residual ( $R_{WP}$ ) 8.4 %

Figure 52. Quantitative Rietveld X-ray fine structure analysis for fly ash based geopolymer mortar FA-1.25-75.

### FA-1.25-75 Exposed to 800°C



Refinement residual ( $R_{WP}$ ) 6.8 %

Figure 53. Quantitative Rietveld X-ray fine structure analysis for fly ash based geopolymer mortar FA-1.25-75-800.

**3.9.2.4 Mercury intrusion porosimetry (MIP).** The mercury intrusion porosimetry (MIP) was performed on the same mixtures that were chosen for the XRD analysis and for the same reasons explained in section 3.9.2.3. These mixtures are FA-1.25-45, FA-1.25-75 and FA-1.25-75-800. The MIP results are shown in Table 20 and Figure 54. As presented in Table 20, increasing the initial curing temperature from 45° to 75°C resulted in a reduction in the threshold pore diameter and an increase in the percentage of macro pores and porosity. The reduction in the threshold diameter seems to agree with the finding of previous study by Sindhunata (2006). Smaller pore size and threshold diameter could contribute to specimen strength and durability. When specimen exposed to an elevated temperature their internal structure get destroyed due to the thermal expansion incompatibility between the aggregate and the geopolymer, as explained in section 3.9.2.2. Accordingly, the MIP results for FA-1.25-75-800 show an

increase in the porosity and the threshold diameter as well as a major decrease in the percentage of the micro pores.

Table 20. Fly ash based geopolymer mortars MIP results.

Mixture	Porosity (%)	Threshold Pore Diameter ( $\mu\text{m}$ )	Percentage of Small Pores ( $<0.1\mu\text{m}$ ) (%)
FA-1.25-45	14.3	0.05	68.43
FA-1.25-75	16.5	0.04	60.93
FA-1.25-75-800	22.3	0.08	41.55

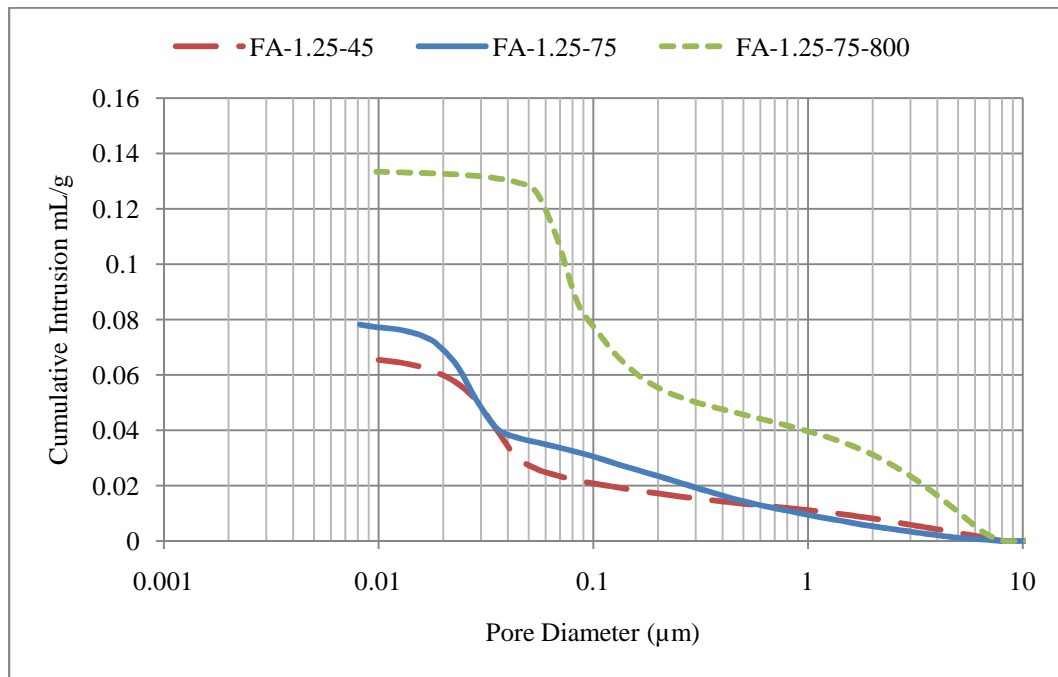


Figure 54. Relationship between the threshold diameter and the cumulative intrusion for fly ash based geopolymer mortars.



### **3.10 Metakaolin Based Geopolymer**

The following sections will cover the preparation and testing of the metakaolin based geopolymer mortars. Tests results of different metakaolin based geopolymer mortars will be compared and discussed.

#### **3.10.1 Methodology.**

**3.10.1.1 Metakaolin based geopolymer mortars mix proportion.** Following the sand to cement ratio of standard cement mortar suggested by ASTM C 109 (2002), the fine aggregate to metakaolin ratio was set to be 2.75. The same alkaline solution prescribed in section 3.9.1.1 was used to prepare the metakaolin based geopolymer mortars. To study the effect of the alkaline solution on the properties of the geopolymer, four different ratios of sodium silicate to potassium hydroxide (0.75, 1.00, 1.25, and 1.50) were used. The alkaline solution to metakaolin ratio by mass was kept constant at 1.5 to maintain a mortar flow of  $110 \pm 5\%$  following ASTM C 109 (2002).

**3.10.1.2 Metakaolin based geopolymer mortars mixing procedure.** This procedure was followed in mixing all metakaolin based geopolymer mortars. The mixing was conducted using the same mixer prescribed in section 3.9.1.2. See Figure 55. The mixing procedure is illustrated in Figure 56.



Figure 55. Metakaolin based geopolymer mortars preparation.

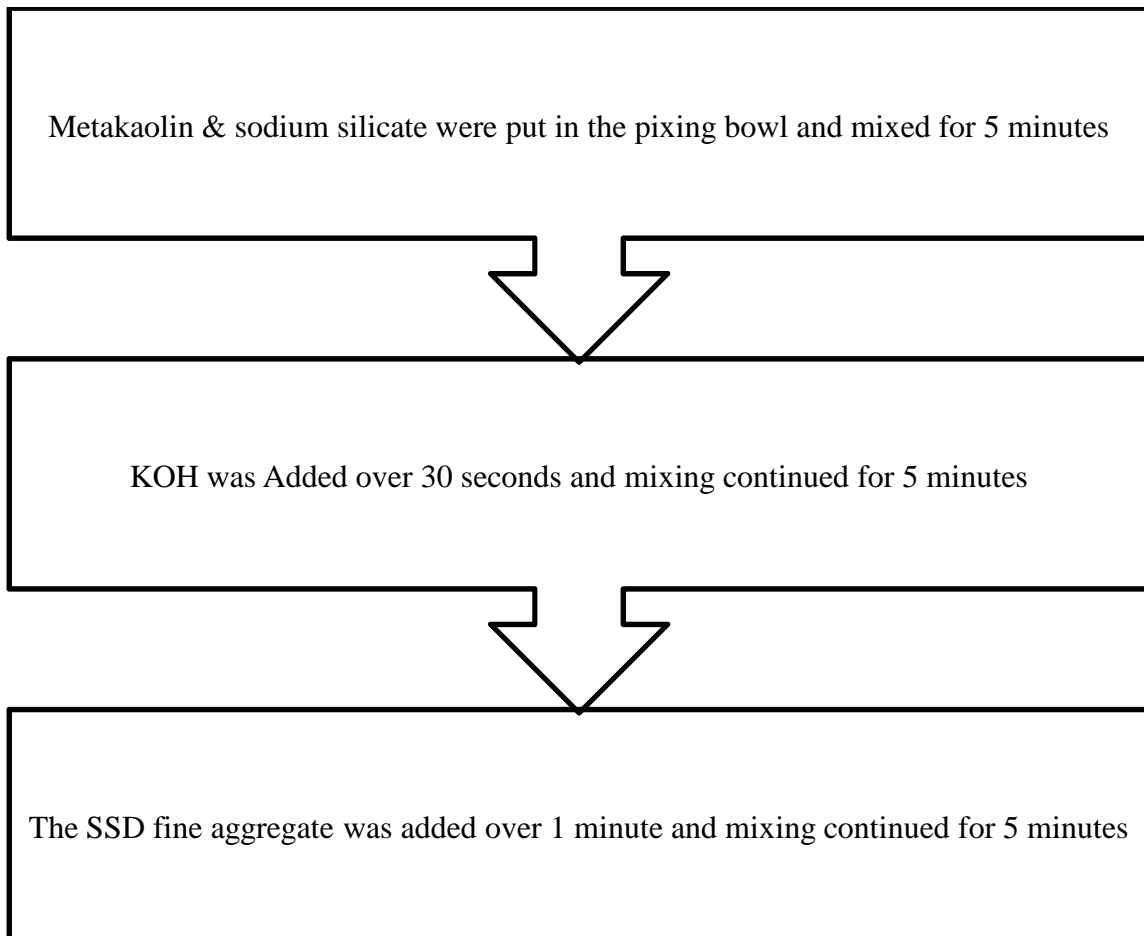


Figure 56. Metakaolin based geopolymer mortars mixing procedure.

The total mixing time was 16.5 minutes. After mixing, the geopolymer mortar specimens were prepared according to section 3.7. The mixture was named as follows:

Meta-X-Y

Where: Meta: Is Metakaolin

X: Is the sodium silicate to potassium hydroxide ratio.

Y: Is the initial curing temperature.

The number 800 was added at the end if the specimen was exposed to 800°C i.e. Meta-X-Y-800.

**3.10.1.3 Metakaolin based geopolymer mortars testing.** The same procedure prescribed in section 3.9.2 was followed to test the metakaolin base geopolymer mortars.

### **3.10.2 Metakaolin based geopolymer mortars tests results and discussions.**

The following sections will present the results of all tests performed on the metakaolin based geopolymer mortars.

**3.10.2.1 Metakaolin based geopolymer mortars compressive strength.** This section will discuss the effect of the curing regime, alkaline solution, and the exposure to 800°C on the development of the metakaolin based geopolymer mortars compressive strength. The compressive strength results for all the metakaolin geopolymer mortars are illustrated in Table 21.

**3.10.2.1.1 Effect of the Curing Regime and the Age of Testing.** Figures 57 and 58 shows the compressive strength of the metakaolin based geopolymer mortars prepared at different initial curing temperatures. In general, the metakaolin based geopolymer mortars compressive strength increase with the increase of the curing temperature. However, when the initial curing temperature increased from 45°C to 60°C there was

insignificant decrease in the 3 day compressive strength for mortars made with sodium silicate to potassium hydroxide ratios of 0.75, 1.00, and 1.50. When 75°C initial curing was used, all the metakaolin geopolymer mortars experienced an increase in the compressive strength. Table 21 shows that increasing the initial curing from 60°C to 75°C caused an increase in the compressive strength ranged between 290 and 930 psi. Figure 59 illustrates the increase in the compressive strength for the metakaolin geopolymer mortars when the initial curing temperature changed from 45°C to 75°C. As presented in Figure 59, it is obvious that mixture with a sodium silicate to potassium hydroxide ratio of 1.25 showed the highest increase in strength (3210 psi). As shown in Table 21, the metakaolin geopolymer mortars change in compressive strength with age was insignificant. This seems to agree with the finding of other studies by Kong and Sanjayan (2008); Lloyd and Rangan (2009).

Table 21. Metakaolin based geopolymer mortars compressive strength.

Geopolymer mortars cured at 75°C				
Mortar Name	sodium silicate to potassium hydroxide liquid ratio by mass	Compressive strength (psi)		
		3 Days	7 Days	7 Days Exposed to 800°C
Meta-0.75-75	0.75	4280	3840	2180
Meta-1-75	1.00	4420	4500	2120
Meta-1.25-75	1.25	4660	4970	2490
Meta-1.5-75	1.50	1370	1200	-
Geopolymer mortars cured at 60°C				
Meta-0.75-60	0.75	3350	3310	2070
Meta-1.00-60	1.00	3740	4070	2110
Meta-1.25-60	1.25	3940	4110	2060
Meta-1.50-60	1.50	1080	1370	-
Geopolymer mortars cured at 45°C				
Meta-0.75-45	0.75	3520	3500	1940
Meta-1.00-45	1.00	3920	3640	1790
Meta-1.25-45	1.25	1450	1710	1837
Meta-1.50-45	1.50	1310	1700	-

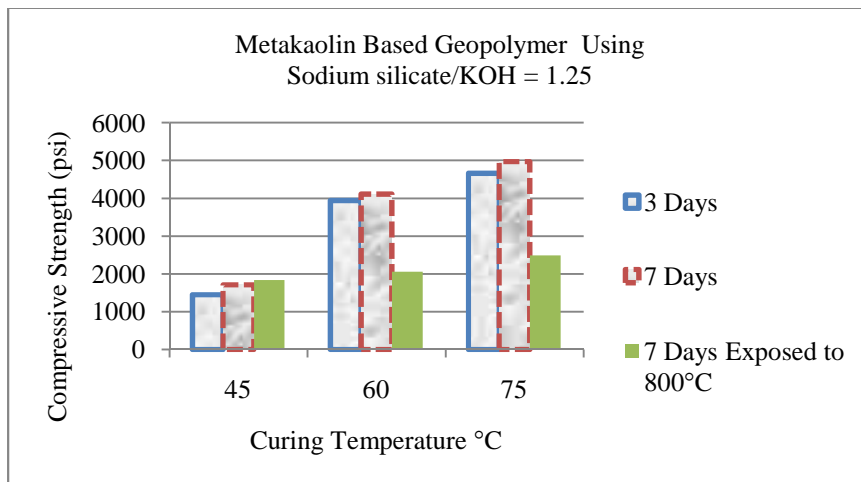
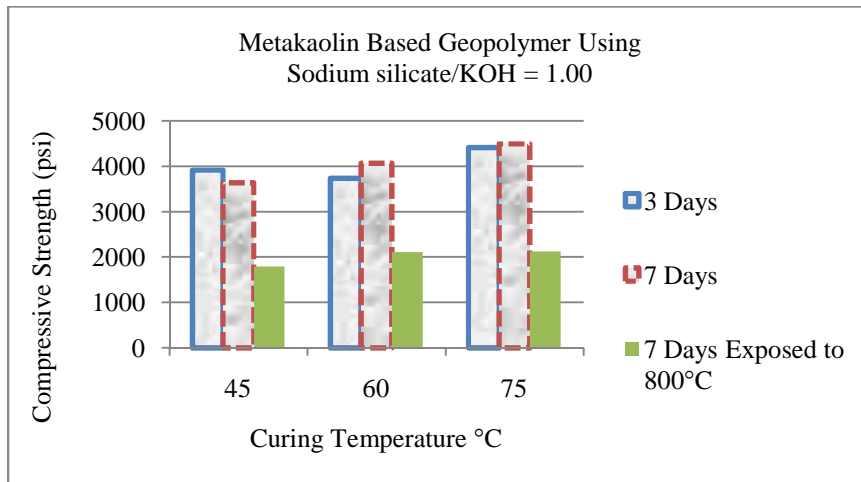
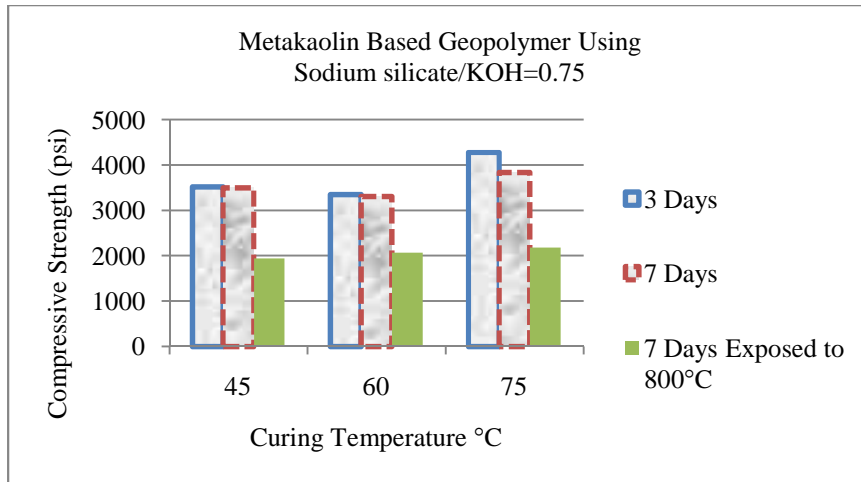


Figure 57. Relationship between the curing temperature and the compressive strength for metakaolin geopolymer mortars made with Sodium silicate to potassium hydroxide ratios of 0.75, 1.00, and 1.25.

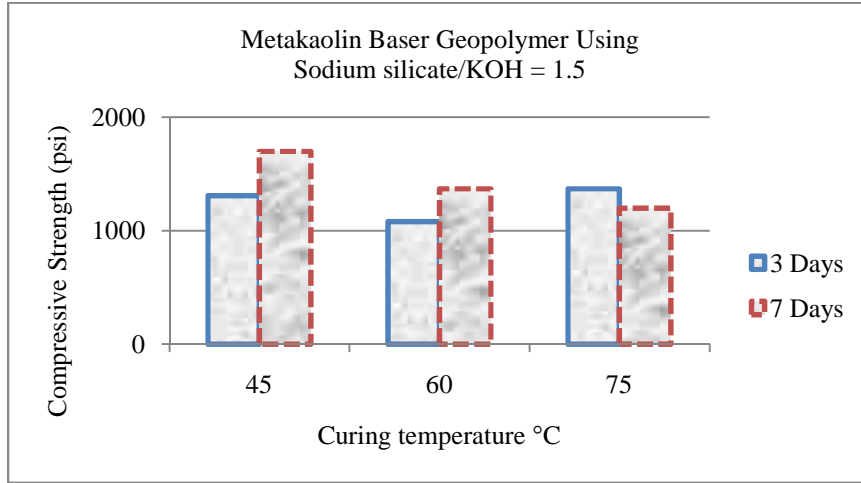


Figure 58. Relationship between the curing temperature and the compressive strength for metakaolin geopolymer mortars made with Sodium silicate to potassium hydroxide ratio of 1.50.

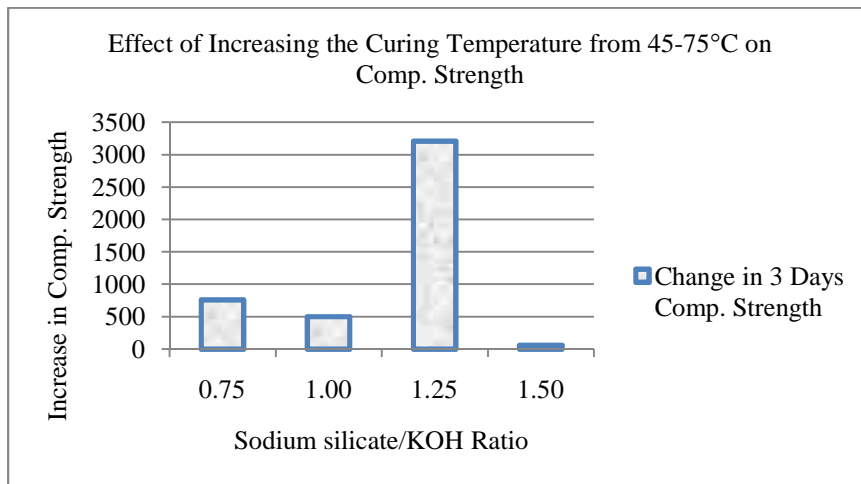


Figure 59. Effect of increasing the curing temperature from 45°C to 75°C on the compressive strength of different geopolymer mortars.

3.10.2.1.2 *Effect of the sodium silicate to potassium hydroxide ratio.* Figure 60 shows the relationships between the sodium silicate to potassium hydroxide ratio and the geopolymer mortars compressive strength for different initial curing temperatures. As shown in Figure 60, the sodium silicate to potassium hydroxide required to acquire the highest compressive strength depends on the initial curing temperature. When the initial curing temperature was 45°C the optimum sodium silicate to potassium hydroxide ratio was 1.00. Increasing the sodium silicate to potassium hydroxide ratio above 1.00 caused a dramatic loss in compressive strength under the same curing conditions. However, this was not the case for the geopolymer mortars cured at 60°C and 75°C as the optimum sodium silicate to potassium hydroxide ratio was 1.25. It should be noted that the highest compressive strength was obtained when the sodium silicate to potassium hydroxide ratio was 1.25 and the specimens were cured at 75°C. Using sodium silicate to potassium hydroxide ratio more than the optimum ratio causes a rapid decrease in the geopolymer mortars compressive strength. This decrease is related to the excess of the sodium silicate in the geopolymer, which delays water evaporation and structural formation (Kong & Sanjayan, 2008).



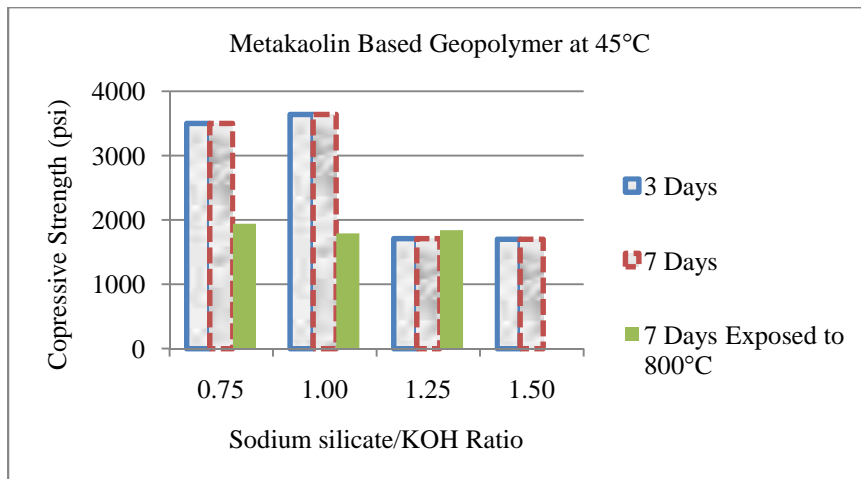
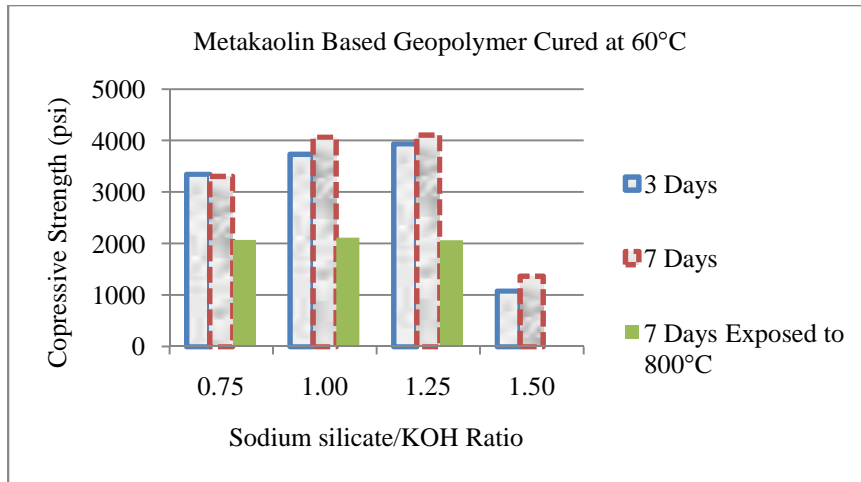
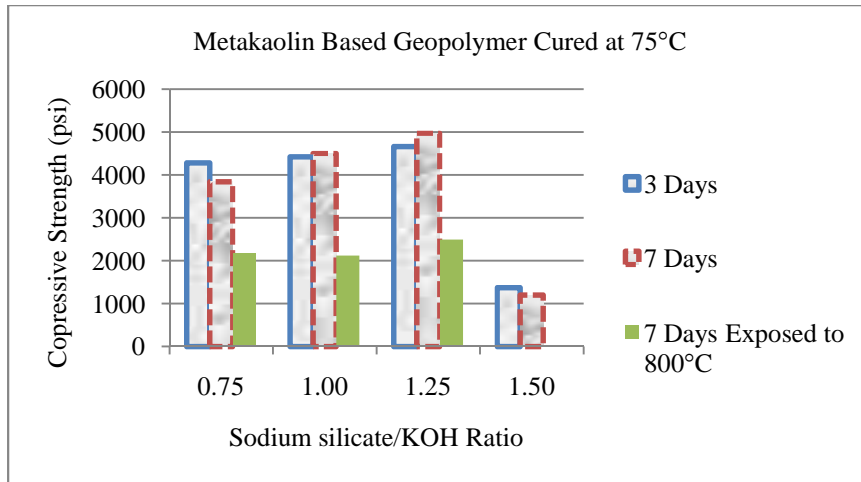


Figure 60. Effect of the sodium silicate to potassium hydroxide ratio by mass on the compressive strength of the metakaolin based geopolymer mortars cured at different temperatures.

*3.10.2.1.3 Effect of the exposure to 800°C.* To study the heat resistant of the metakaolin based geopolymer mortars, the mortar specimens were subjected to 800°C as prescribed in section 3.8. Figure 61 shows a metakaolin geopolymer mortar specimen before and after exposure to 800°C. Figures 57, 58, and Table 21 illustrate the compressive strength results for the metakaolin geopolymer mortars with and without exposure to 800°C. In general, all the mixtures showed a reduction in strength after they were exposed to 800°C. This reduction in compressive strength ranged between 1240 and 2480 psi. However, specimens prepared with a sodium silicate to potassium hydroxide ratio of 1.25 and cured at 45°C showed insignificant (127 psi) increase in compressive strength after they were exposed to 800°C. This increase could be a result of unfinished polymerization existed before the exposure to 800°C. Table 21 also shows that all tested mortars maintained a compressive strength after they were exposed to 800°C. This compressive strength ranged between 1837 and 2490 psi.

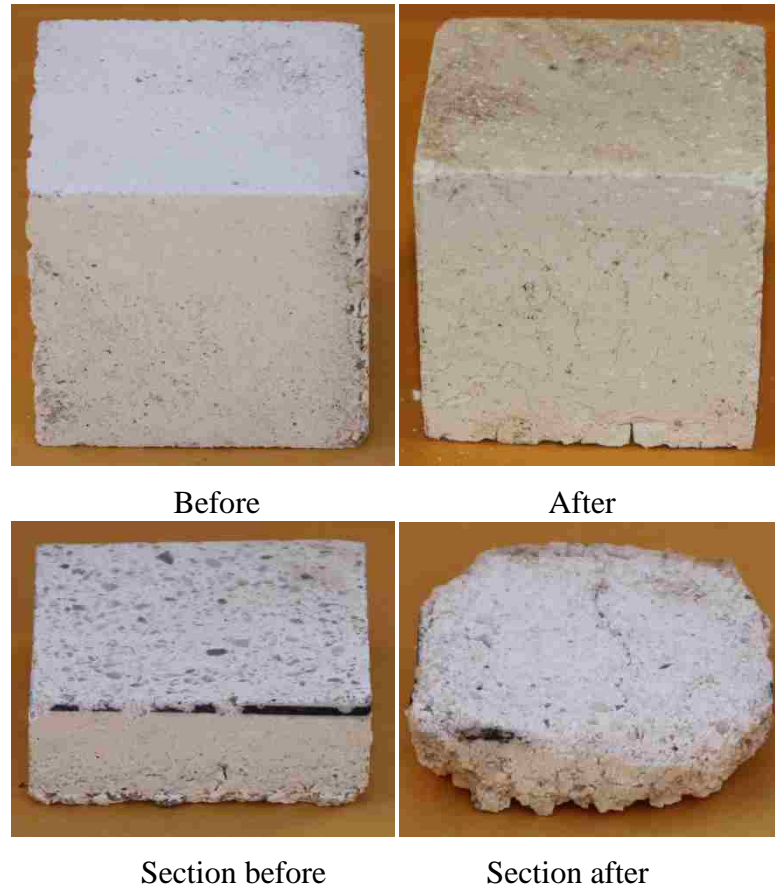


Figure 61. Metakaolin based geopolymer mortar before and after the exposure to 800°C.

**3.10.2.2 Changes in Volume and Mass after the Exposure to 800°C.** Table 22 shows the change in mass and volume of the metakaolin geopolymer mortars after they were exposed to 800°C. As presented in Table 22, all geopolymer mortars experienced a loss in mass. The loss in mass was more than 20% for all tested specimens. Some of these specimens experienced a loss in volume too. The loss in volume for the metakaolin geopolymer mortars ranged between 0.00 and 2.20%. Both the loss in mass and the loss in volume are related to the loss of water in the geopolymer mortars.

Table 22. Metakaolin based geopolymer mortars changes in mass and volume.

Mixture Name	Reduction in mass (%)	Reduction in volume (%)
Geopolymer mortars cured at 75°C		
Meta-0.75-75	20.6	2.2
Meta-1.00-75	21.2	1.8
Meta-1.25-75	20.3	0.4
Geopolymer mortars cured at 60°C		
Meta-0.75-60	28.6	0.1
Meta-1.00-60	29.0	1.1
Meta-1.25-60	28.3	0.0
Geopolymer mortars cured at 45°C		
Meta-0.75-45	31.7	1.5
Meta-1.00-45	31.0	1.3
Meta-1.25-45	31.8	1.5

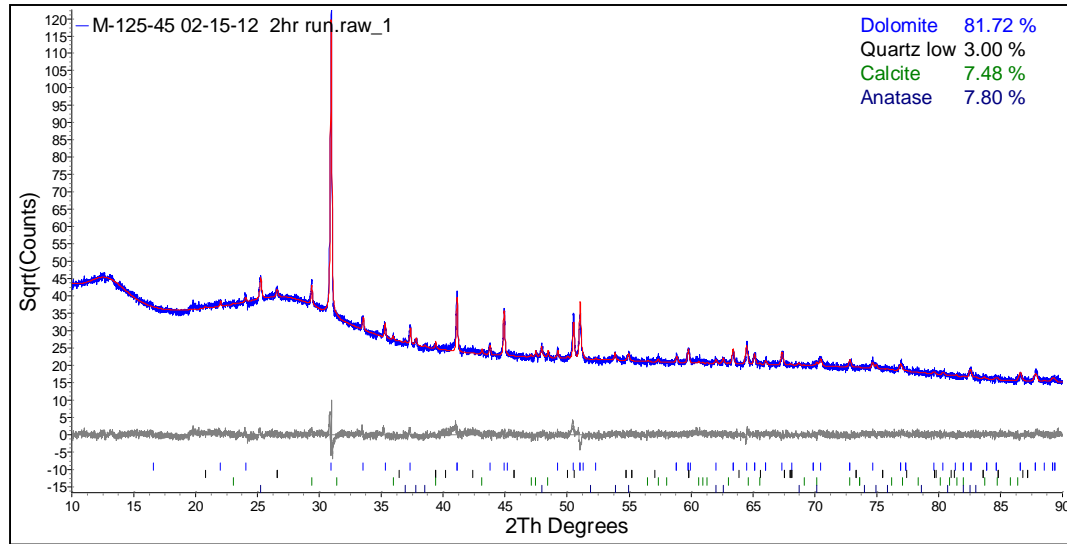
**3.10.2.3 X-ray diffraction analysis (XRD).** For the same reasons prescribed in section 3.9.2.3, three powder samples from three different specimens were used to perform the XRD analysis. These three samples are Meta-1.25-75, Meta-1.25-45 and Meta-1.25-75-800. The XRD results are illustrated in Figures 62, 63, and 64 and Table 23. As presented in Table 23, more than 80% of both Meta-1.25-45 and Meta1.25-75 is Dolomite. However, increasing the initial curing temperature from 45°C to 75°C caused a reduction in the percentage of Anatase and an increase in the percentage of Calcite.

Exposing the specimens to 800°C for one hour caused a significant change in the geopolymer mortar crystal structure. Hence, the Dolomite phase was vanished and substituted by Periclase, CaO and an increase in the Calcite. It should be noted that a high percentage of the Dolomite was near-ordered glass.

Table 23. Metakaolin based geopolymer mortars XRD results.

	Metakaolin	Geopolymer mortar name		
		Meta-1.25-45	Meta-1.25-75	Meta-1.25-75-800
Anatase %	-	7.8	1.44	1.54
CaO %	-	-	-	4.14
Calcite %	-	7.48	11.49	47.51
Dolomite %	-	81.72	81.91	-
Kaolinite %	77	-	-	-
Metakaolinite %	20	-	-	-
Mullite %	-	-	2.63	-
Periclase %	-	-	-	28.84
Portlandite %	-	-	-	16
Quartz Low %	-	3	2.53	2.17
Zeolite %	3	-	-	-

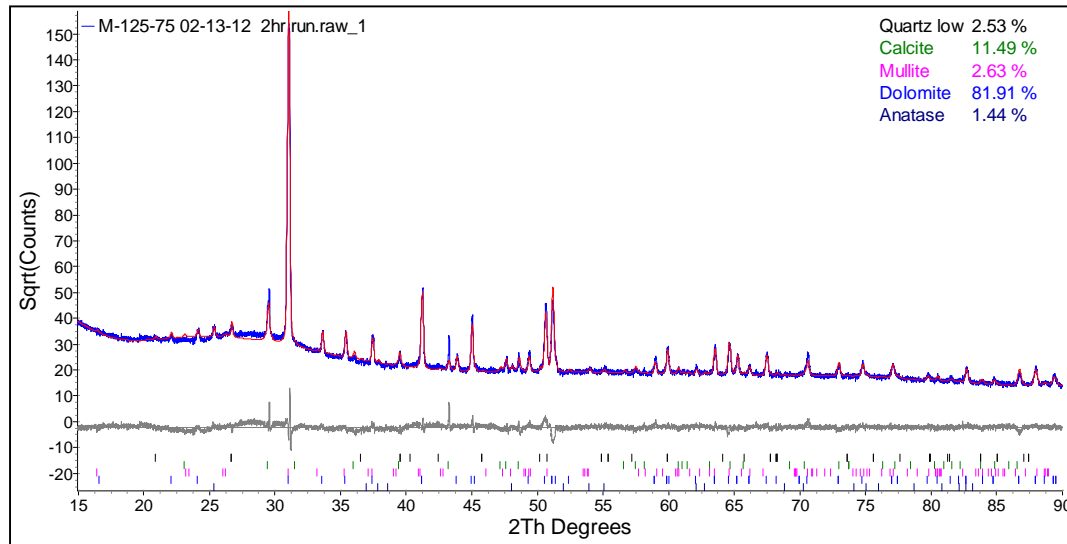
### Meta-1.25-45



Refinement residual ( $R_{WP}$ ) 5.2 %

Figure 62. Quantitative Rietveld X-ray fine structure analysis for the metakaolin based geopolymer mortar Meta-1.25-45.

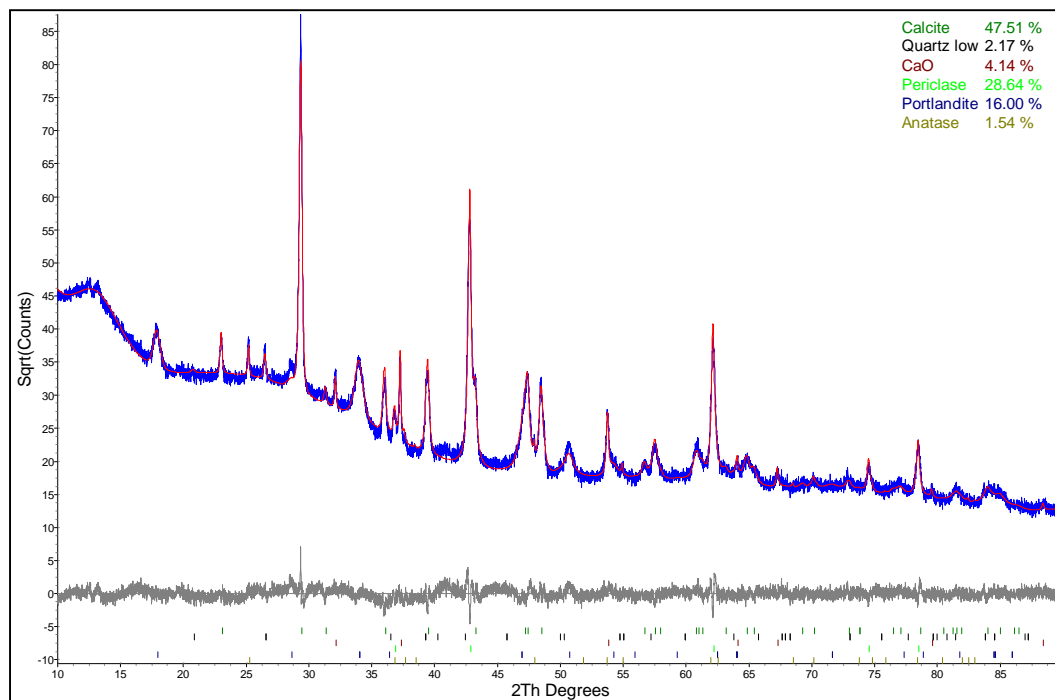
### Meta-1.25-75



Refinement residual ( $R_{WP}$ ) 7.8 %

Figure 63. Quantitative Rietveld X-ray fine structure analysis for the metakaolin based geopolymer mortar Meta-1.25-75.

Meta-1.25-75-800



Refinement residual ( $R_{WP}$ ) 5.8 %

Figure 64. Quantitative Rietveld X-ray fine structure analysis for the metakaolin based geopolymer mortar Meta-1.25-75-800.

**3.10.2.4 Mercury intrusion porosimetry (MIP).** The same three specimens that were chosen for the XRD analysis were chosen for the MIP test and for the same reasons explained in the previous section. The MIP results are illustrated in Table 24 and Figure 65. Table 24 shows that increasing the initial curing temperature from 45°C to 75°C caused a reduction in the threshold diameter and an increase in the percentage of micro pores. This finding aligns with the increase in the compressive strength for the specimens that were initially cured at 75°C and disagree with the finding of previous study by Rovnaník (2010). Due to the thermal expansion incompatibility between the aggregate and the geopolymer when the geopolymer mortar specimen was exposed to 800°C the

percentage of macro pores in the specimen was increased. This finding also supported by the reduction in strength for specimens exposed to 800°C.

Table 24. Metakaolin based geopolymer mortars MIP results.

Mixture	Threshold Pore Diameter ( $\mu\text{m}$ )	Percentage of Small Pores ( $<0.1\mu\text{m}$ ) (%)
Meta-1.25-45	0.10	82.72
Meta-1.25-75	0.08	87.49
Meta-1.25-75-800	0.08	71.81

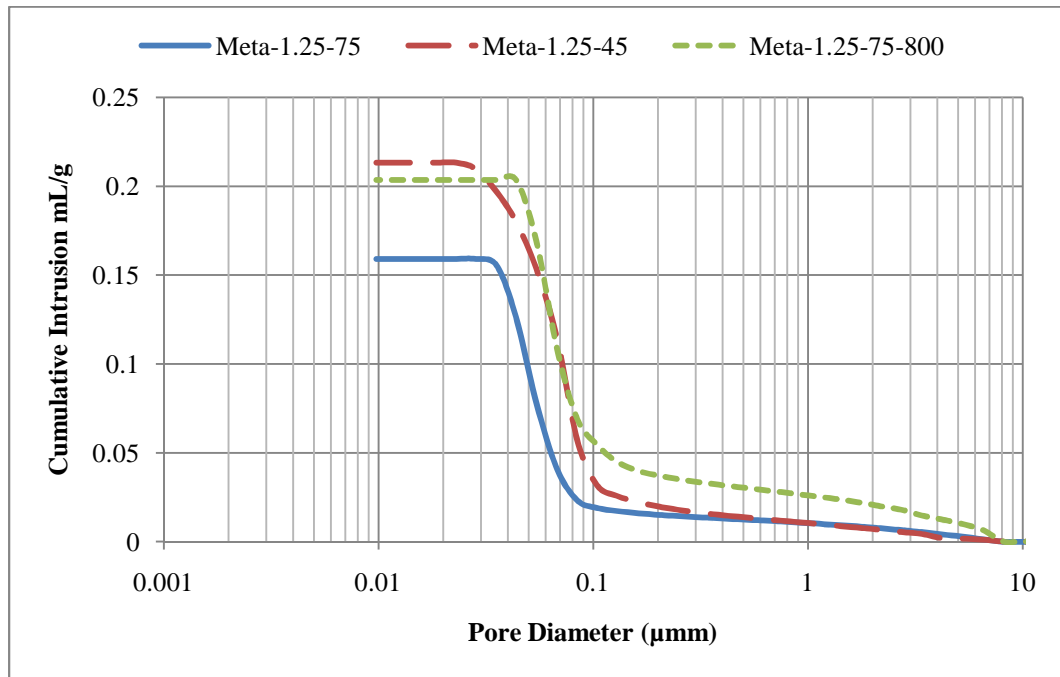


Figure 65. Relationship between the threshold diameter and the cumulative intrusion for metakaolin based geopolymer mortars.



## Conclusion and Recommendations

This thesis on investigating the use of pozzolans in portland cement concrete and inorganic polymer mortar consisted of two phases. Phase 1 investigated the use of two types of class N pozzolan as a partial replacement of OPC in concrete in two separate applications. Phase 2 focused on synthesizing geopolymer mortars using both metakaolin and fly ash in two separate applications. Four goals were set for this thesis in chapter 1. These goals are:

1. To develop mixtures proportions for the use of class N pozzolans as a partial replacement of OPC in concrete;
2. To study and evaluate the performance of the new concretes;
3. To synthesize pozzolan based geopolymer mortars;
4. To study and evaluate the performance and heat resistant of the geopolymer mortars.

### 4.1 Developing Concrete Mixture Proportions Incorporating Class N Pozzolans

Four different concrete mixtures containing class N pozzolan were developed in Phase 1. Three of which used Pozzolete as a partial replacement of OPC and the fourth used Lassenite SR. In general, the new mixtures created high performance concrete. However, there was a decrease in performance and alternations were needed for some of the mixtures.

### 4.2 Performance of the New Concretes

The performance of the new concretes varied according to the type of class N pozzolan that was used and to the percentage of OPC that was replaced. However, the

effects of incorporating class N pozzolan on all concrete mixtures can be summarized as follows:

- Superior reduction in workability accompanied the use of class N pozzolan in concrete. This was overcome by using a suitable amount of super-plasticizer.
- The use of class N pozzolan had no major effect on concrete density and air content.
- Class N pozzolan caused a reduction and a delay in concrete peak adiabatic temperature. In addition, a lower cooling slope was evident for concretes containing class N pozzolan.
- Although all concretes made with class N pozzolan maintained compressive strength higher than 7850 psi at 28 days, class N pozzolan effect on concrete strength varied according to the type and dosage of pozzolan.
- Concrete incorporated class N pozzolan continued to gain strength with time.
- The use of Pozzolete caused a minor reduction in concrete compressive strength at all ages up to 360 days.
- Concrete with high strength at early age (7520 psi at 3 days and 9410 psi at 28 days) was created using Lassenite SR. The increase in the 3 days compressive strength was more than 36% compare to the control mixture. The higher strength could be a result of the less porous transition zone, which improves the aggregate-matrix bond.
- All concretes maintained splitting tensile strength equal to 10% of their compressive strength.

- The static modulus of elasticity and the dynamic Young's modulus of elasticity follow the same trend as the 28 days compressive strength for concretes incorporated Pozzolete and reduced with the increase of Pozzolete while there was no major change in modulus of elasticity when Lassenite SR was used.
- The physical chloride ion migration test (RMT) was more accurate than RCPT in evaluating chloride ion penetration for concretes containing different percentages of class N pozzolan.
- Although concretes containing Pozzolete show higher chloride ion permeability than their control mixture at early ages, their impermeability improves with time and they could show lower chloride ion permeability than the control mix after 90 days of curing depending on the percentage of Pozzolete used.
- A major reduction in concrete rapid chloride ion permeability was achieved by the use of Lassenite SR class N pozzolan.

#### **4.3 Pozzolan based Geopolymer Mortars**

Geopolymer mortars were successfully synthesized in Phase 2 using both artificial and natural pozzolans in two separate applications. The artificial pozzolan used was class F fly ash, while the metakaolin was used as a form of natural pozzolan. Geopolymer mortar proportions were designed for both pozzolans using different ratios of sodium silicate to potassium hydroxide. The ratio of alkaline solution/pozzolan associated with each type of pozzolan was maintained to provide a flow of  $110 \pm 5\%$ .

#### **4.4 Performance and Heat Resistant of the Geopolymer Mortars**

After evaluating the performance and heat resistant of the geopolymer mortars the following can be concluded:

- Both the initial curing temperature and the ratio of sodium silicate to potassium hydroxide highly affect the performance of the geopolymer.
- The optimum ratio of sodium silicate to potassium hydroxide is highly related to the type of pozzolan used and to the initial curing temperature.
- All geopolymer mortars maintained some strength after they were exposed to 800°C for one hour. The strength of the geopolymer mortars after the heat exposure is highly related to their initial strength before the exposure.
- Geopolymer mortars made with class F fly ash showed higher strength and heat resistant than the geopolymer mortars made with metakaolin.
- A significant increase in the ratio of alkaline solution/pozzolan was needed to maintain workable mortar when metakaolin was used compare to fly ash.
- The crystal structure of the geopolymer mortars is highly affected by the initial curing temperature. Moreover, exposing the geopolymer mortars to elevated temperatures significantly changed the crystal structure of the mortars.
- Likewise, the pore structure of the geopolymer mortars is highly related to the initial curing temperature and smaller threshold pore diameter was associated with higher initial curing temperature (75°C).
- Exposing the geopolymer mortars to 800°C for one hour caused a major damage to the mortars pore structure and a relatively significant increase in macro pores was recorded.

#### 4.5 Future Recommendation

The use of class N pozzolans in concrete has the advantage of lower cost, lower heat of hydration and a positive impact on the surrounding environment as a result of reducing the use of OPC. The use of Pozzolete and Lassenite SR as a partial replacement of concrete was investigated in this study. However, further investigation is recommended to evaluate concrete durability. This can be achieved by measuring concrete resistance to freeze-thaw cycles, resistance to surface scaling, resistance to abrasion and the pore structure of the cement.

In this thesis the use Pozzolete showed a disadvantage of lowering the compressive strength of concrete. This disadvantage could be overcome by increasing the reactivity of Pozzolete by means of thermal activation. Activating Pozzolete should be investigated in great details.

In this thesis geopolymer mortars were synthesized using fly ash and metakaolin in two separate applications. The effect of several factors on the properties of geopolymer mortars was studied. However, investigating the effect of other factors like the delay time before curing, initial curing time, and the concentration of KOH is recommended.

## References

- ACI Committee 207 (1996). Mass concrete. (ACI 207.1R-96), Farmington Hills, M.I.: American Concrete Institute.
- ACI Committee 211 (1991). Standard practice for selecting proportions for normal, heavyweight, and mass concrete. (ACI 211.1-91), Farmington Hills, M.I.: American Concrete Institute, Reapproved 2002.
- ACI Committee 232 (2001). Use of raw or processed natural pozzolans in concrete. (ACI 232.1R-00), Farmington Hills, M.I.: American Concrete Institute, Reapproved 2006.
- ACI Committee 232 (2003). Use of fly ash in concrete. (ACI 232.2R-03), Farmington Hills, M.I.: American Concrete Institute.
- ASTM C 39 (2003). Standard test method for Compressive Strength of Hydraulic Cement Mortars, USA: American Society for Testing and Materials.
- ASTM C 109 (2002). Standard test method for compressive strength of hydraulic cement Mortars, USA: American Society for Testing and Materials.
- ASTM C 128 (2001). Standard test method for density, relative density (specific gravity), and absorption of fine aggregate, USA: American Society for Testing and Materials.
- ASTM C 136 (2001). Standard test method for sieve analysis of fine and coarse aggregates, USA: American Society for Testing and Materials.
- ASTM C 138 (2001). Standard test method for density (unit weight), yield, and air content (Gravimetric), USA: American Society for Testing and Materials.

- ASTM C 143 (2003). Standard test method for slump of hydraulic-cement concrete, USA: American Society for Testing and Materials.
- ASTM C 150 (2004). Standard specification for portland cement, USA: American Society for Testing and Materials.
- ASTM C 192 (2002). Standard practice for making and curing concrete test specimens in the laboratory, USA: American Society for Testing and Materials.
- ASTM C 215 (2002). Standard test method for fundamental transverse, longitudinal and torsional resonant frequencies of concrete specimens, USA: American Society for Testing and Materials.
- ASTM C 230 (2003). Standard specification flow table for use in Tests of hydraulic cement, USA: American Society for Testing and Materials.
- ASTM C 231 (2003). Standard test method for air content of freshly mixed concrete by the pressure method, USA: American Society for Testing and Materials.
- ASTM C 311 (2002). Standard test method for sampling and testing fly ash or natural pozzolans for use in portland-cement concrete, USA: American Society for Testing and Materials.
- ASTM C 469. (2002). Standard test method for static modulus of elasticity and poisson's ratio of concrete in compression, USA: American Society for Testing and Materials.
- ASTM C 494 (2004). Standard specification for Chemical Admixtures for Concrete. USA: American Society for Testing and Materials.
- ASTM C 496. (2004). Standard test method for splitting tensile strength of cylindrical concrete specimens. USA: American Society for Testing and Materials.

- ASTM C 595 (2003). Standard specification for blended hydraulic cements. USA:  
American Society for Testing and Materials.
- ASTM C 617 (1998). Standard practice for Capping Cylindrical Concrete Specimens1.  
USA: American Society for Testing and Materials, Reapproved (2003).
- ASTM C 618 (2003). Standard specification for coal fly ash and raw of calcined natural  
pozzolan for use as a mineral admixture in portland cement concrete, USA:  
American Society for Testing and Materials.
- ASTM C 1064 (2003). Standard test method for temperature of freshly mixed portland  
cement concrete, USA: American Society for Testing and Materials.
- ASTM C 1202 (1997). Standard test method for electrical indication of concrete's ability  
to resist chloride ion penetration, USA: American Society for Testing and  
Materials.
- ASTM C 1231 (2000). Standard practice for use of unbonded caps in determination of  
compressive strength of hardened concrete cylinders, USA: American Society for  
Testing and Materials.
- Bakharev, T. (2006). Thermal behaviour of geopolymers prepared using class F fly ash  
and elevated temperature curing. *Cement and Concrete Research*, 36(6), 1134-  
1147.
- Ballard, Z. J., Caires, W. S., Peters, S. R., Cesare, J., Colorado. Dept. of Transportation.  
Research Branch, & United States. Federal Highway Administration. (2008).  
Alternate mitigation materials for alkali-silica reaction (ASR) in concrete  
Colorado Dept. of Transportation, DTD Applied Research and Innovation Branch.



- Bondar, D., Lynsdale, C., Milestone, N. B., Hassani, N., & Ramezaniapour, A. (2010). Effect of type, form, and dosage of activators on strength of alkali-activated natural pozzolans. *Cement and Concrete Composites*,
- Bondar, D., Lynsdale, C., Milestone, N., Hassani, N., & Ramezaniapour, A. (2011a). Effect of adding mineral additives to alkali-activated natural pozzolan paste. *Construction and Building Materials*,
- Bondar, D., Lynsdale, C., Milestone, N., Hassani, N., & Ramezaniapour, A. (2011b). Effect of heat treatment on reactivity-strength of alkali-activated natural pozzolans. *Construction and Building Materials*,
- Bondar, D., Lynsdale, C. J., Milestone, N. B., Hassani, N., & Ramezaniapour, A. (2011). Engineering properties of alkali-activated natural pozzolan concrete. *ACI Materials Journal*, 108(1), 64-72.
- Chen, H., Soles, J. A., & Malhotra, V. M. (1993). Investigations of supplementary cementing materials for reducing alkali-aggregate reactions. *Cement and Concrete Composites*, 15(1-2), 75-84. doi:DOI: 10.1016/0958-9465(93)90039-C
- Chindaprasirt, P., Chareerat, T., & Sirivivatnanon, V. (2007). Workability and strength of coarse high calcium fly ash geopolymer. *Cement and Concrete Composites*, 29(3), 224-229.
- Cook, R. A., & Hover, K. C. (1999). Mercury porosimetry of hardened cement pastes. *Cement and Concrete Research*, 29(6), 933-943.
- Davidovits, J. (1989). Geopolymers and geopolymeric materials. *Journal of Thermal Analysis and Calorimetry*, 35(2), 429-441.

- Davidovits, J. (1999). Chemistry of geopolymeric systems, terminology. *Geopolymere*, 99, 9-39.
- Davis, R. E. (1950). A review of pozzolanic materials and their use in concretes. Paper presented at the Symposium on use of Pozzolanic Materials in Mortars and Concretes, 3.
- Davraz, M., & Gunduz, L. (2005). Engineering properties of amorphous silica as a new natural pozzolan for use in concrete. *Cement and Concrete Research*, 35(7), 1251-1261. doi:DOI: 10.1016/j.cemconres.2004.11.016
- Doležal, J., Škvára, F., Kopecký, L., Pavlasová, S., Lucuk, M., Dvořáček, K., . . . Šulc, R. Concrete based on fly ash geopolymers. Proceedings of 16th Intern.Baustofftagung IBAUSIL 2006
- Duxson, P. (2006). University of Melbourne, Dept. of Chemical and Biomolecular Engineering). The Structure and Thermal Evolution of Metakaolin Geopolymers,
- Duxson, P., Lukey, G. C., & van Deventer, J. S. J. (2006). Thermal evolution of metakaolin geopolymers: Part 1-physical evolution. *Journal of Non-Crystalline Solids*, 352(52-54), 5541-5555.
- Duxson, P., Lukey, G. C., & van Deventer, J. S. J. (2007). The thermal evolution of metakaolin geopolymers: Part 2-phase stability and structural development. *Journal of Non-Crystalline Solids*, 353(22-23), 2186-2200.
- Duxson, P., Mallicoat, S., Lukey, G., Kriven, W., & Van Deventer, J. (2007). The effect of alkali and Si/Al ratio on the development of mechanical properties of metakaolin-based geopolymers. *Colloids and Surfaces A: Physicochemical and Engineering Aspects*, 292(1), 8-20.

- Edouard, J. (2011). Experimental evaluation of the durability of fly ash-based geopolymer concrete in the marine environment. (M.S., Florida Atlantic University). ProQuest Dissertations and Theses, Retrieved from <http://search.proquest.com/docview/876102896?accountid=3611>. (MSTAR\_876102896)
- Fernández-Jiménez, A., Pastor, J. Y., Martín, A., & Palomo, A. (2010). High-Temperature resistance in Alkali-Activated cement. *Journal of the American Ceramic Society*, 93(10), 3411-3417.
- Ghrici, M., Kenai, S., & Said-Mansour, M. (2007). Mechanical properties and durability of mortar and concrete containing natural pozzolana and limestone blended cements. *Cement and Concrete Composites*, 29(7), 542-549. doi:DOI: 10.1016/j.cemconcomp.2007.04.009
- Gourley, J., & Johnson, G. (2005). Developments in geopolymer precast concrete. Paper presented at the World Congress Ceopolymer, 139-143.
- Güneyisi, E., Özturan, T., & Gesoglu, M. (2011). Examining the electrical properties of plain and blended cement concretes: Relationship between charge passed and initial current. *Composites Part B: Engineering*,
- Hardjito, D., & Rangan, B. (2005). Development and properties of low-calcium fly ash-based geopolymer concrete. Research Report GC, 1
- Hardjito, D., Wallah, S., Sumajouw, D., & Rangan, B. (2004a). On the development of fly ash-based geopolymer concrete. *ACI Materials Journal-American Concrete Institute*, 101(6), 467-472.

- Hardjito, D., Wallah, S., Summajouw, D., & Rangan, B. (2004b). Properties of geopolymer concrete with fly ash as source material: Effect of mixture composition. Paper presented at the Proceedings of the 7th CANMET/ACI International Conference on Recent Advances in Concrete Technology, 109-118.
- Hardjito, D., Wallah, S., Sumajouw, D., & Rangan, B. (2005a). Effect of mixing time and rest period on the engineering of fly ash-based geopolymer concrete. Paper presented at the Geopolymer, Green Chemistry and Sustainable Development Solutions: Proceedings of the World Congress Geopolymer 2005, 145.
- Hardjito, D., Wallah, S., Sumajouw, D., & Rangan, B. (2005b). Fly ash-based geopolymer concrete. *Australian Journal of Structural Engineering*, 6(1), 77-84.
- Irassar, E., Di Maio, A., & Batic, O. (1996). Sulfate attack on concrete with mineral admixtures. *Cement and Concrete Research*, 26(1), 113-123. doi:DOI: 10.1016/0008-8846(95)00195-6
- Jirasit, F., & Lohaus, L. (2005). Effects of high silica-content materials on fly ash-based geopolymeric cement properties. Paper presented at the Geopolymer, Green Chemistry and Sustainable Development Solutions: Proceedings of the World Congress Geopolymer 2005, 107.
- Kaid, N., Cyr, M., Julien, S., & Khelafi, H. (2009). Durability of concrete containing a natural pozzolan as defined by a performance-based approach. *Construction and Building Materials*, 23(12), 3457-3467. doi:DOI: 10.1016/j.conbuildmat.2009.08.002

- Khan, M. I. & Alhozaimy, A. M. (2005). King Saudi University, College of Engineering). Performance of concrete utilizing the natural pozzolanic material available in the Kingdom of Saudi Arabia
- Khan, M. I., & Alhozaimy, A. M. (2011). Properties of natural pozzolan and its potential utilization in environmental friendly concrete. *Canadian Journal of Civil Engineering*, 38(1), 71-78. doi:10.1139/L10-112
- Kong, D. L. Y, & Sanjayan, J. G. (2008). Damage behavior of geopolymer composites exposed to elevated temperatures. *Cement and Concrete Composites*, 30(10), 986-991.
- Kong, D. L. Y., & Sanjayan, J. G. (2010). Effect of elevated temperatures on geopolymer paste, mortar and concrete. *Cement and Concrete Research*, 40(2), 334-339.
- Kong, D. L. Y., Sanjayan, J. G., & Sagoe-Crentsil, K. (2007). Comparative performance of geopolymers made with metakaolin and fly ash after exposure to elevated temperatures. *Cement and Concrete Research*, 37(12), 1583-1589.
- Kong, D. L. Y., Sanjayan, J. G., & Sagoe-Crentsil, K. (2008). Factors affecting the performance of metakaolin geopolymers exposed to elevated temperatures. *Journal of Materials Science*, 43(3), 824-831.
- Kouloumbi, N., Batis, G., & Malami, C. (1994). The anticorrosive effect of fly ash, slag and a greek pozzolan in reinforced concrete. *Cement and Concrete Composites*, 16(4), 253-260. doi:DOI: 10.1016/0958-9465(94)90037-X
- Kumar, S., Kumar, R., Alex, T., Bandopadhyay, A., & Mehrotra, S. (2005). Effect of mechanically activated fly ash on the properties of geopolymer cement. Paper

- presented at the Geopolymer, Green Chemistry and Sustainable Development Solutions: Proceedings of the World Congress Geopolymer 2005, 113.
- Lee, W. K. (2002). University of Melbourne, Dept. of Chemical Engineering). Solid-Gel Interactions in Geopolymers,
- Lloyd, N., & Rangan, V. (2009). Geopolymer concrete-sustainable cementless concrete. Paper presented at the Proceedings of the 10th ACI International Conference on Recent Advances in Concrete Technology and Sustainability Issues, 33-54.
- López, M., & Castro, J. T. (2010). Effect of natural pozzolans on porosity and pore connectivity of concrete with time. *Rev.Ing.Constr*, , 419-431.
- Lovewell, C., & Hyland, E. J. (1974). A method of proportioning structural concrete mixtures with fly ash and other pozzolans. *Special Publication*, 46, 109-140.
- Luping, T., & Nilsson, L. O. (1993). Rapid determination of the chloride diffusivity in concrete by applying an electric field. *ACI Materials Journal*, 89(1)
- Mandal, K. K., Thokchom, S., & Roy, M. (2011). Effect of Na<sub>2</sub>O content on performance of fly ash geopolymers at elevated temperature.
- Mather, B. (1956). The partial replacement of portland cement in concrete. *Am Soc Testing & Matls Spec Tech Publ*,
- Mehta, P. K. (1981). Studies on blended portland cements containing santorin earth. *Cement and Concrete Research*, 11(4), 507-518. doi:DOI: 10.1016/0008-8846(81)90080-6
- Meissner, H. (1949). Pozzolans used in mass concrete Bureau of Reclamation.
- Meyer, C. (2009). The greening of the concrete industry. *Cement and Concrete Composites*, 31(8), 601-605. doi:DOI: 10.1016/j.cemconcomp.2008.12.010

- Najafi Kani, E., & Allahverdi, A. (2009). Effects of curing time and temperature on strength development of inorganic polymeric binder based on natural pozzolan. *Journal of Materials Science*, 44(12), 3088-3097.
- Najafi Kani, E., Allahverdi, A., & Provis, J. L. (2011). Efflorescence control in geopolymer binders based on natural pozzolan. *Cement and Concrete Composites*,
- Naseer, A. N. A., Jabbar, A. J. A., Khan, A. N. K. A. N., Ali, Q. A. Q., Hussain, Z. H. Z., & Mirza, J. M. J. (2008). Performance of pakistani volcanic ashes in mortars and concrete. *Canadian Journal of Civil Engineering*, 35(12), 1435-1445.
- Nili, M., & Salehi, A. M. (2010). Assessing the effectiveness of pozzolans in massive high-strength concrete. *Construction and Building Materials*, 24(11), 2108-2116. doi:DOI: 10.1016/j.conbuildmat.2010.04.049
- Nili, M., & Zaheri, M. (2011). Deicer salt-scaling resistance of non-air-entrained roller-compacted concrete pavements. *Construction and Building Materials*, 25(4), 1671-1676. doi:DOI: 10.1016/j.conbuildmat.2010.10.004
- Pacheco-Torgal, F., Moura, D., Ding, Y., & Jalali, S. (2011). Composition, strength and workability of alkali-activated metakaolin based mortars. *Construction and Building Materials*,
- Palomo, A., Grutzeck, M., & Blanco, M. (1999). Alkali-activated fly ashes:: A cement for the future. *Cement and Concrete Research*, 29(8), 1323-1329.
- Pan, Z., Sanjayan, J. G., & Rangan, B. (2009). An investigation of the mechanisms for strength gain or loss of geopolymer mortar after exposure to elevated temperature. *Journal of Materials Science*, 44(7), 1873-1880.

- Pan, Z., & Sanjayan, J. G. (2010). Stress–strain behaviour and abrupt loss of stiffness of geopolymer at elevated temperatures. *Cement and Concrete Composites*, 32(9), 657-664. doi:10.1016/j.cemconcomp.2010.07.010
- Papadakis, V. G., & Tsimas, S. (2005). Greek supplementary cementing materials and their incorporation in concrete. *Cement and Concrete Composites*, 27(2), 223-230. doi:DOI: 10.1016/j.cemconcomp.2004.02.011
- Provis, J. L., & Van Deventer, J. (2009). *Geopolymers: Structure, processing, properties and industrial applications* Woodhead Publ. Limited.
- Ramezaniapour, A. A., Pilvar, A., Mahdikhani, M., & Moodi, F. (2011). Practical evaluation of relationship between concrete resistivity, water penetration, rapid chloride penetration and compressive strength. *Construction and Building Materials*, 25(5), 2472-2479. doi:DOI: 10.1016/j.conbuildmat.2010.11.069
- Rangan, B. V., Hardjito, D., Wallah, S. E., & Sumajouw, D. M. J. (2005). Studies on fly ash-based geopolymer concrete. Paper presented at the Proceedings of the World Congress Geopolymer. France: Saint Quentin, 133-137.
- Rovnaník, P. (2010). Effect of curing temperature on the development of hard structure of metakaolin-based geopolymer. *Construction and Building Materials*, 24(7), 1176-1183.
- Shannag, M. J. (2000). High strength concrete containing natural pozzolan and silica fume. *Cement and Concrete Composites*, 22(6), 399-406. doi:DOI: 10.1016/S0958-9465(00)00037-8



- Shannag, M. J., & Yeginobali, A. (1995). Properties of pastes, mortars and concretes containing natural pozzolan. *Cement and Concrete Research*, 25(3), 647-657. doi:DOI: 10.1016/0008-8846(95)00053-F
- Shi, C. (2003). Another look at the rapid chloride permeability test (ASTM C1202 or ASSHTO T277). FHWA Resource Center, Baltimore,
- Sideris, K., & Savva, A. (2001). Resistance of fly ash and natural pozzolans blended cement mortars and concrete to carbonation, sulfate attack and chloride ion penetration. *Special Publication*, 199, 275-294.
- Sindhunata, D. S. (2006). University of Melbourne, Department of Chemical and Biomolecular Engineering). A Conceptual Model of Geopolymerisation
- Sumajouw, D. M. J., Hardjito, D., Wallah, S. E., & Rangan, B. V. (2005). Fly ash-based geopolymer concrete: An application for structural members. Paper presented at the Geopolymer, Green Chemistry and Sustainable Development Solutions: Proceedings of the World Congress Geopolymer 2005, 149.
- Sun, P. (2006). Wayne State University). Fly Ash Based Inorganic Polymeric Building Material,
- Tagnit-Hamou, A., Petrov, N., & Luke, K. (2003). Properties of concrete containing diatomaceous earth. *ACI Materials Journal*, 100(1)
- Targan, S., Olgun, A., Erdogan, Y., & Sevinc, V. (2003). Influence of natural pozzolan, colemanite ore waste, bottom ash, and fly ash on the properties of portland cement. *Cement and Concrete Research*, 33(8), 1175-1182. doi:DOI: 10.1016/S0008-8846(03)00025-5

- Taylor, H. F. W. (1986). Proposed structure for calcium silicate hydrate gel. *Journal of the American Ceramic Society*, 69(6), 464-467
- Temiz, H., Kose, M. M., & Koksai, S. (2007). Effects of portland composite and composite cements on durability of mortar and permeability of concrete. *Construction and Building Materials*, 21(6), 1170-1176. doi:DOI: 10.1016/j.conbuildmat.2006.06.011
- Temuujin, J., Van Riessen, A., & MacKenzie, K. (2010). Preparation and characterisation of fly ash based geopolymer mortars. *Construction and Building Materials*, 24(10), 1906-1910.
- Townsend, C. L. (1966). Control of temperature cracking in mass concrete United States. Dept. of the Interior, Bureau of Reclamation.
- Tuthill, L. H., & Adams, R. F. (1972). Cracking controlled in massive, reinforced structural concrete by application of mass concrete practices.
- USGBC, L. (2009). For new construction and major renovations.
- Uzal, B., Turanli, L., & Mehta, P. K. (2007). High-volume natural pozzolan concrete for structural applications. *ACI Materials Journal*, 104(5)
- Van Dam, T. J. (2010). Geopolymer Concrete, Retrieved from <http://www.fhwa.dot.gov/pavement/concrete/pubs/hif10014/index.cfm>
- Van Jaarsveld, J., & Van Deventer, J. (1999a). Effect of the alkali metal activator on the properties of fly ash-based geopolymers. *Industrial & Engineering Chemistry Research*, 38(10), 3932-3941.

- Van Jaarsveld, J., & Van Deventer, J. (1999b). The effect of metal contaminants on the formation and properties of waste-based geopolymers. *Cement and Concrete Research*, 29(8), 1189-1200.
- Van Jaarsveld, J., Van Deventer, J., & Lukey, G. (2002). The effect of composition and temperature on the properties of fly ash-and kaolinite-based geopolymers. *Chemical Engineering Journal*, 89(1-3), 63-73
- Wallah, S., Hardjito, D., Sumajouw, D., & Rangan, B. (2005a). Performance of geopolymer concrete under sulfate exposure. *ACI SPECIAL PUBLICATIONS*, 225, 27.
- Wallah, S. E., Hardjito, D., Sumajouw, D. M. J., & Rangan, B. V. (2005b). Performance of fly ash-based geopolymer concrete under sulfate and acid exposure. Paper presented at the Geopolymer, Green Chemistry and Sustainable Development Solutions: Proceedings of the World Congress Geopolymer 2005, 153.
- Wallah, S., & Rangan, B. V. (2006). Low-calcium fly ash-based geopolymer concrete: Long-term properties. *Research Report GC*, 2
- Washburn, E. W. (1921). Note on a method of determining the distribution of pore sizes in a porous material. *Proceedings of the National Academy of Sciences of the United States of America*, 7(4), 115.
- Waugh, W. R. (1963). Corps of engineers experience with pozzolans. Paper presented at the Symposium on Mass Concrete, 89-101.
- Wu, H. C., & Sun, P. (2010). Effect of mixture compositions on workability and strength of fly ash-based inorganic polymer mortar. *ACI Materials Journal*, 107(6)

Xu, H., & Van Deventer, J. (2000). The geopolymerisation of aluminosilicate minerals.

International Journal of Mineral Processing, 59(3), 247-266.

Yip, C. K., Provis, J. L., Lukey, G. C., & van Deventer, J. S. J. (2008). Carbonate mineral

addition to metakaolin-based geopolymers. Cement and Concrete Composites,

30(10), 979-985.

Yunsheng, Z., Wei, S., & Zongjin, L. (2008). Synthesis and microstructural

characterization of fully-reacted potassium-poly (sialate-siloxo) geopolymeric

cement matrix. ACI Materials Journal, 105(2)

## VITA

Graduate College  
University of Nevada, Las Vegas

Omar Abdelmalek Saleh

### Degrees

Associate of Applied Science in Computer Aided Design-Drafting, 2006  
Delgado Community College

Bachelor of Science in Civil Engineering, 1995  
University of Mosul, Iraq

### Special Honors

Golden Key International Honour Society  
Tau Beta Pi The Engineering Honor Society  
The honor Society of Phi Kappa Phi

### Publications:

Said, A and Saleh, O., (2012). Investigating the use of class N pozzolan as a partial replacement of Ordinary portland cement in concrete. [In progress]

Said, A and Saleh, O., (2012). Fly ash-based geopolymer mortars exposed to elevated temperature. [In progress]

Said, A and Saleh, O., (2012). Metakaolin-based geopolymer mortars exposed to elevated temperature. [In progress]

Thesis Title: Investigating the Use of Pozzolans in Portland Cement Concrete and Inorganic Polymer Mortar

### Thesis Examination Committee:

Chairperson, Dr. Aly Said, Ph.D., P.E.

Committee Member, Dr. Moses Karakouzian, Ph.D., P.E.

Committee Member, Dr. Samaan Ladkany, Ph.D., P.E.

Graduate Faculty Representative, Dr. Jan 'Matt' Pedersen, Ph.D.